Technical Program for Long-Term Management of Canada's Used Nuclear Fuel – Annual Report 2022

Nuclear Waste Management Organization (S. Briggs, ed.)

nwmo

NUCLEAR WASTE MANAGEMENT ORGANIZATION   SOCIÉTÉ DE GESTION DES DÉCHETS NUCLÉAIRES

Technical Program for Long-Term Management of Canada's Used Nuclear Fuel – Annual Report 2022

NWMO-TR-2023-01

May 2023

Nuclear Waste Management Organization (S. Briggs, ed.)

Document History

Title:	Technical Program for Long-Term Management of Canada's Used Nuclear Fuel – Annual Report 2022		
Report Number:	NWMO-TR-2023-01		
Revision:	R000	Date:	May 2023
Nuclear Waste Management Organization			
Authored by:	NWMO (S. Briggs, ed.)		
Reviewed by:	P. Gierszewski, K. Glenn, R. Habib, S. Hirschorn		
Approved by:	C. Boyle		

ABSTRACT

Title: **Technical Program for the Long-Term Management of Canada's Used Nuclear Fuel – Annual Report 2022**
Report No.:   **NWMO-TR-2023-01**
Author(s):   NWMO (S. Briggs, ed.)
Company: Nuclear Waste Management Organization
Date: May 2023

Abstract

This report is a summary of activities and progress in 2022 for the Nuclear Waste Management Organization's Technical Program. The primary purpose of the Technical Program is to support the implementation of Adaptive Phased Management (APM), Canada's approach for the long-term management of used nuclear fuel.

The work continued to develop the repository design; to understand the engineered barrier, geological and other processes important to the safety case; and to assess the siting areas.

NWMO continued to participate in international research activities, including projects associated with Posiva Encapsulation Plant for spent nuclear fuel, the Mont Terri Underground Rock Laboratory, the SKB Äspö Hard Rock Laboratory, the ONKALO facility, the Grimsel Test Site, and the OECD (Organisation for Economic Co-operation and Development) Nuclear Energy Agency.

NWMO's technical program supported technical presentations at national and international conferences, issued 14 NWMO technical reports and published 17 journal articles.

TABLE OF CONTENTS

LIST OF TABLES

LIST OF FIGURES

1   INTRODUCTION

The Nuclear Waste Management Organization (NWMO) is implementing Adaptive Phased Management (APM) for the long-term management of used nuclear fuel. This is the approach recommended in *"Choosing a Way Forward: The Future Management of Canada's Used Nuclear Fuel"* (NWMO 2005) and selected by the Government of Canada in 2007.

The technical objective of the APM approach is a Deep Geological Repository (DGR) that provides long-term containment and isolation, to ensure safety of people and the environment while the radioactivity in the used fuel decays.

The deep geological repository is a multiple-barrier system designed to safely contain and isolate used nuclear fuel over the long term. It will be constructed at a depth of more than 500 metres, depending upon the geology of the site, and consist of a series of tunnels leading to a network of placement rooms where the used nuclear fuel will be contained using a multiple-barrier system. A conceptual design for a DGR is illustrated in Figure 1-1 for a generic rock setting (the design will be varied for actual rock conditions).

The NWMO is presently in the Site Selection phase. No site has been selected to host the DGR. The process for selecting a site is described in *Moving Forward Together: Process for Selecting a Site for Canada's Deep Geological Repository for Used Nuclear Fuel* (NWMO 2010). The steps for evaluating the geological suitability of willing and informed host communities consists of a) initial screenings to evaluate the suitability of candidate sites against a list of preliminary screening criteria, using readily available information; b) preliminary assessments to further determine if candidate sites may be suitable for developing a safe used fuel repository; and c) detailed field investigations to confirm suitability of one site.

Initially, 22 communities had expressed interest in the program. By 2022 the number of areas engaged in the site selection process had been narrowed to two, the Revell Site in the Wabigoon Lake Ojibway Nation (WLON)-Ignace area and the South Bruce site in the Saugeen Ojibway Nation (SON)-South Bruce area, based on preliminary assessments of potential geological suitability and potential for the project to contribute to community well-being. The location of these potential sites is shown in Figure 1-2. Reports documenting the site selection process to date are available on the NWMO website (http://www.nwmo.ca/sitingprocess_feasibilitystudies).

The NWMO continues to conduct technical work to support design, site assessment and safety case for a DGR, in parallel with work to engage with and establish partnerships with communities. This report summarizes technical work conducted in 2022. In the near term, this information will support selection of a preferred site, anticipated to be selected in 2024. In the longer term, this will support an impact assessment and licence applications at the selected site. NWMO's overall implementation plan is described in *Implementing Adaptive Phased Management* 2023-2027 (NWMO 2023).
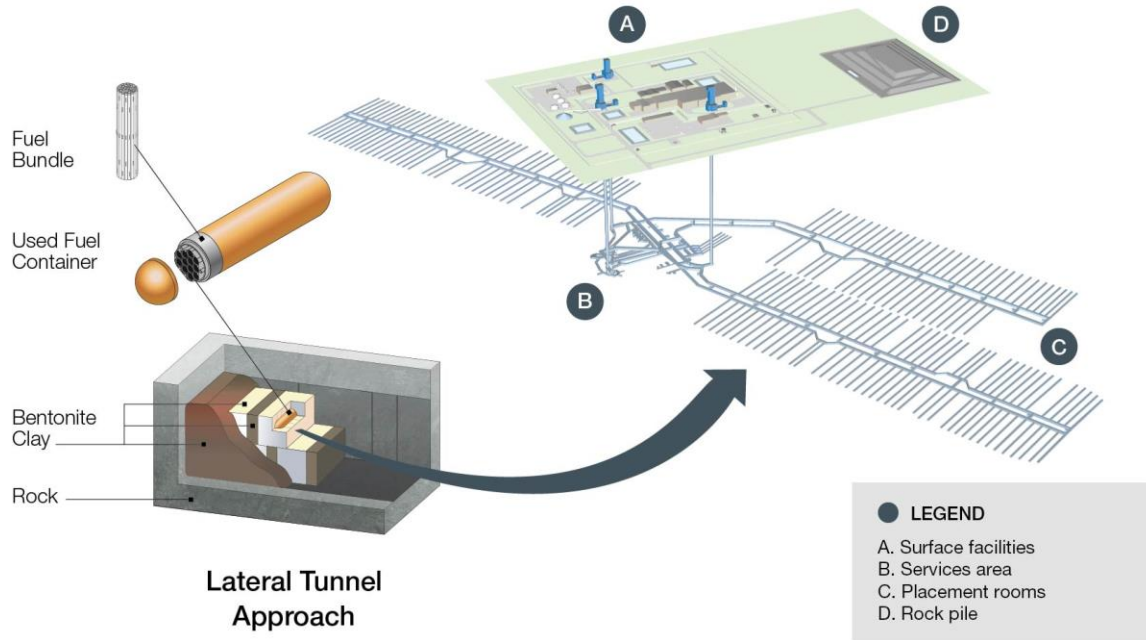
Figure 1-1: Illustration of a Deep Geological Repository Reference Design

Figure 1-2: Interested Community Status as of 31 December 2022

2   OVERVIEW OF NWMO TECHNICAL PROGRAMS

The NWMO Technical Program includes site investigations, preliminary design and proof testing, and developing the safety case for a used fuel DGR. Work conducted during 2022 is summarized in this report. Prior years work is summarized in NWMO (2022a).

The work is summarized in the following sections divided into Engineering, Geoscience, Repository Safety, and Site Assessment.

This work involved 17 universities (including 15 Canadian universities), as well as a variety of industrial and governmental research partners. A list of the 2022 technical reports produced by NWMO is provided in Appendix A.1. Appendix A.2 provides a list of journal articles on work supported by NWMO.

An important aspect of the NWMO's technical program is collaboration with radioactive waste management organizations in other countries. In 2022, the NWMO had agreements with ANDRA (France), INER (Taiwan), KORAD (South Korea), Nagra (Switzerland), NDA (United Kingdom), NUMO (Japan), ONDRAF (Belgium) and SKB (Sweden) to exchange information arising from their respective national programs to develop a deep geologic repository for nuclear waste, and collaborated with other organizations on specific projects.

Some of this collaboration is work undertaken at underground research facilities. In 2022, NWMO supported projects at the Mont Terri Underground Rock Laboratory in Switzerland, the SKB Äspö Hard Rock Laboratory in Sweden, the ONKALO facility in Finland, and the Grimsel Test Site (GTS) in Switzerland. These provide information in both crystalline (Äspö, ONKALO, GTS) and sedimentary (Mont Terri) geological environments.

NWMO was involved with the following joint experimental projects in 2022:

- Full-scale In-Situ System Test (FISST/EBBO) demonstration project at ONKALO,
- The Mont Terri Project and Rock Laboratory including:
  - Diffusion across 10-year-old concrete/claystone interface (CI, CI-D),
  - Long-term Diffusion experiment (DR-B),
  - Analysis of Geochemical Data (GD)
  - Geomechanical in-situ Characterization of Opalinus Clay (GC-A)
  - Full Scale Emplacement Experiment (FE-G, FE-M),
  - Hydrogen Transfer (HT) test,
  - Iron Corrosion – Bentonite (IC-A) test,
  - Long-term Pressure Monitoring (LP-A),
  - Microbial Activity (MA),
  - Porewater Gas-characterisation Methods for Reactive and Noble Gases (PC-D),
  - Seismic imaging ahead of and around underground infrastructure (SI-A)
  - Permanent nanoseismic monitoring (SM-C), and
  - Large-scale Sandwich seal experiment (SW-A).
- POST Project (Fracture Parameterization for Repository Design & Post-closure Analysis),
- Materials Corrosion Test (MaCoTe) at GTS.
- Gas-Permeable Seal Test (GAST) at GTS.
- Enhanced Sealing Project (ESP) at Whiteshell Labs, Canada,
- MICA Michigan International Copper Analogue project, and

- International Bentonite Longevity project.

NWMO was involved with the following modelling or information exchange projects in 2022:
- DECOVALEX thermal-hydraulic-mechanical modelling,
- Aspo Groundwater Modelling Task Force,
- Post-closure criticality working group,
- CatchNET cold climate hydrology modelling,
- BIOPROTA biosphere models, and
- Joint projects with SKB on modelling fractured rock, including HM coupling, Skempton/Biot coefficient, fracture statistics.

The NWMO continued to participate in the international radioactive waste management program of the Organisation for Economic Co-operation and Development (OECD) Nuclear Energy Agency (NEA). Members of this group include the major nuclear energy countries, including waste owners and regulators. NWMO is involved with the following NEA activities:

- Radioactive Waste Management Committee (RWMC),
- Integration Group for the Safety Case (IGSC),
- Working Group on the Characterization, the Understanding and the Performance of Argillaceous Rocks as Repository Host Formations (i.e., Clay Club),
- Expert Group on Geological Repositories in Crystalline Rock Formations (i.e., Crystalline Club),
- Expert Group on Operational Safety (EGOS),
- Thermochemical Database (TDB) Project, and
- Working Party on Information, Data and Knowledge Management (WP-IDKM).

This report aligns with the RD2019 - NWMO's Program for Research and Development for Long Term Management of Used Nuclear Fuel (NWMO 2019). The RD2019 report describes the major technical research and development directions of the NWMO. It is complementary to NWMO activities in site selection, site characterization, design and engineering proof testing, and considers the full lifecycle of the repository. A key point is that underlying science studies will continue throughout the repository phases in order to support future licence decisions. The current annual technical report includes an update on work that supports this science basis.

3 REPOSITORY ENGINEERING AND DESIGN

During 2022, research and development progressed as planned in the Engineering Program:

1. A full-scale Emplacement trial of the Engineered Barriers System in a simulated rock emplacement room was completed successfully, proving the NWMO system design for emplacement of the UFC container and bentonite buffer.
2. As part of the Proof Test Program, serial production of 17 UFCs continued during the year with eleven fully completed and the balance at various stages of assembly.
3. A beyond-design pressure test was performed on one of the completed UFCs. The container plastically buckled at a pressure of 63 MPa, demonstrating a 40% design margin against buckling. Finally, the container was fully flattened. Following the tests, helium leak testing confirmed that the container had not failed.
4. Refinements and optimization of the manufacturing processes for electrodeposition, cold spraying and machining of the copper coating continued as planned.
5. Assessment of primary and alternative routes to the potential DGR sites of Revell and South Bruce continued.
6. Work continued on the Used Fuel Packaging Plant (UFPP) on technical feasibility and risk assessment as part of the next phase of the facility design to support Impact Assessment and Licensing activities.
7. Assessment of potential underground DGR layouts for 5.5 million bundles storage capacity continued for the two potential sites at Revell (crystalline rock) and South Bruce (sedimentary rock).
8. A study was completed assessing three transfer equipment concepts for the Loaded Buffer Box Transfer Cask to select a preferred option.

Summaries of these activities in 2022 are provided in the following sections.

3.1 DESIGN REQUIREMENTS

In 2022, no further design requirements work was initiated following the development of the three high-level design requirements (DR) documents completed in 2021. Details on the three documents can be found in the 2021 ATR (NWMO 2022a). They provide the basis for the development of more detailed sub-tier design requirements and program requirements, and will be used to inform safety assessment, site evaluation, and project cost estimate updates.

3.2 USED FUEL TRANSPORTATION

3.2.1 Used Fuel Transportation Systems

Canada's used nuclear fuel is currently safely managed in facilities licensed for interim storage. These facilities are located at nuclear reactor sites in Ontario, Québec, and New Brunswick, as well as Atomic Energy of Canada Limited's nuclear sites at Whiteshell Laboratories in Manitoba, and Chalk River Laboratories in Ontario. The long-term management of Canada's used nuclear fuel will require transport of the used nuclear fuel from these interim storage facilities to the DGR.

NWMO is currently in a site selection process for the repository and has narrowed its focus to two potential siting areas: the WLON-Ignace area in northwestern Ontario; and the SON-South

Bruce area in southern Ontario. The locations of the interim storage facilities and the potential siting areas are illustrated in Figure 3-1.

● Interim storage facilities
1. Whiteshell Laboratories, Man.
2. Bruce Nuclear Generating Station, Ont.
3. Pickering Nuclear Generating Station, Ont.
4. Darlington Nuclear Generating Station, Ont.
5. Chalk River Laboratories, Ont.
6. Gentilly Nuclear Generating Station, Que.
7. Point Lepreau Nuclear Generating Station, N.B.

■ Assessments underway in the area
1. The Wabigoon Lake Ojibway Nation-Ignace area, Ont.
2. The Saugeen Ojibway Nation-South Bruce area, Ont.

Figure 3-1: Interim Storage Facilities and Potential Siting Areas

NWMO's current reference Used Fuel Transportation System (UFTS) is an all-road system which uses two types of transportation packages: Used Fuel Transportation Packages (UFTPs) for OPG owned fuel; and conceptual Basket Transportation Packages (BTPs) for all other fuel. Both UFTPs and BTPs are to be transported using conventional tractor-trailers.

An alternative UFTS is being considered by the NWMO which uses Dry Storage Container Transportation Package (DSC-TP) for the transport of OPG owned fuel currently stored in Dry Storage Containers (DSCs). Superload or heavy-load trucks and railcars are being considered for these DSC-TP shipments. As in the reference UFTS, conceptual BTPs are to be used to transport non-OPG owned fuel, on conventional tractor-trailers.

NWMO's responsibility includes the development of a robust UFTS to ensure the safe and secure transport of Canada's used fuel. Projects in the areas of transportation routing, estimating transportation environmental releases, transportation security, transportation accident analysis and transport package performance, as well as supporting the Whiteshell Fuel Transfer Project were all areas of work in 2022.

3.2.2 Used Fuel Transportation System – Routing Assessment

NWMO progressed an assessment aimed at establishing representative primary and alternate routes from each interim storage facility to both potential repository site locations, for the two UFTS concepts being considered, as described above.

This assessment used routing considerations and factors identified through: literature review; benchmarking against established industry programs; criteria identified through public engagement; technical factors; safety criteria; regulatory guidance and legislative factors.

3.2.3 Transportation Accident Data and Mitigation Assessment

In 2022, NWMO initiated a study to analyze historical transportation accident data relevant to the types of conveyances considered in the above-noted UFTS concepts to understand accident scenarios, contributing factors, and strategies that can be implemented to mitigate them.

The study leveraged provincial road accident data from Ontario, Québec, and New Brunswick, as well as other relevant data from federal sources (Transportation Safety Board, Transport Canada, Canadian Nuclear Safety Commission) for both road and rail transport modes.

The objective of the study is to analyze the accident data utilizing probabilistic risk methods, thus providing a statistical breakdown of common accident scenarios, as well as the likelihood of occurrence for accidents of concern. The results of the study will be leveraged to identify preventative and mitigative measures that can be implemented in NWMO's future transportation campaign.

This project is ongoing.

3.2.4 Confidence in Used Fuel Transportation Package Performance

In 2022, NWMO initiated a project aimed at presenting, in a clear and concise manner, how the regulations and requirements pertaining to Type B transportation packages ensure that inherent safety is built into their design. The performance requirements and test criteria of certified Type B packages will be outlined. The work will draw from existing legislations and regulations, as well as extra-regulatory demonstration tests and real-world accident reconstructions, in order to provide further evidence that the transport of used fuel in certified Type B packages is safe. This project is ongoing.

3.2.5 Whiteshell Fuel Transfer Project

NWMO is currently collaborating with Canadian Nuclear Laboratories (CNL) to support the Whiteshell Fuel Transfer Project aimed at consolidating used fuel storage. Used fuel currently stored at Whiteshell Laboratories in Pinawa, Manitoba, will be transported to the interim waste management facility in Chalk River, Ontario. To accomplish this, CNL has leased NWMO's Used Fuel Transportation Package (UFTP-1).

As part of this project, it is anticipated that CNL will use the UFTP to transport mixed fuel types (MFT) from the Concrete Canister Storage Facility at Whiteshell Laboratories to CNL. NWMO will be engaging in additional work to expand allowable contents of the UFTP transport

certificate to include MFT. As such, NWMO is collaborating with CNL to develop a new application which will be submitted to the CNSC in 2023 to include such contents.

3.3 USED FUEL PACKAGING PLANT

The Used Fuel Packaging Plant (UFPP) is a key surface facility at the DGR site. The UFPP will have all the provisions required for receiving the transportation casks known as Used Fuel Transportation Packages (UFTP) for fuel being transported in storage modules or Basket Transportation Packages (BTP) for fuel in sealed baskets, equipment for fuel handling, designated facilities for the encapsulation of the fuel in Used Fuel Containers (UFCs) and their dispatching for emplacement in the underground repository.

The NWMO completed its first iteration of the conceptual design for the UFPP in early 2021. The overall conceptual layout of the UFPP is shown in Figure 3-2. The process operations for handling the used fuel and its encapsulation in the UFCs are described in the Annual Technical Report for 2020 (NWMO, 2021b).
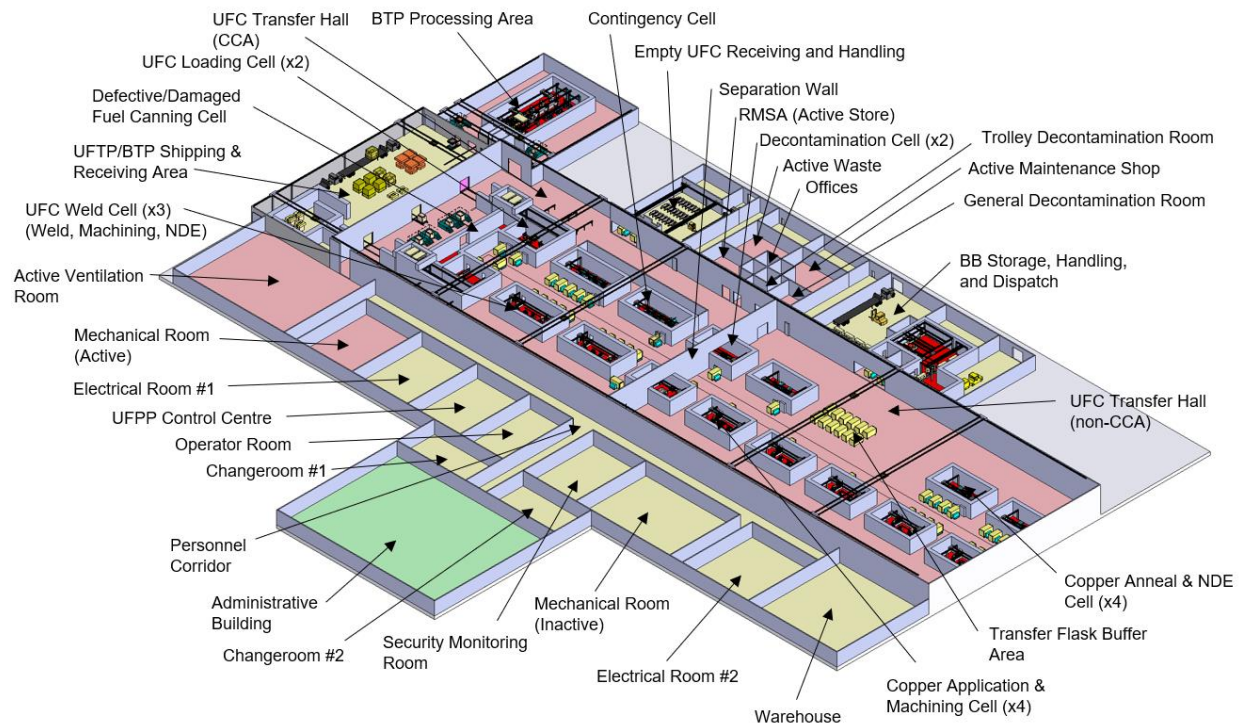
Figure 3-2: Concept Layout of the Used Fuel Packaging Plant (UFPP)*

*The key acronyms denoting processing areas and components are: CCA (Contamination-controlled Area), Non-CCA (non-contaminated control area), BB (Buffer Box), BTP (Basket Transportation Package), UFTP (Used Fuel Transportation Package), UFC (Used Fuel Container), NDE (Non-destructive Examination), and RMSA (Radioactive Material Storage Area).

3.3.1 Process Systems Development Description

The conceptual design for the UFPP is followed up in 2022 with a review of the projected used fuel inventory and the packaging process development to date. The purpose of this assessment is to realign the design inputs to support the next major work packages associated with the

UFPP: support of the Impact Assessment and Licence to Prepare Site Applications; and the next phase of design for the UFPP.

The projected used fuel inventory was updated and select characteristics of the used fuel were documented as input for the next phase of work. The final inventory projection of used fuel expected at the DGR site was adjusted to align with new estimates from the operating nuclear power stations for operational life and nuclear fuel consumption.

While the development of the used fuel packaging processes and the UFC design have not been finalized, the maturing UFPP design will be developed alongside the maturing packaging process and UFC design. The understanding of key UFPP systems to date are described in the UFPP process development report to support this plan. Twelve key systems have been identified at this time for the purpose of this report: 1. Transportation package receipt; 2. used fuel storage; 3. used fuel inspection; 4. UFC handling; 5. UFC welding; 6. weld machining; 7. weld NDE; 8. copper application; 9. copper heat treatment; 10. copper machining; 11. copper NDE; 12. loaded buffer box assembly and dispatch.

3.3.2   Impact Assessment and Licence to Prepare Site Activities

The preparation for and launch of the contract to support the Impact Assessment (IA) and License to Prepare Site (LTPS) were underway in 2022. The purpose of this contract is to strategically advance the previous development of the Used Fuel Packaging Plant (UFPP) to align with the needs of the IA and LTPS applications.

This contract will require completing design activities for some UFPP systems, and preparation of the construction plan, operations plan, and decommissioning plan for the UFPP. The deliverables from this contract will be used as an input to NWMO's Effects Assessment work. For example, the UFPP utilities (e.g., electricity, natural gas, water usage), waste generation, etc. will be quantified and emissions/effluents calculated.

3.3.3   Collaboration with Posiva Solutions Oy Finland

Finland is the current leader in the implementation of used nuclear fuel packaging and underground disposal technologies (Mikhailova, 2019). The Onkalo disposal facility developed by Posiva will be the world's first deep geological repository for spent nuclear fuel. Posiva has accumulated over 40 years of engineering research and development experience in used fuel packaging for their facility, which encompasses both the canister design and the machinery for safely handling the fuel during the packaging process. The civil construction for the Onkalo encapsulation plant has been completed, and the equipment needed for the used fuel packaging process inside the plant is being installed and commissioned.

NWMO has initiated a collaborative project with Posiva to engage their technical experts in used fuel packaging and handling to draw from this extensive experience. Through this joint work, NWMO has received valuable technical review of our project requirements and conceptual design documentation, and we have been granted access to Posiva's documentation to use as a technical reference for our project. This work has been complemented by webinars, which allow the technical teams from both organizations to openly discuss our designs and the implementation of our project together.

Through this collaboration, our Used Fuel Packaging Plant team, and other groups within NWMO, have been able to leverage the accumulated knowledge and lessons learned from Posiva's experts and apply this to our designs, to improve the safety, efficiency, and reliability of used fuel packaging in Canada.

3.3.4 UFC Closure Technology – Technical Feasibility and Risk Assessment Study

NWMO initiated an assessment aimed at evaluating the UFC design for implementation in a production environment and to identify risks associated with the automation of tooling required to package fuel bundles by remote and robotic methods into Used Fuel Containers (UFCs). This assessment was based on NWMO's current throughput requirement of 120,000 spent CANDU fuel bundles per year.

Three (3) nuclear automation vendors with experience in design of reliable automated and remotely controlled tooling for a radiation environment were asked to review the UFC closure weld and copper spray processes. This review was performed through observation of the welding and copper spray demonstrations at research and development facilities.   Other associated processes were assessed through a detailed document review and discussions with NWMO. Following the observation of the demonstration processes, each vendor was asked to host a workshop with key NWMO stakeholders and deliver a report summarizing their assessments based on feasibility and risks in developing automated tooling to remotely operate in a high-radiation environment. The workshop and associated report discussed the following:

1. Practical feasibility of the welding and copper spray process operations for use in a fully automated high-volume production environment considering NWMO's current throughput requirement of 120,000 spent CANDU bundles per year.

2. Practical feasibility of the welding and copper spray process operations for reliable use in a hot cell/ radiation environment.

3. Identification, assessment and quantification of risks associated with implementation of the processes and tooling. Risk evaluation based on UFPP annual throughput and safety requirements.

The assessment made by three (3) separate nuclear automation vendors allowed NWMO to compare the independent reviews on risks and feasibility from companies with automation nuclear experience based on different applications and operating experiences. The information from this work will inform the next design phases of UFC and UFPP to incorporate the industry knowledge and experience in nuclear and automation.

3.4 BUFFER AND SEALING SYSTEMS

The NWMO continues to support the development of the buffer and sealing systems including optimized manufacturing, storage, and emplacement technology for the Highly Compacted Bentonite (HCB) blocks that are placed directly around the UFCs.

3.4.1 Full Scale Emplacement Trial

The full-scale emplacement trial was completed in April 2022 after several years of engineering development. Its main purpose was to demonstrate the NWMO's engineered barrier system by testing, assembling and placing full-scale prototype system components in a simulated emplacement room. This allowed to perform an operational demonstration of the concept, a

verification of equipment performance and an assessment of the feasibility of the reference concept in achieving emplacement of the containers, the bentonite buffer and backfill.

The scope of the trial was to fill the first 6 m of the mock emplacement room (approximately half the length of the room). Filling the first 6 m of the emplacement room requires:

1. Installation of the gap fill observation room ('aquarium') and dummy gap fill material at the end of the emplacement room. These will represent the initial fill in the deep geological repository.

2. Scanning and measuring the volume of the room and buffer materials to calculate the as-placed dry-density.

3. Placement of 7 complete, loaded buffer box (LBB) assemblies. (Note: Loaded for this trial means with representative weight, not actual used fuel).

4. Placement of 16 floor tablets and 21 filler blocks.

5. Placement of granulated gap fill material.

6. Scanning and measurement of the as-placed material.

7. Disassembly and inspection of all buffer materials and retrieval of the buffer box Emplacement Trial Requirements

This trial was to replicate the NWMO reference concept, which is to place copper coated used fuel containers, encased in highly compacted bentonite into an underground emplacement room, and then back-fill with underground emplacement room with gap fill material. Upon completion of this process, the UFC is in the state necessary for long-term storage. This concept is generic in nature, with modifications to room and back fill material geometry to manage container surface temperature and repository thermal load, in both sedimentary and crystalline repository geospheres that are under consideration in Canada.

To simplify this test, the additional highly compacted bentonite spacers used for thermal balancing and the required staggering of buffer boxes are omitted (as thermal performance was not a consideration for this demonstration). The delivery of additional highly compacted bentonite spacer blocks would be identical to the buffer box and therefore these omissions do not impact our ability to assess the delivery of buffer boxes, spacer blocks or gap fill material.

The basic requirements of this test are:

1. To fill the excavated volume (mock emplacement room) of the emplacement room with:

2. Buffer boxes with representative weight.

3. Gap Fill Material; and

4. Achieve an average as-placed, gap fill material dry density ≥1.41 g/cm^3

3.4.1.1 Emplacement Trial Materials

The buffer portion of the engineered barrier system between the used fuel container and the surrounding geosphere is bentonite clay-based and consists of the following:

1. Highly Compacted Bentonite (HCB) blocks, spacers, and bricks interfacing directly with the used fuel container, and;

2. Gap Fill Material (GFM) used to fill the voids between the HCB and the rock in the placement room.

Bentonite, specifically sodium bentonite, is used as a buffer material because of its unique ability to absorb large amounts of water and effectively create a seal around the used fuel container. This is important to help preserve the integrity of the used fuel container for many thousands of years.

Refer to Figure 3-3: for the emplacement trial arrangement.
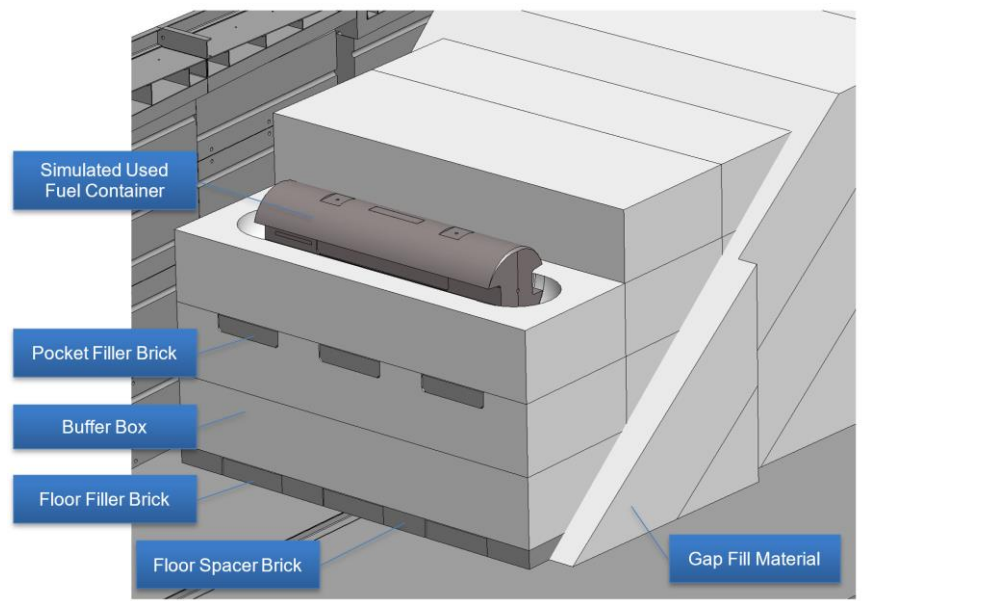
Figure 3-3: Emplacement Room Materials

3.4.1.1.1 Highly Compacted Bentonite

Highly compacted bentonite is pressed using the cold isostatic pressing (CIP) method. Cold isostatic pressing is also known as wet bag pressing, where the material to be pressed is loaded into a flexible rubber bag, inside a perforated metallic container. The bag is sealed and placed in a pressure vessel where it is hydrostatically compressed at high pressure. The CIP method produces a highly compacted bentonite block with a uniform density throughout since the bentonite is uniformly compressed from all directions.

The raw material is procured and blended with water to a moisture content between 19 and 21%, this results in highly compacted bentonite blocks with dry densities >1.7g/cm^3 (Birch and Mielcarek, 2016). Approximately 4000 kg of blended bentonite is loaded into the custom designed, perforated steel container lined with a latex rubber bag assembly to make HCB blocks for the buffer box. The loaded container is then lowered into a pressure vessel and pressurized to 100 MPa. The blocks are then machined to the exact dimensions required. This includes the cavity to house the used fuel container.

Highly compacted bentonite is sensitive to the relative humidity in the environment and as a result, the blocks are immediately wrapped in a vapour barrier and stored in a humidity-controlled room. Shaping is completed in a humidity-controlled room by a 6-axis robot with

machining spindle. The completed blocks are again wrapped in vapour barrier and placed back into storage until ready for assembly.

A total of 7 buffer boxes were used for the emplacement trial, requiring 14 HCB blocks. Additional HCB blocks were pressed and cut down to fabricate the required floor spacer, filler, and pocket filler bricks.

3.4.1.1.2 Gap Fill Material

NAGRA have developed a bentonite-based granulate for their placement concept that has been adopted as a GFM in the NWMO concept. GFM is produced by reducing the moisture content of as-delivered MX-80 bentonite (or equivalent) to 3-6% and then granulating it to increase dry density. The granules are then milled and sieved to the desired particle distribution (Table 3-1) for optimum packing efficiency. To date, the NWMO has had difficulty sourcing a North American supplier for GFM in the test quantities, so for the emplacement trial, 60 tonnes was purchased from NAGRA.

Table 3-1: GFM Particle Size Distribution Envelope

Particle Size (mm)	Cumulative Weight Percent Passing (%)
8.0	100
4.75	70-100
1.18	30-55
0.3	10-30
0.075	0-12

3.4.1.1.3 Used Fuel Container

One of the requirements of this trial was test the ability to deliver and emplace buffer box assemblies. A complete, loaded buffer box assembly with full used fuel container would weigh approximately 8000kg. Testing with used fuel bundles is not possible, so simulated containers were fabricated to match the weight of a loaded used fuel container. Additionally, 2 copper-coated containers loaded with concrete plugs as weight were used in the trial to assess the impact handling of the HCB material might have on the copper surface finish of the container.

3.4.1.2 Emplacement Trial Equipment

3.4.1.2.1 Mock Emplacement Room

The mock emplacement room (MER) is an above ground representation of the NWMO reference DGR emplacement room. The room has been designed and fabricated from structural steel to the reference DGR internal dimensions (Figure 3-4) and lined with polyurethane panels molded to replicate the drill and blast excavation technique (Figure 3-5) The floor is poured smooth concrete.
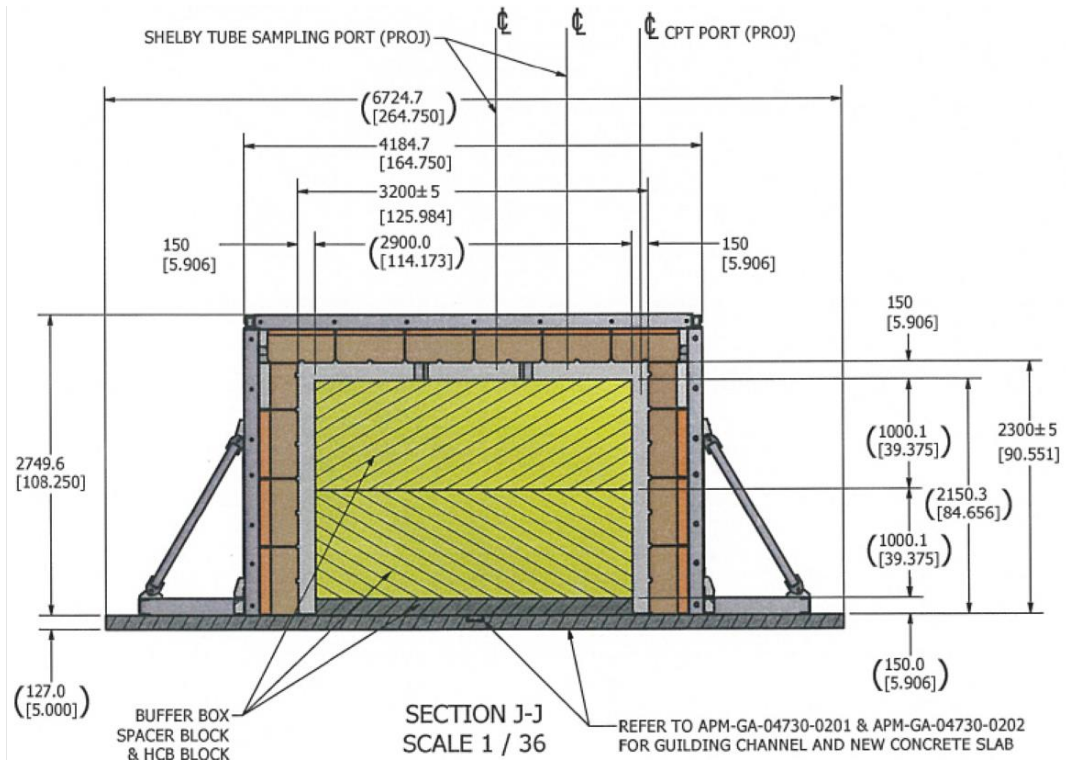
Figure 3-4: Mock Emplacement Room Section View and Dimensions (Ref. APM-GA-04730-0204 R000)

Figure 3-5: Mock Emplacement Room

3.4.1.2.2 Observation/Inspection Room

Inside the mock emplacement room, an observation/inspection room (Figure 3-6, informally referred to as the aquarium) was designed and built to allow for observation of the distribution of the gap fill material as the MER is being filled. This room is made from structural steel to support GFM loads and acrylic wall panels to allow observation of the GFM as it is delivered into the MER. It is dimensionally identical to 3 rows of buffer boxes and is installed at the back of the mock emplacement room. Access to the room is through the back of the mock emplacement room.

Figure 3-6: "Aquarium" From the Entrance to Mock Emplacement Room

3.4.1.2.3 Buffer Box Delivery Equipment

The buffer box delivery equipment (Figure 3-7 and Figure 3-8) is a modified electric Versa Lift 25/35 lift truck with a custom end attachment specifically designed to handle buffer box assemblies and a custom designed and built mast to fit inside the mock emplacement room. The current emplacement room is conceptual and generic in size to deal with both potential Canadian geospheres for a deep geological repository. As such, there was no intent at this stage to custom design a specific piece of production ready equipment to demonstrate the buffer box delivery concept. The initial plan was to build and test the custom attachment that can be used with a conventional forklift to pick up and place buffer boxes. Once the custom attachment had been validated, the NWMO would source a vehicle with load capacity and dimension that could fit within the constraints of the mock emplacement room. The custom attachment would be fitted to that vehicle, and this would become our emplacement machine. A review for a vehicle was conducted and some suitable mining vehicles were identified. This review also found that the NWMO's existing Versa Lift 25/35 only needed a shorter mast to fit inside the emplacement room. Purchasing or renting the mining vehicles would have been at a significant cost when compared to replacing the existing Versa Lift mast with a shorter one, so the decision was made to design and build a shorter mast for the Versa Lift.

The custom end attachment features include three 16-inch-wide, adjustable/removable tines with independent hydraulic load levelling. It has Inflatable air bags that apply a compressive load to the buffer box assembly as a countermeasure against cracking and to help with retrieval. The attachment was designed and built with flexibility in mind to test for different configurations. The reference design relies on lifting the buffer boxes with 3 tines, but future testing and optimization may try to reduce that to only 2 tines. This would reduce the number of filler blocks required and improve delivery times. The inflatable airbags apply a compressive load of 1000 kg to the ends of the buffer box assembly. This load helps keep the bentonite blocks in compression (HCB in tension can influence the development of cracks), depending on the position of the tines, but more importantly, prevents the HCB from separating should there be a crack or a break.

Given the high radiation fields in the real DGR, the intent was to demonstrate buffer box delivery remotely. To help with this, the Versa Lift and attachment functions are remote controlled. The clearance between the room walls and the attachment is minimal, making driving the equipment straight without contacting the walls difficult. As such, the Versa Lift was modified with sensors and can self-steer down the length of the emplacement room. It can also sense when it is approaching the end of the room, or an object – floor spacer blocks or an already placed buffer box. These features allow us to position the buffer box as close as possible with minimal manual positioning refinement required. The refinement is necessary because the precision of the Versa Lift is not sufficient for current placement requirements and was deemed to be suitable given the goal of the emplacement trial. The aforementioned is prototype equipment for demonstration only and is not intended to be used in the real DGR, where precise emplacement equipment with autonomous or remote-controlled positioning refinement will be used.
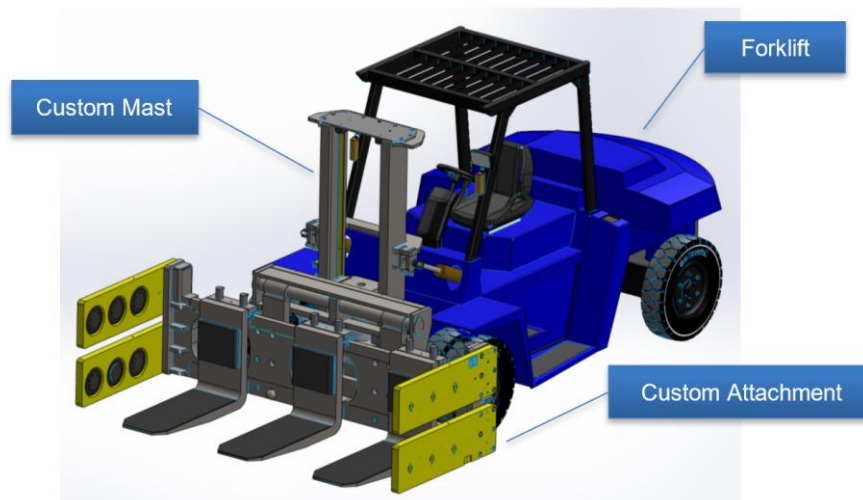
Figure 3-7: Buffer Box Delivery Equipment (drawing)

Figure 3-8: Buffer Box Delivery Equipment

3.4.1.2.4 Brick Delivery Equipment

Backfilling the floor and pocket filler bricks is not considered high-risk to this concept and as such, is completed with relatively simple manual loading equipment. The manual equipment utilizes a tray and push mechanism (Figure 3-9) to load the filler block into the pocket, either on the floor or the buffer box. A filler brick is loaded onto the tray and the equipment moves in front of the opening. The tray is then adjusted via linear actuator up or down and by manual hand crank left or right. Once aligned, the brick is pushed into position.

The push bar keeps the block inside the pocket while the slip skid is retracted. A small vacuum lift will be used to lift and place the filler blocks into the brick filler tooling and place spacer blocks on the floor for the bottom layer of the Buffer Box assemblies.
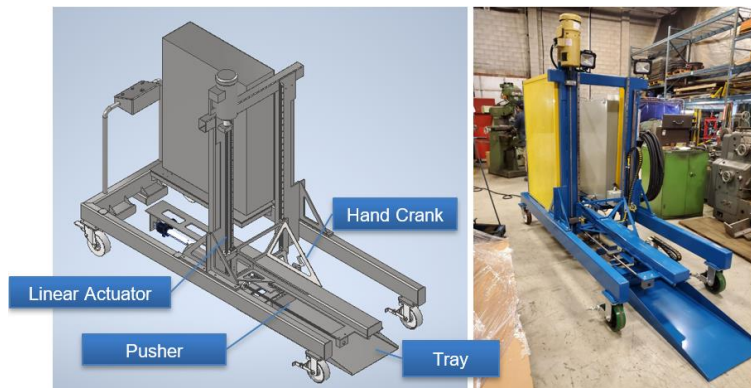
Figure 3-9: Brick Delivery Equipment

3.4.1.2.5 Gap Fill Material Delivery Equipment

The gap fill material delivery equipment (Figure 3-16) was commissioned at the start of the emplacement trial. The equipment travels into the emplacement room and places gap fill material in the space between the buffer boxes and the interior walls and ceiling of the mock emplacement room.

The gap fill delivery equipment is a complex piece of equipment with many systems. Several tests were conducted, and small-scale prototypes built and tested leading to the development of a full-scale piece of equipment.

Initial testing involved understanding the characteristics of gap fill material and which methods are suitable to increase density. Gap fill material was compressed with hydraulic rams (Figure 3-10) and vibrated (Figure 3-11) to assess compaction and 'bridging' of the material in small spaces, i.e., what would be expected in the narrow sections of the emplacement room.
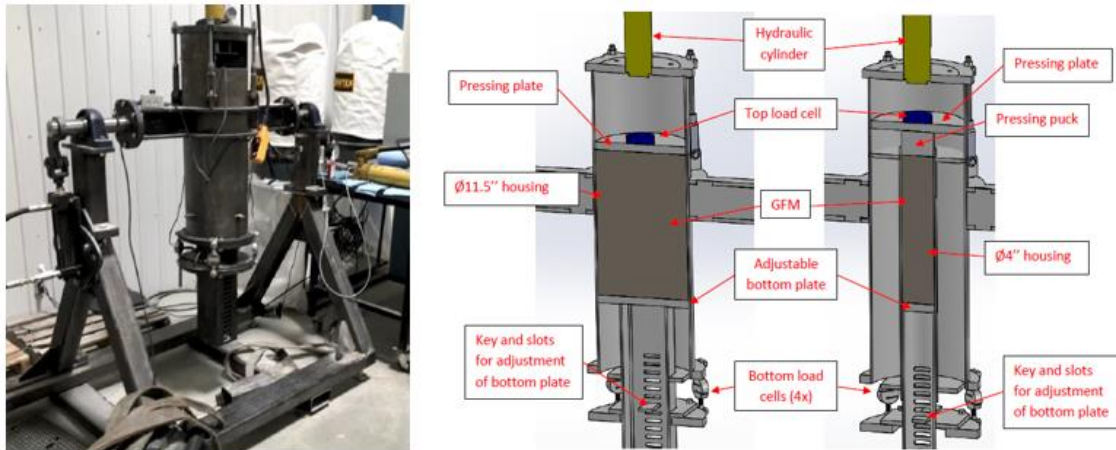
Figure 3-10: GFM Compression Testing

Figure 3-11: GFM Vibration Testing

Building on the preliminary testing, prototypes were built to assess the delivery performance for both the vertical and horizontal voids between the buffer boxes and the mock emplacement room (Figure 3-12). It was found that for the vertical voids, vibration alone was suitable for achieving dry density requirements and a combination of compression and vibration was needed for the horizontal portion of the room. Additionally, given the height constraints of the room, the ability to get the gap fill material from the hopper to the screws on top was identified as a risk and a prototype was built and tested to verify the concept before building the real equipment.

Figure 3-12: Vertical and Horizontal GFM Void Prototypes

The full-scale gap fill material delivery equipment is a complex piece of equipment composed of several subsystems. An overview of the system as it is setup in the NWMO Test Facility is shown in Figure 3-13.
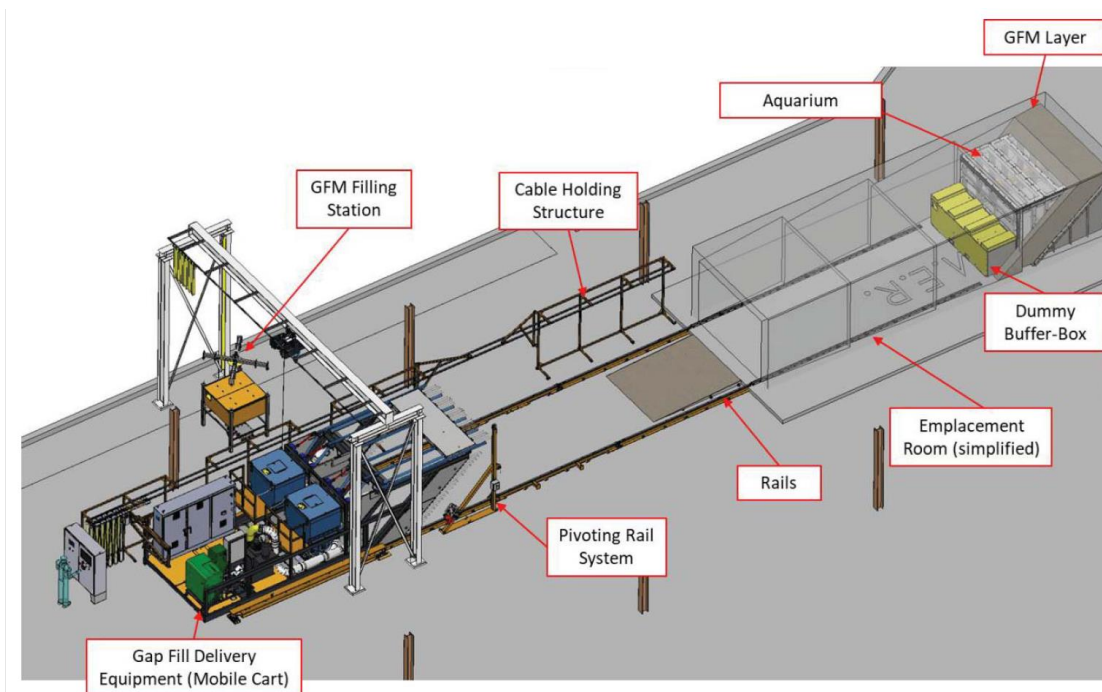
Figure 3-13: Gap Fill Delivery Equipment Layout

The main piece of equipment is the mobile cart (Figure 3-14), which contains the GFM feed, vibration, compressed air, dust collection, electrical panel, motive, and the sensor systems. The GFM feed system consists of two large hoppers, elevating screws, and the feed screws. This is the system that delivers the GFM into the vertical and horizontal voids in the emplacement room. The vibration system is a series of vibrating rods used for densifying/compacting the GFM in both the vertical and horizontal voids. The vibrating rods are driven by pneumatic vibrators that are powered by the compressed air distribution system. The mobile cart also has a contained dust collection system to minimize airborne gap fill material dust during the filling sequence in the room. This dust collection system also controls the amount of airborne gap fill

material dust when filling the hoppers. The electrical panel houses all the electrical systems on the cart. The Motive Power System allows the mobile cart to advance and/or reverse in and out of the emplacement room. Given the tight tolerances inside the emplacement room and the overall length of the mobile cart, the mobile cart travels on rails to ensure the GFM feed and vibration systems fit into the void between the buffer boxes and the interior surface of the mock emplacement room. Sensors are located throughout to measure various parameters related to the amount of gap fill material placed and the position of the mobile cart.
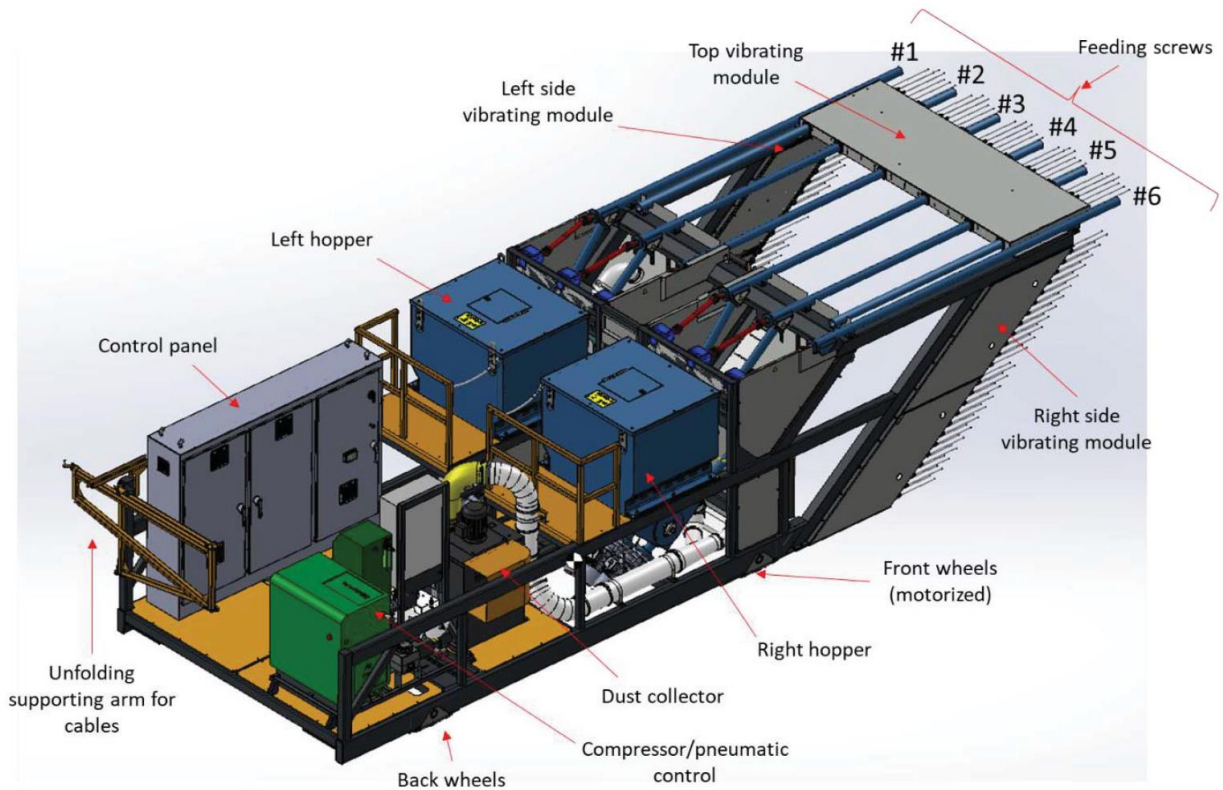
Figure 3-14: Gap Fill Delivery Equipment Mobile Cart

The gap fill delivery mobile cart also relies on several supporting systems (Figure 3-15). These are a weighing station, a fill station, the main panel, a cable management system, and a pivoting rail to allow access to the room for the buffer box and brick delivery equipment.

The weighing station is used to measure the mass of the material delivered. This value, along with the volume of the material added and measured by 3-D scanning, was used to calculate the density of the placed gap fill material. The fill station consists of a separate loading hopper and overhead crane to load the hoppers on the mobile cart in a controlled and safe manner. The main panel controls the gap fill delivery equipment and provides all systems feedback to the operator to control the filling sequence. A cable management system manages the power and communications cables between the main control panel and the mobile cart as it travels in and out of the emplacement room. Finally, the rail system has a pivoting rail that lifts when the mobile cart is parked to allow for the buffer box and brick delivery equipment access to the emplacement room.

The gap fill delivery equipment has alarms to indicate to personnel in the area that the equipment is operating. There are emergency stops located throughout to shut down the system in the event of an emergency. All motorized drives and potential hazards are guarded to ensure safe operation of the equipment. A more comprehensive description of the gap fill delivery equipment (Figure 3-16) and its operation can be found in the operating manual.
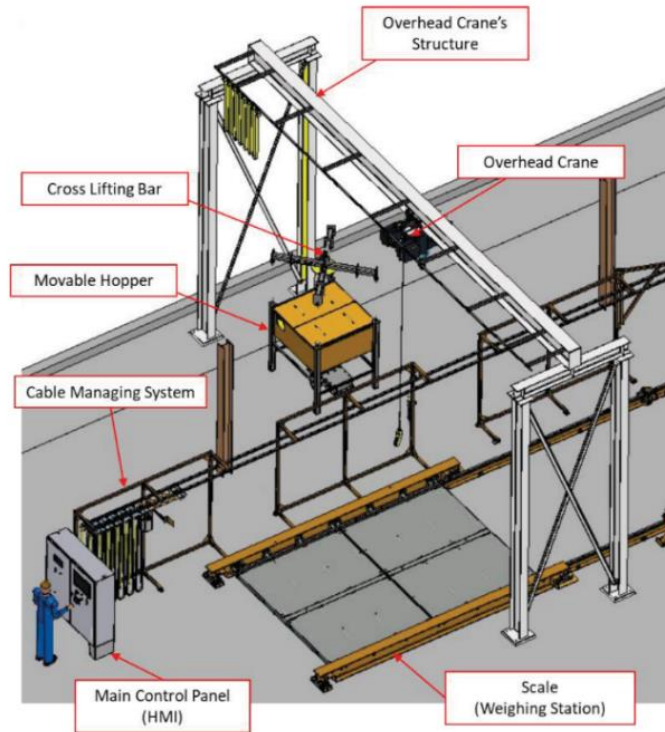
Figure 3-15: Gap Fill Delivery Equipment Supporting Systems

Figure 3-16: Gap Fill Material Delivery Equipment

3.4.1.3 Emplacement Trial Test Setup

The emplacement test was performed in the NWMO Oakville Test Facility. In the year prior to the emplacement trial, a test was performed to remove some of the top roof sections of the mock emplacement room. This was to help develop a procedure to remove the roof sections safely and accurately in a manner that would least disrupt the as-placed gap fill material.
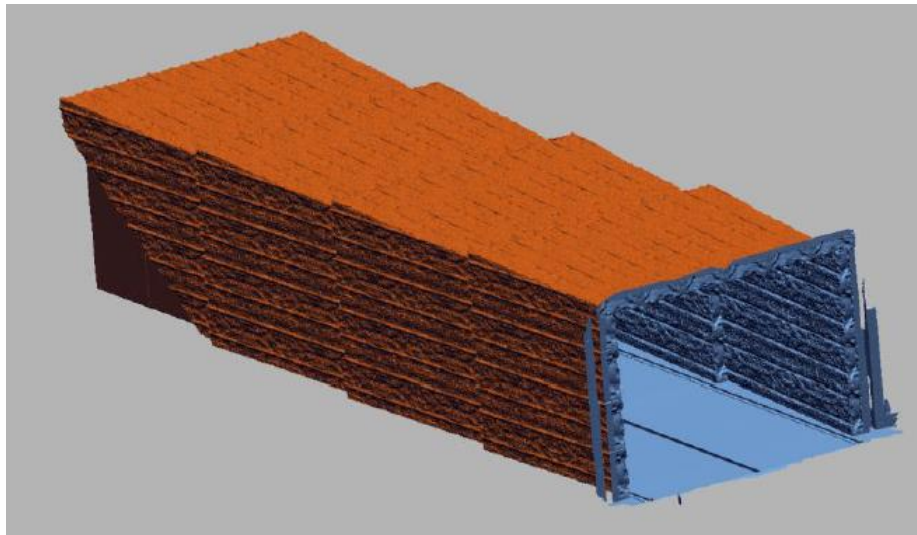
Figure 3-17: Mock Emplacement Room Interior Scan

Additionally, all gaps between the polyurethane panels were filled or sealed to prevent gap fill material from flowing between panels. At this stage, the room was 'design frozen' and in May 2021 the interior volume of the mock emplacement room was scanned to measure the internal volume (Figure 3-17). This measurement was critical since one of the methods to calculate the

gap fill material density was to measure the volume and the mass of the material placed. The aquarium was also scanned prior to being installed inside the mock emplacement room.
The two, copper-coated used fuel containers that were used in the trial were inspected prior to assembly inside buffer boxes. This was to identify any damage or areas of concern on the copper coating so that they are not attributable to damage because of emplacement activities.
In the week prior to the trial, the floor area around the emplacement room and gap fill delivery equipment was cleaned and cleared. The mock emplacement room was cleaned of gap fill material from previous testing and the line follower tape for the buffer box delivery equipment was cleaned and checked against a laser level for straightness. To monitor the humidity and temperature, a hygrometer (Traceable Model 6520) was installed inside the emplacement room. Three NIKON DSLR cameras were set up overhead in the facility to take pictures once every minute for the duration of the trial. Two were setup on roof trusses at the east (Figure 3-18) and west (Figure 3-19) ends of the warehouse space, and one on a south (Figure 3-20) column to capture all movements during the trial. Three GoPro cameras were setup inside the aquarium to capture video footage of the gap fill material being delivered (Figure 3-21).

Figure 3-18: East Overhead Camera

Figure 3-19: West Overhead Camera

Figure 3-20: South Overhead Camera
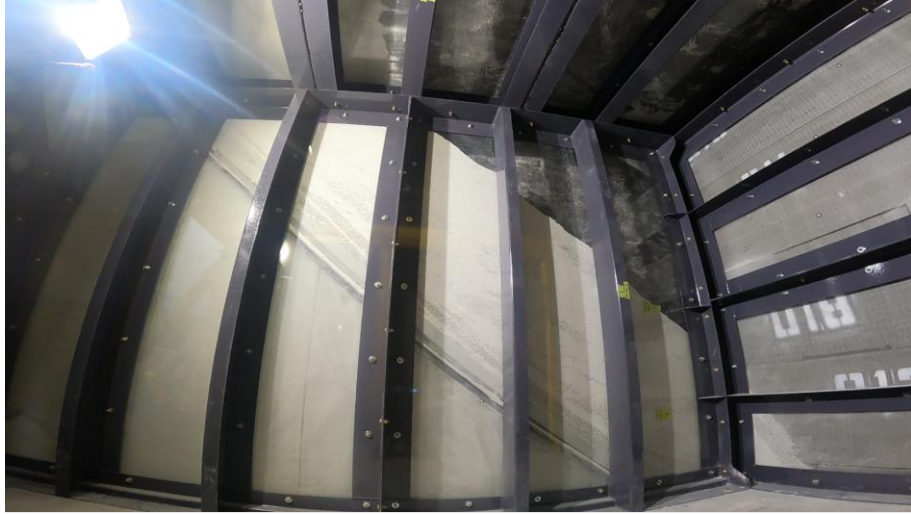
Figure 3-21: GoPro Camera View Inside Aquarium

3.4.1.4 Emplacement Trial Results and Discussion

The emplacement trial started on April 18, 2022, and finished on April 23, 2022. The placement of all highly compacted floor spacers, floor and pocket filler bricks, and buffer box assemblies were completed by Ancam Solutions. Similarly, the operation of the gap fill delivery equipment and placement of gap fill material was completed by Novika staff. All steps were completed under NWMO supervision where applicable.

As stated in section 7, the basic requirements of this test are to fill the mock emplacement with room buffer boxes with representative weight, gap fill material, and achieve an average as-placed, gap fill material dry density ≥ 1.41 g/cm^3.

Placement of the highly compacted bentonite spacer bricks was completed using the NWMO vacuum lift and then positioned manually according to the specifications of the inspection and test plan. Similarly, filler bricks for the floor and the pockets bricks were placed using the brick delivery equipment and then positioned manually. There was no issue in performing these low-risk operations. All measurements were recorded directly into the inspection and test plan document.

Five buffer boxes were assembled with cast iron plugs and two were assembled with copper coated containers, all of which were weight-representative of actual used fuel containers loaded with fuel (Table 3-2).

Table 3-2: Emplacement Trial Buffer Boxes

Buffer Box	HCB Blocks Numbers	Weight	Notes
1	018 (top) & 012 (bottom)	7307 kg	Iron plug
2	019 (top) & 011 (bottom)	7620 kg	Iron plug
3	021 (top) & 027 (bottom)	7267 kg	Copper coated container
4	029 (top) & 001 (bottom)	7602 kg	Copper coated container
5	020 (top) & 013 (bottom)	7135 kg	Iron plug
6	003 (top) & 016 (bottom)	7697 kg	Iron plug
7	023 (top) & 028 (bottom)	7298 kg	Iron plug

Prior to emplacement, each buffer box was inspected, and notes, sketches and photos were taken to document the condition of each buffer box. Buffer boxes were picked up with the delivery equipment, trammed down the length of the room and emplaced. Each buffer box was positioned precisely between the gap fill delivery equipment rails and with a specified gap from the previously placed buffer box. Position dimensions were measured and recorded, and a post-emplacement inspection was performed to document the placement of each buffer box assembly. Figure 3-22 shows the position of the buffer boxes within the room. Each buffer box was scanned prior to emplacement and then placed during the post-processing of the gap fill material layer data.

Figure 3-22: Scanned Buffer Box Positions Inside Emplacement Room

The buffer box delivery equipment performed as expected (Figure 3-23 and Figure 3-24). It was modified to self-steer down the length of the room and sense an object to position itself and the buffer box before the operator placed the load. These features worked very well and simplified the operations of buffer box placement. Originally, the intent was to remotely position and place the buffer box to replicate how it would have to be done in the real repository. However, precision limitations of the Versa Lift 25/35 forklift prevented achieving this. It is important to note that the buffer box delivery equipment is based off a conventional heavy forklift (Versa Lift 25/35) and that the forklift was never designed to have the precise movements that were required for placement of buffer boxes in this trial. So as a result, staff had to fine-tune the final placement position of the buffer box assembly, which involved operator skill to advance, and side shift the controls to position the buffer box within the required tolerances. Although manual fine-tuning was necessary, it was not unexpected, and we were able to demonstrate that placement of buffer boxes is feasible. Specialized equipment would be required should the design constraints remain the same in the future underground emplacement room design.

Figure 3-23: Buffer Box Delivery Equipment Ready for Delivery

Figure 3-24: Buffer Box 1 Inside Mock Emplacement Room

As with the buffer box delivery equipment, the gap fill delivery equipment also performed as expected. Four layers of gap fill material were delivered following the filling procedure for the gap fill delivery equipment described in the operating manual. The first layer of material is approximately 1.25 m in length with each subsequent layer approximately 1 m. To measure the amount of gap fill material delivered, the gap fill delivery equipment was weighed before and after each layer. After each layer was delivered, the filled surface was scanned and this surface was merged with the volume scans of the empty room, the aquarium, and the buffer boxes as applicable to establish the volume occupied by the gap fill material (Figure 3-25 and Figure 3-26). With the volume and the mass of the material placed, the density of the fill was calculated. This was completed for each layer delivered and an average dry density was calculated for all four layers of the placed gap fill material.
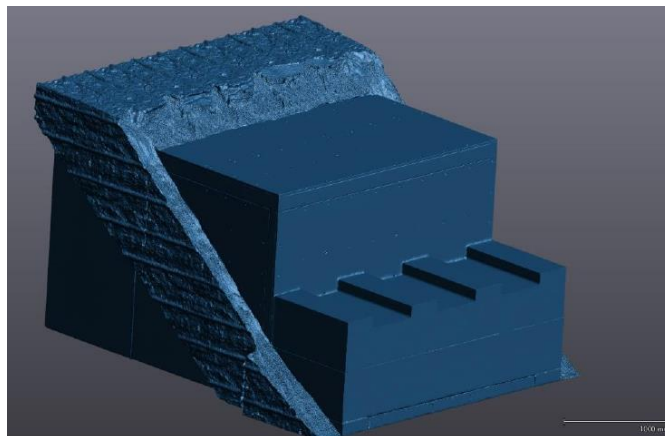
Figure 3-25: First Gap Fill Material Layer Merged Volume Scan
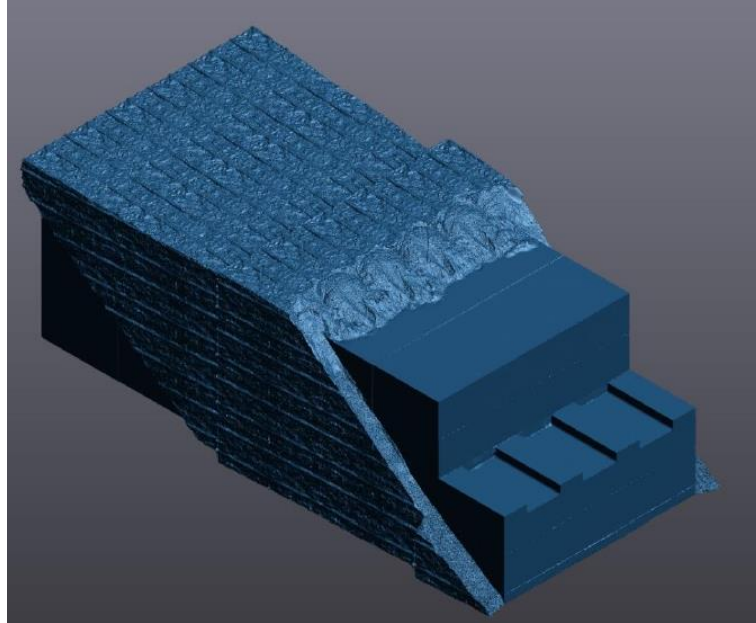
Figure 3-26: Completed Trial Merged Volume Scan

Once the trial was completed, the emplacement room roof panels directly over the placed gap fill material were removed for observation and further scanning (Figure 3-27). The top surface scan was compared against the scan of the empty room volume to help determine if the top surface was completely filled. The scan identified areas that the gap fill material did not reach, and which were not easily visible by the naked eye. These voids were included when calculating the average dry density.

Figure 3-27: Emplacement Room Top Panels Removed

Further to considering the voids identified by the top surface scan, the amount of gap fill material that fell into the gaps between buffer boxes was estimated as well. When the trial was deconstructed and the buffer boxes were removed, it was visible where the gap fill material was and from this, an amount of gap fill material that went in between the boxes was estimated and this amount was considered when calculating the final dry density (Figure 3-28).

The final dry density calculated was 1.457 g/cm^3 with an uncertainty of approximately ±0.008 g/cm^3. Therefore, it can be concluded that the gap fill delivery equipment was successful in achieving the as-placed dry density requirement of ≥1.41 g/cm^3.

Figure 3-28: Indication of Gap Fill Material Between Buffer Boxes

The overall estimated dry density of all the placed bentonite buffer materials was calculated to be 1.63 g/cm^3. This value is determined by averaging the measured gap fill material dry density and the air gap adjusted dry density achieved for the highly compacted bentonite during the emplacement trial.

3.5 SITE AND REPOSITORY

3.5.1 Non-Nuclear Materials Handling Study

It was identified that a non-nuclear materials handling study was required in order to determine the demand on the security checkpoint gates, the requirements for the Service Shaft, and the overall traffic flow on site at the Revell Site. There are two parts to this study, a surface materials handling study, and Service Shaft study reviewing the materials sent underground via the Service Shaft. The results of this study for the Revell Site are equally applicable to the South Bruce Site.

3.5.2 Loaded Buffer Box (LBB) Transfer Cask Equipment: Part I Study

The purpose of this study is to assess three transfer equipment concepts for the LBB Transfer Cask (rubber tired Towed Cart, Automated Guided Vehicle (AGV) Rail Cart, and Self-propelled Modular Transfer Equipment) and select the preferred concept. The LBB Transfer Cask transfer

equipment concept development includes consideration of processes, equipment, and comparison to commercially available solutions.

Concept 1 (rubber tired Towed Cart) and concept 2 (AGV Rail Cart) were assigned high scores. The difference in the scores of the two concepts is not sufficient to eliminate either option or make a decision at this time. As a result, Hatch and NWMO have agreed that further investigation is required under the next stage of design of this study before a concept can be selected.

3.5.3   Site Framework Layouts – Crystalline & Sedimentary Site

In general, the updates include the following:

1. Updates to the overall site layout to fit the Revell Site and the South Bruce Site land assemblages.
2. Coordination with the Used Fuel Packaging Plant (UFPP) design.

The original adaptive facility layout was updated based on the following information:

1. Site topography and existing local infrastructure.
2. Regional water flow and on-site water flow (i.e., pond locations and number of discharge points).
3. Updates to UFPP design.
4. Preliminary input from facility systems.
5. On-site vehicle and pedestrian traffic considerations.

3.5.4   Underground Services Area and Amenities: General Arrangement Drawings

General arrangement drawings were prepared for various underground amenities and infrastructure including:

1. 25 and 100 worker refuge stations
2. 100 worker lunchroom and office area
3. Typical Latrine
4. Battery Swapping Station
5. Explosives & Detonator Magazines
6. Rock-breaker Station
7. Domestic Waste Handling Facility
8. Concrete Receiving Station and Flush Water Sump
9. Road Ballast Crushing Station
10. Mobile Equipment Wash Bay
11. Various maintenance shops: Electrical, Lube Bay, Mobile Equipment, Emulsion Cassette, Welding bay and Fixed Plant Mechanical
12. Loading pocket feeder and conveyor
13. Construction material storage bay

3.5.5 Headframe Construction Type: Literature Review

A literature review was conducted as part of the trade-off study comparing a reinforced concrete headframe to a steel headframe structure. The purpose of this was to determine the estimated life for both reinforced concrete and steel. Initially, this literature review examines examples of existing reinforced concrete and steel headframes in addition to other structures. Then, the study investigates the causes of degradation of steel and reinforced concrete structures, and the measures that can be considered to achieve a durable design such as by retrofitting of the deteriorated parts. In addressing the full life cycle of the structures, recycling methods for both options were detailed. Finally, both reinforced concrete and steel headframe structures were compared by considering parameters such as durability, fire resistance, maintenance, repair, and sustainability.

This study finds that concrete headframes can have an expected design life of 150 years. Minimal maintenance is expected to be required for the concrete shell if the design provides adequate cover to reinforcement and limits the maximum crack width to 0.3 mm. Fibre reinforced polymer (FRP) as a replacement for steel reinforcement should be considered if a design life of more than 150 years is required. A concrete mix designed for durability should also be utilised. The structural steel inside the concrete headframe will need to be painted every 15 years.

The steel headframe will also have an expected design life of 150 years provided the corrosion protection system is maintained every 15 years. A duplex corrosion protection system (galvanizing plus paint) is recommended. It is anticipated that the side cladding and roof sheeting will need to be replaced every 30 to 50 years.

3.5.6 UG Repository Layouts for 5.5M Bundles – Crystalline & Sedimentary

Preliminary underground repository layouts for the two potential site locations were developed based on updated understanding of the site-specific considerations:

Revell Site (Crystalline)

- Geoscience information including the Inferred Fracture Zone (IFZ) model based on drilling results.

South Bruce Site (Sedimentary)

- NWMO owned or optioned land assemblage
- Cobourg formation target elevation

3.5.7 Aboveground Amenities: Design Requirements Document

The purpose is to specify the design requirements of the Aboveground Amenities. Most of the requirements will apply to the operational phase, however, additional requirements for site preparation, construction, monitoring, and decommissioning are also listed.

This study defines the requirements for works related to the DGR Project within the scope of the DGR Surface Facilities. Also, other Design Requirements documents are being considered for

the requirements of associated systems (e.g., building electrical systems, fire protection systems, heating systems, etc.). The provisions of the Design Requirements document apply to:

1. Equipment and building foundations.

2. Building structural frames constructed of reinforced concrete or structural steel.

3. Above ground facilities (or surface structures buried wholly or partially in the ground) constructed of reinforced concrete or steel.

4. Stairs, ladders, platforms, and walkways.

5. Bridge crane, monorail, and other crane or hoist structures.

3.5.8 Best Management Practices for Mitigation of Nuisance Effects

An evaluation was performed of best industry practices for construction and operations of the DGR facilities that would reduce nuisance effects, including noise, dust, vibration, visual impact, light and odour. A gap analysis was completed to evaluate where current design and construction concepts could be improved to reflect best management practices for nuisance mitigation.

This work is preliminary and was based on a review of regulatory standards and guidelines along with a review of publicly available information from other projects. It was focused on potential effects on human receptors, and indirect effects are yet to be considered.

3.5.9 Non-Nuclear Waste Management Facilities

The DGR Project will have a non-nuclear Waste Management System in place to manage waste generated onsite. The design of the non-nuclear Waste Management System includes considerations for the segregation, handling, storage, and disposal of the waste generated. Additionally, minimization of waste through reuse, repair, and recycling is considered where practical.

To develop the design, non-nuclear waste was identified and categorized into eight separate waste streams generated from the surface and underground DGR:

1. Domestic Waste

2. Industrial/Process Waste

3. Recyclable Waste

4. Excess Soil/Treatment Solids

5. Stabilized Sewage Sludge

6. Reusable/Repairable Equipment and Materials

7. Compostable Waste

8. Hazardous Waste.

As the DGR facility continues to be developed, additional information will become available to refine this design.

3.5.10 Water Storage, Treatment, and Distribution System Design

The water demand for the Domestic and Service Water Systems for the surface and underground facilities was updated based on recent studies; and a base case of equipment was defined and sized, including piping, water and sewage treatment equipment, pumps, storage equipment, and building footprints. The update, which placed an emphasis on recycling as much of the water as possible, was carried out for the following treatment, storage, and distribution systems:

1. Raw Water System;

2. Domestic Water System where water is treated to potable levels in accordance with the Ontario Safe Drinking Water Act;

3. Service Water System for non-potable water that is used for general services and operations, including industrial processes, facilities, and installations on the surface and underground;

4. Industrial and DGR Drainage Systems;

5. Fire Water System; and

6. Domestic Sewage System.

3.5.11 Service and Stormwater Management Systems

For the design of the Service Water and Stormwater Management Systems, the following were reviewed and assessed:

1. Existing and pre-development site conditions;

2. Determination of post-development catchment areas and associated peak flows based on the site framework layout, finished grading design, preliminary road design, and

3. Hydraulic calculations for the sizing of drainage infrastructure (i.e., ditches, culverts, storm sewers, catch basins).

The drainage concept ensures there is adequate drainage for stormwater runoff while considering all potential construction and operational concerns of proposed infrastructure. This is achieved through incorporating a drainage concept to control surface water runoff by overland flow into storm sewers, catch basins, manholes, culverts, and open channels to a stormwater management pond and associated engineered wetland. This concept ensures ponding and headwater elevations of water shall be below elevations that could potentially impact proposed infrastructure such as site roads and buildings. The proposed stormwater management infrastructure has sufficient capacity to store and release the post-development runoff to pre-development conditions. The discharge will not cause any water quality, flood hazards, or erosion concerns.

3.5.12 Compressed Air System

The purpose was to review, update, and advance the existing calculation for the Compressed Air System. The Compressed Air System includes the following subsystems:

1. Breathing Air Systems that provides purified Breathing Air to the UFPP at the surface and to each of the refuge stations underground.

2. A Service Air System that provides Service Air to a range of facilities and equipment at the surface and underground.

Also, this study was performed to document the latest design of the Compressed Air System for the DGR and to provide a description of the air compressors and the drying, storage, purification/filtration, and distribution systems in the Revell Site. The design was advanced based on new information from on-site air consumers and processes to include major mechanical equipment, piping, and buildings. Additionally, recommendations were provided for future work to further develop the system design.

4 ENGINEERED BARRIER SYSTEM

The engineered barrier system (EBS) is a major component of the underground design. It includes the used nuclear fuel bundles, container (Figure 4-1), buffer and sealing systems. Summaries of these activities are provided in the following sections. Wasteform durability is discussed in Section 6.2.
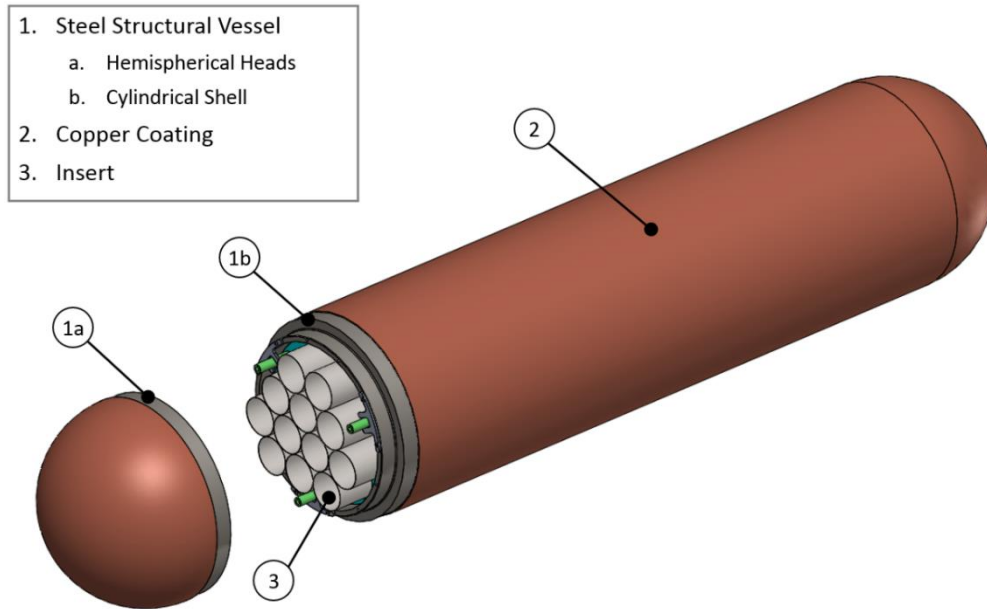
Figure 4-1: Illustration of Used Fuel Container Reference Design

4.1 USED FUEL CONTAINER

In 2022, the NWMO continued the execution of the Proof Test Program to validate the reference (conceptual) design of the Used Fuel Container (shown in Figure 4-1). The demonstration of UFC manufacturing/inspection/testing via NWMO's Serial Production project is ongoing. Progress in UFC proof testing, R&D, and design analysis activities are summarized in the subsections below.

4.1.1 UFC Design

In 2022, the NWMO design team worked toward concluding the structural integrity evaluations on the steel structural vessel of the UFC. Additional loading conditions were identified, which led to the scope expansion of the UFC design qualification program. New calculations were performed and issued to cover conditions such as non-uniform external pressure, significant uneven buffer swelling, plastic ratcheting under 10 cycles of glacial load, and beyond design basis unilateral compression. The last major structural evaluation, the container drop and impact analysis, was also progressing as planned. At the same time, copper coating mechanical performance evaluation was launched. Copper coating delamination, reduction of thickness due to mechanical processes, and cracking were identified as the main areas of investigation. Analysis and testing work was initiated to address these issues.

As an action item from a meeting held with the CNSC in 2021, the NWMO design team initiated the preparation of a white paper to present a systematic approach in the development of the design criteria for disposal containers. The white paper is intended to *i)* describe the design philosophy of the UFC; *ii)* provide explanations on how NWMO's UFC design criteria were established; and *iii)* identify the contents of the existing standards that can be applied to the UFC construction. This work progressed steadily with the advance of the Proof Test Program.

4.1.2   UFC Serial Production Project

4.1.2.1   Fabrication of UFC Prototypes

In 2022, the NWMO continued the execution of its UFC Serial Production project to achieve its target of manufacturing 17 UFCs. In this past year, an additional 10 UFCs were completed (similar to the first unit completed in 2021 shown in Figure 4-2). The remainder of the total of 17 UFC's are in various stages of assembly as summarized in Table 4-2. Ongoing feedback from Serial Production and parallel R&D programs is allowing further optimization of select manufacturing processes which are being implemented in subsequent UFC units.

Figure 4-2: Used Fuel Container Reference Design – Serial Production Unit #1

Throughout the Serial Production project in 2022, drawings, manufacturing, inspection & test plans, and related documentation such as procedures and inspection report templates were created and revised to support machining, welding, copper coating, and non-destructive examination (NDE) work on UFC components.

In 2021, an alteration was made to the plan for fabrication of 5 of the 17 UFCs for Serial Production. This change was driven by the need to develop resilience in the supply chain for the production of electrodeposited coatings. In this regard, a new Vendor with expertise in the application of electrodeposition of copper coatings to cylindrical geometry was contracted for the supply of copper coated UFC shell components. In comparison to the "Reference Assembly Method" (copper coated lower assembly + copper coated upper head) the "Alternate Assembly Method" would have 3 copper coated components for assembly: lower head, shell and upper

head. The Alternate Assembly Method necessitates the application of cold spray coating to both the lower and closure weld zones. A comparison between the reference assembly method and alternate assembly method is presented in Table 4-1.

In 2022, a need to conduct additional external pressure testing was identified. Two additional UFCs were built without copper coating to support the testing work (steel structural vessel portion). One of the existing planned UFCs with copper coating will be identified to support the testing work (with copper coating).

The UFC completion status at the end of 2022 of the planned total of 17 Serial Production UFCs is shown in Table 4-2, broken down by major components. Moving forward, a significant effort will be spent in completing the remaining UFCs, targeted by mid-2023.

Table 4-1: Reference vs. Alternate Assembly Method Comparison

Reference Assembly Method	
Reference Assembly Method Schematic	**Steps:** 1. Steel Components • 2 Hemi-heads • Shell 2. Weld Lower Assembly 3. Copper Coating • Lower Assembly • Upper Hemi-head 4. Closure Weld 5. Copper Coating over Closure Zone Photo of Reference Assembly Method at Step 3
Alternate Assembly Method	
Alternate Assembly Method Schematic	**Steps:** 1. Steel Components • 2 Hemi-heads • Shell 2. Copper Coating • Lower Hemi-head • Shell • Upper Hemi-head 3. Lower Assembly Weld 4. Copper Coating over Lower Assembly Weld 5. Closure Weld 6. Copper Coating over Closure Zone Photo of Alternate Assembly Method at Step 2

Table 4-2: 2022 UFC Serial Production Status (Cumulative)

UFC No.	Reference Assembly Method		
	Copper Lower Assembly	**Copper Upper Hemi-head**	**UFC Assembly**
1	🟩	🟩	🟩
2	🟩	🟩	🟩
3	🟩	🟩	🟩
4	🟩	🟩	🟩
5	🟩	🟩	🟩
6	🟩	🟩	🟨
7	🟩	🟩	🟨
8	🟩	🟩	🟨
9	🟩	🟩	🟥
10	🟩	🟩	🟥

UFC No.	Alternate Assembly Method			
	Copper Lower Hemi-head	**Copper Shell**	**Copper Upper Hemi-head**	**UFC Assembly**
11	🟩	🟩	🟩	🟩
12	🟩	🟩	🟩	🟩
13	🟩	🟩	🟩	🟩
14	🟩	🟩	🟩	🟨
15	🟩	🟩	🟩	🟩

UFC No.	External Pressure Testing (Steel Structural Vessel)			
	Steel Lower Hemi-head	**Steel Shell**	**Steel Upper Hemi-head**	**UFC Assembly**
16	🟩	🟩	🟩	🟩
17	🟩	🟩	🟩	🟩

Legend	Completed	In Process	Not Started
Definitions	All work complete.	Work has started on the base material or assembly.	Work has not started on the base material or assembly.

4.1.3   UFC Copper Coating Development

4.1.3.1   Electrodeposition Process Development

The electrodeposition of copper from a sulfuric acid based chemistry has been used extensively and has been in service for many years in the industry. When coupled with the use of a pulse-reverse applied current, the ability to deposit smooth uniform thick copper coatings with good physical properties may be realized. Process development at prime contractor Integran Technologies, Inc. ("Integran", Mississauga, Ontario, Canada) were initiated leading to a copper material that was sufficiently pure (> 99.9%) and ductile (> 10% elongation). Following this, scale-up was performed with UFC components. With extensive optimization, the process was demonstrated to be scalable and soon after deemed ready to resume Serial Production in 2021 to which nine upper hemi-heads and five lower assemblies were successfully produced and submitted for component level machining.

In parallel to serial production in 2021, another refinement of processing parameters was sought with the objective of improving robustness with respect to deposit quality, additive control and copper purity. In early 2022, the refined process parameters were scaled and further trialed in the production tanks on a coupon level (i.e., pipes) using the current production tanks. The results were indicative of improved surface quality and purity (see Table 4-3).

Table 4-3: Purity Results from Refined Processing Parameters Using "Quality Assurance" Coupons.

Sample Type	Cu (> 99.9 %)	S (<0.0012 %)	P (<0.010 %)	C (<0.005 %)	O (<0.010 %)	H (<0.001 %)
Short Pipe	>99.9	0.0001	<0.005	0.0008	0.0009	0.0002
Long Pipe	>99.9	<0.0001	<0.005	0.0007	0.0005	0.0001

Following confirmation of scalability, the newly refined process was implemented at the UFC component level (i.e., upper hemi-heads and lower assemblies) to complete the remainder of the Serial Production units at Integran including five additional upper hemi-heads and five lower assemblies (see **Error! Reference source not found.** and **Error! Reference source not fo und.**, respectively).

In general, the outcome of the Serial Production project was considered to be a success with minor opportunities for improvement. One improvement in particular would be to completely eliminate the occurrence of infrequent nodules that may result in a coating defect. Other future work may include an effort to increase the plating rate, thereby reducing the processing time and improving cost effectiveness.

Figure 4-3: Copper Coated Serial Production Upper Hemi-head using Refined Acid Copper Electrodeposition Process Parameters.

Figure 4-4: Copper Coated Serial Production Lower Assembly using Refined Acid Copper Electrodeposition Process Parameters.

4.1.3.2 Cold Spray Process Development

In 2022, an additional nine UFC's were processed at the PolyCSAM Industrialization Centre (Boucherville, QC) located within the NRC facilities and operated by Polycontrols, Inc. (Brossard, QC). Of the nine, four had one closure weld zone (Figure 4-5) and, five of which had two closure weld zones (Figure 4-6) for cold spray copper application. The UFC's with two closure weld zones were those belonging to the "Alternate assembly" manufacturing method where shells were copper coated using electrodeposition and two copper coated upper hemi-heads were subsequently assembled by welding.

Figure 4-5: Copper Coated Closure Weld Zone on Reference Assembly UFC.
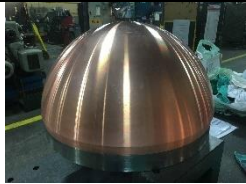
Figure 4-6: Copper Coated Closure Weld Zones on Alternate Assembly Method UFC.

The Serial Production project thus far was not without challenges. Over the course of this effort, numerous practical improvements were made to better assure the quality of the copper coating; however, some engineering efforts will be required in 2023 to resolve sensitivities to certain processing parameters, for example, stand-off distance. During the Serial Production project thus far, it was determined that stand-off distance of the cold spray gun nozzle during the laser-assisted bond layer application was a critical parameter to achieve a uniform copper bond at the steel substrate. Thus, an effort was launched to improve process control by implementing a laser tool to track stand-off distance and dynamically correct it on the robot arm. This is expected to be implemented in the first half of 2023.

4.1.4   UFC Copper Components Machining

Table 4-4 shows pictures of each component as it moves from as-machined steel condition though copper coating and final machining.

Table 4-4: UFC Copper Coated Components Stages of Manufacture

UFC Component	Copper Coating Stages		
	Steel	Bulk Copper	Machined Copper
Hemi-head			
Shell			
Lower Assembly			
Closure Zone			

In 2022, continued progress was made in developing the final machining operation applied to the UFC. After the closure weld and closure zone cold spray copper coating are completed, the copper in the closure zone must be machined to match the surrounding copper surfaces on either side (cylindrical surface of the Copper Coated Lower Assembly and spherical surface of the Copper Coated Upper Hemi-head). Some challenges were identified in the machining of the closure zone copper due to the unique characteristics of the cold spray product form (i.e., powder metallurgy for cold spray versus wrought metallurgy for electrodeposition). Optimization of machining parameters, including introduction of a blending operation and a modified machine profile are being investigated as a means to achieve the required surface roughness for non-destructive examination.

4.1.5 UFC Non-Destructive Examination

In 2022, the Non-Destructive Examination (NDE) program focused on improving volumetric flaw detection and sizing capability in the copper coating by fabrication of a custom ultrasonic probe for phased array ultrasonic testing (PAUT). Simulations of the current "flat" PAUT probe showed that a small feature (1 mm or less in diameter) is likely to go undetected – especially when located near the copper surface. For a simulated curved probe (curved in the secondary axis, as shown in Figure 4-7), the probability of detection is increased for smaller features (1 mm or less in diameter) but still challenging.
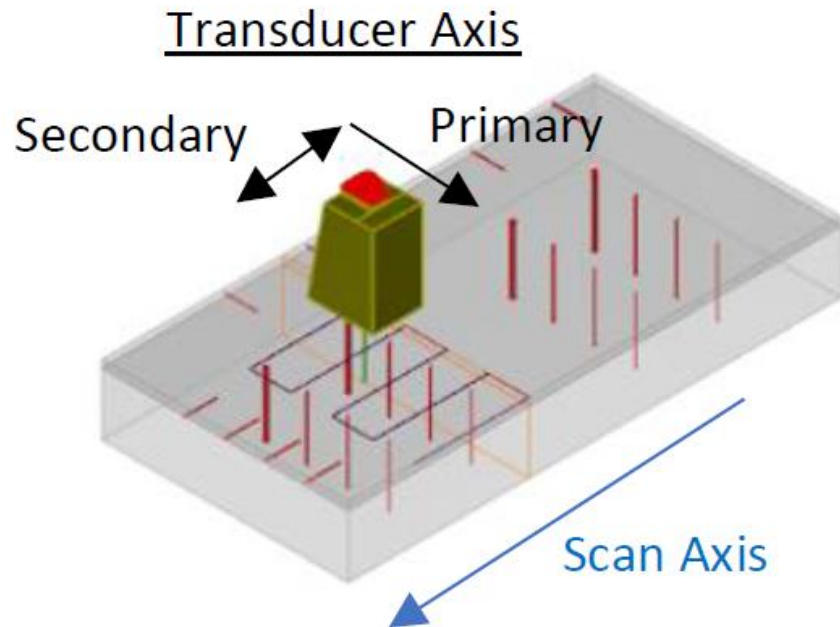
Figure 4-7: PAUT probe layout.

Improved flaw sizing is achieved by reduction of the beam diameter in the secondary probe axis (as shown in Figure 4-8). For flaw sizing, the standard "flat" probe is within +3 mm of the simulated FBH diameter (3 mm). Reduction in the beam width allows the curved probe to be within +1 mm from the simulated FBH diameter (3 mm) (see, Figure 4-9). The sizing is still limited by the UT beam width, but the reduced beam diameter allows reduction of the sizing error. The custom curved probe has been fabricated and will be used in experimental trials and UFC component inspections in 2023.
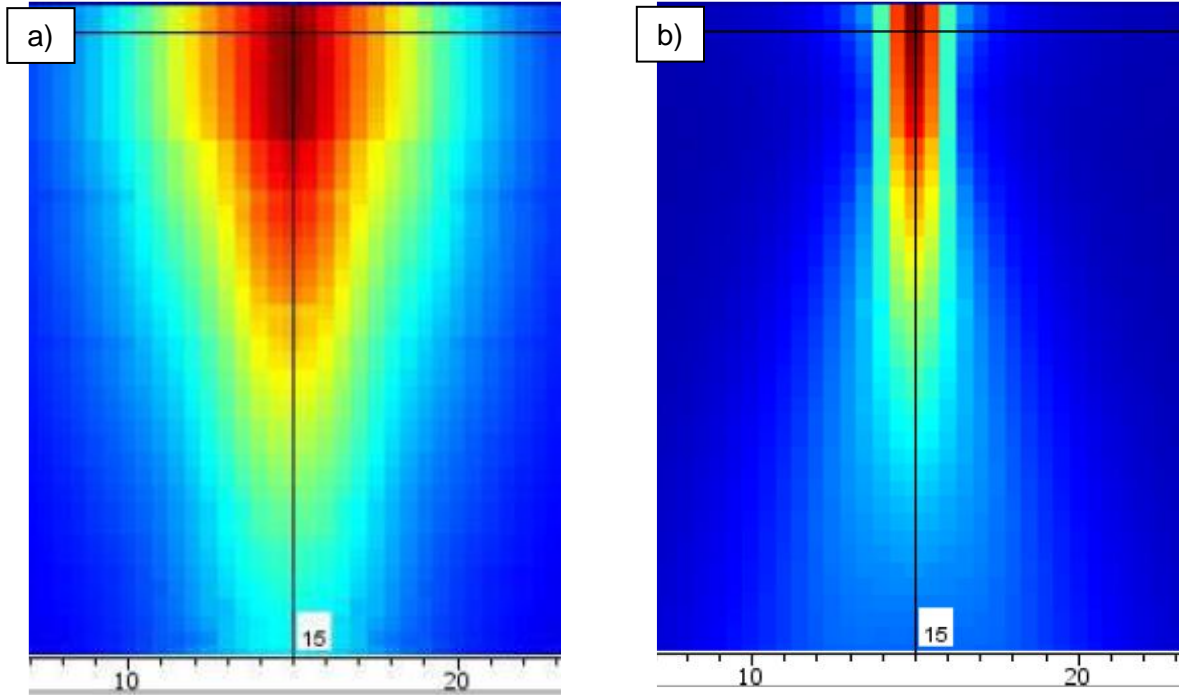
Figure 4-8: Secondary Axis Simulated Beam Width of a) Standard "Flat" and b) Curved PAUT Probes.
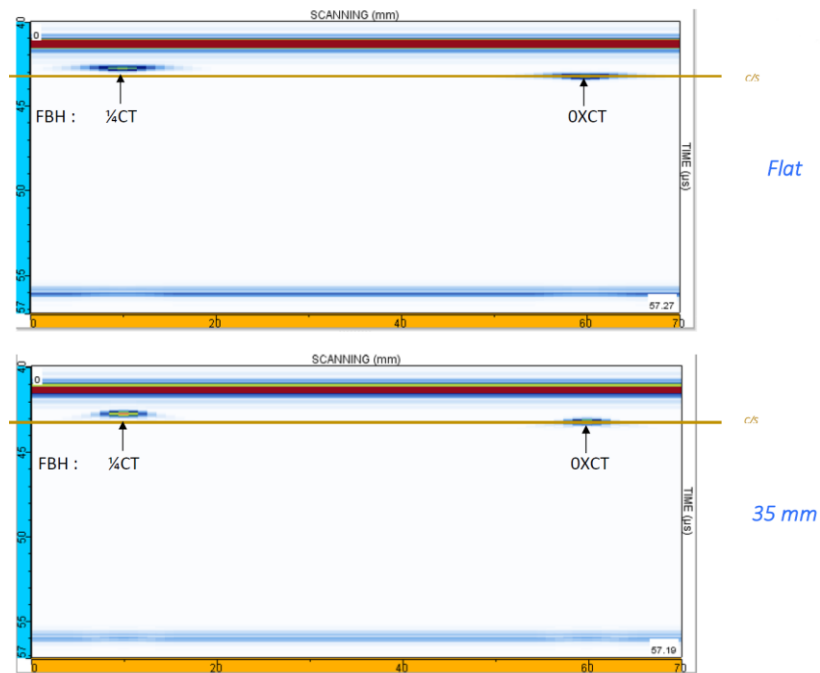
Figure 4-9: Inspection Simulation of 3mm Diameter Flat Bottom Hole (FBH) Using "Flat" (Standard) Probe vs. 35mm Curved Probe.

4.1.6 UFC External Pressure Testing

In 2022, the NWMO conducted a new external pressure test on a Serial Production UFC unit. The test was performed at the C-FER Technologies in Edmonton, Alberta. In this test, a steel UFC was pressurized to the glacial design load (45 MPa) and held for 24 hours, then the pressure was slowly varied between 5 and 45 MPa for 10 cycles. This loading condition was intended to demonstrate that the UFC can withstand 10 cycles of glaciation each with the theoretical bounding load without significant plastic deformation. A helium leak test was conducted following the cyclic test to confirm the intactness of the containment boundary. Geometric laser scanning was also performed to confirm that no significant permanent deformation occurred after the test. Next, the UFC was pressurized beyond the design load and plastically buckled at a pressure of 63 MPa. The buckling test demonstrated the 40% design margin against plastic buckling. Finally, the UFC was further collapsed to the maximum degree, i.e., the cylindrical portion of the container was fully flattened until the end effect from the hemispherical heads prevented further propagation of the collapse. Another helium leak test was performed confirming the integrity of the containment boundary; no breach was detected. The UFC before the tests and the collapsed UFC after the tests are shown in Figure 4-10.

(a) UFC Before the Test

(b) Collapsed UFC After the Test

Figure 4-10: UFC Serial Production Unit Before and After the External Pressure Tests

The new pressure tests successfully demonstrated that the UFC is highly durable under the design basis load (45 MPa), design extension condition (buckling) and a condition far beyond the design basis (fully collapsed).

In addition, the previous UFC pressure test conducted in 2016 was reviewed as part of the preparation for the test at C-FER. The measured strain data were analyzed and compared to the simulation results. The results were published in a conference paper (Janson, et al, 2022).

4.2 COPPER DURABILITY

4.2.1 Used Fuel Container Corrosion Studies

4.2.1.1 Anoxic Corrosion of Copper

Following closure of the DGR, oxygen will be present for a short period of time. However, this oxygen will be consumed by mineral reactions, aerobic microbial metabolism and corrosion leading to a highly reducing environment for the majority of the DGR's lifetime. The absence of oxygen creates an environment in which copper, the corrosion barrier of the UFC, is thermodynamically immune to corrosion provided that the pH of the groundwater does not reach extreme low values, which is not anticipated. However, while groundwaters at either potential DGR host site are very low in bisulfide concentration, if sulfide reducing bacteria are present in the vicinity of the DGR it is possible that bisulfide could be created and diffuse to the UFC causing copper corrosion. While the presence of compacted bentonite in the DGR virtually eliminates this possibility, the effects of bisulfide on the integrity of the UFC and the quantification of any such corrosion is important to understand. Additionally, since there remain two potential host sites for the Canadian DGR, the specific groundwater chemistry of each site must be investigated in conjunction with the effect of bisulfide. With respect to corrosion, the dominant species in each case is chloride which is being studied at various concentrations in conjunction with bisulfide.

Work being conducted by NWMO at CanmetMATERIALS (Hamilton, Canada) in collaboration with the University of Toronto investigates the individual and the combined effects of bisulfide and chloride along with pH effects in an anoxic environment. In the absence of oxygen, any potential corrosion reactions will produce hydrogen as a product which can be captured in the headspace of the specialized corrosion cells used in this research, shown in Figure 4-11(a). A detailed description of this apparatus was published by Senior et al. (2020a) in 2020. This hydrogen is then passed through a highly sensitive solid state ceramic sensor which can quantify the hydrogen. Using the known stoichiometry of the potential corrosion reactions, copper corrosion rates are then calculated. Notably, the release of trapped hydrogen from within the copper, or the production of hydrogen from other corrosion reactions within the cell (i.e., through the interaction of steels and water) will be assumed to be copper corrosion using this calculation method, and this will overestimate copper corrosion (Senior et al. 2019). The design of the corrosion cells allows for the online spiking of experiments with gaseous hydrogen sulfide, which dissolves in solution as bisulfide, thereby simulating the potential effects of microbiologically-induced corrosion at 75°C. Sample data showing the cumulative hydrogen measured and the calculated corrosion rates over a period of six years are shown in Figure 1(b) and (c), respectively. Consistently, regardless of immersion environment or the number of hydrogen sulfide additions, the hydrogen generation and therefore the calculated corrosion rates decline with time to below measurable quantities.

The corrosion experiments are ongoing along with hydrogen analysis of repository relevant coppers (i.e., electrodeposited, and cold spray copper). Preliminary results indicate that at this relatively low temperature of 75°C some of the hydrogen being released into the corrosion cells is attributable to hydrogen inside the copper as a result of its manufacturing processes as opposed to copper corrosion. While the relative amounts of hydrogen being produced are not yet definitively assigned, this work indicates that the extremely low corrosion rates being measured in the program are highly conservative. Therefore, the NWMO is well justified in its copper corrosion assessment, which asserts that the total anoxic copper corrosion would produce less than 0.25 mm of damage in 1,000,000 years and is consistent with the conservative NWMO total corrosion allowance of 1.204 mm over that period of time (Hall et al. 2021).
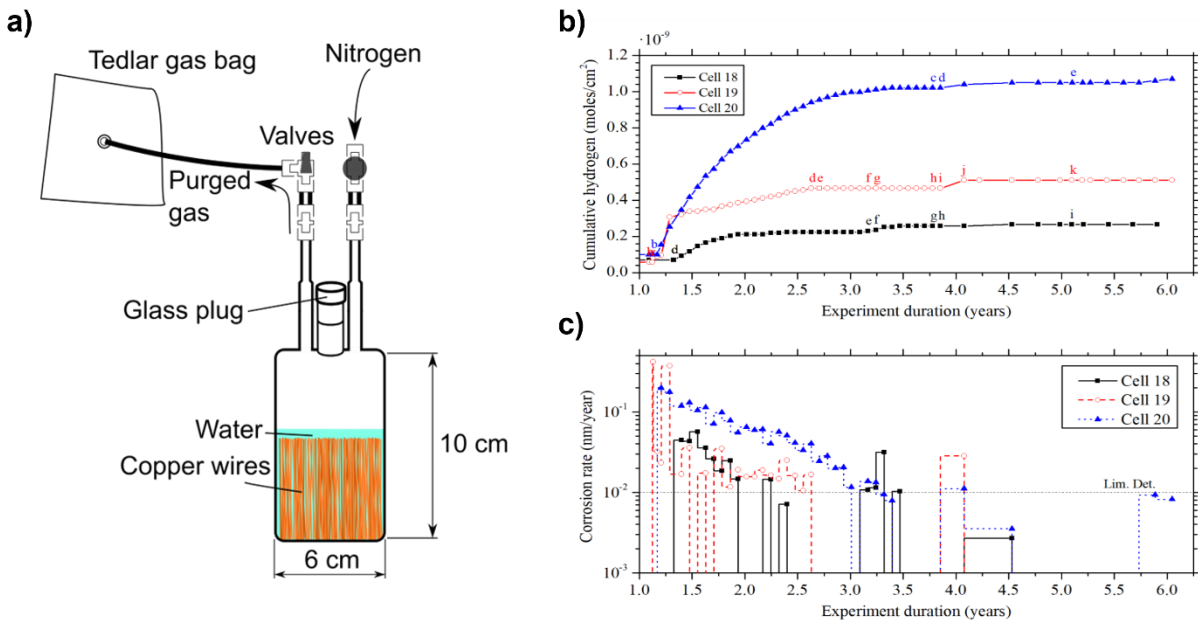
Figure 4-11: (a) Schematic of Test Cells for Anoxic Copper Corrosion Investigations at CanmetMATERIALS; (b) Cumulative measured Hydrogen and Calculated Copper Corrosion Rates for Three Cells Containing Cold Spray, Electrodeposited, and Junction Material, all in Simulated Canadian Groundwater Versus Time.

4.2.1.2 Microbiologically Influenced Corrosion

The repository environment is anticipated to evolve from early oxic conditions to later anoxic conditions. Likewise, degradation processes of the UFCs should transition from the initial oxygen-driven processes to those governed by the availability of sulfide as an oxidant. One feature of this transition is likely to be the conversion of any accumulated (hydr)oxide-type corrosion products produced during the oxic phase to copper sulfide compounds. This conversion is important for determining microbiologically influenced corrosion allowance. A preliminary assessment by (Hall et al. 2021) indicated that where high amounts of previously oxidized copper and high concentrations of aqueous sulfides are considered to occur simultaneously, it is presumed that only some (i.e., 50%) of the previously oxidized copper will convert to copper sulfide. To enhance the confidence of this assessment further investigations on the conversion process was initiated. Based on the recent investigations, during the conversion process, sulfide species could interact with the UFC surface in several ways such as a) chemical conversion, b) galvanically-couple process and c) direct corrosion. Results to date

indicate a rapid and quantitative conversion of oxides according to processes a) and/or b), followed by direct corrosion of the Cu surface by sulfide (Salehi Alaei *submitted*).

Under anaerobic conditions, microbiologically influenced corrosion (MIC) could occur, where sulfate-reducing bacteria produce bisulfide (HS^-) that can transport through HCB and corrode the copper barrier (Md Abdullah et al. 2022). This is an interdisciplinary phenomenon that includes processes such as microbial activity, species transport through the HCB as well as corrosion dynamics. A new experimental work initiated and focused on quantifying HS^- transport through HCB using diffusion experiments under a range of anticipated DGR conditions (e.g., temperature and ionic concentration) as well as HCB densities. Preliminary results indicate that geochemical reactions/sorption of HS^- onto HCB resulted in certain changes in the bentonite composition that may have caused unusual diffusion behaviour (Chowdhury et al. *submitted,* Rashwan et al. 2022). Further studies, including sample analysis (i.e., via SEM-EDS and total sulfur analysis) are underway to better understand the transport dynamics, and the results will aid in assessing the performance of EBS. In addition, it is anticipated that sorption onto bentonite will reduce HS^- transport and minimize the risk of corrosion, therefore, an independent testing is ongoing to systematically investigate the sorption phenomenon of HS^- onto bentonite under various liquid to solid (L:S) ratios (50-200); initial HS^- concentrations (1-5 ppm) and contact time (1-48 hours) (Figure 4-12). Figure 4-12a) and b) also show that the experiments using either 1- or 24-hour contact times exhibited very similar sorption behaviour. This result suggests that most of the sorption of HS^- occurred within the first hour of contact with bentonite. These preliminary results compare well with the hypotheses from Pedersen et al. (2017), who suggested that a large fraction of HS^- will likely immobilize in bentonite due to reacting with the ferric and ferrous ions in the MX-80 bentonite (Chowdhury et al. *submitted).*
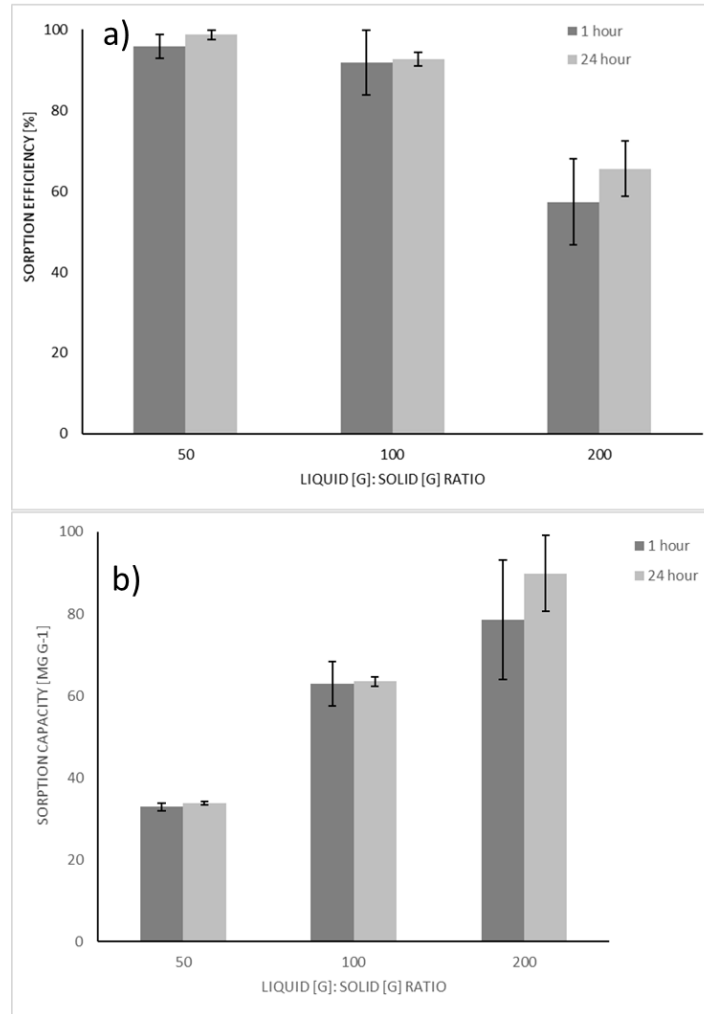
Figure 4-12: The Effect of L:S and Contact Time on the (a) Sorption Efficiency and (b) Sorption Capacity of HS- on MX-80 Bentonite. All Data Bars Represent an Average of Duplicate Experiments, and the Error Bars Note the Maximum and Minimum Measurements from Duplicate Experiments (Chowdhury et al. *submitted*).

4.2.1.3 Corrosion of Copper Coatings

The NWMO has been focusing on identifying or narrowing the chemistry requirements for copper coatings with an intent to create a purity specification for copper coatings that emphasizes corrosion performance. The purity specification of copper coatings includes trace chemical species (metallic and non-metallic) that may be incorporated into the coating during the manufacturing process. Phase I of this project focused on the effect of non-metallic impurities on the corrosion behavior of a wide range of commercial and customized copper samples including cold sprayed and electrodeposited copper coatings. The most recent results from the coating purity program show that amongst different non-metallic impurities, trace oxygen does affect the reactivity of copper in aggressive conditions (e.g. nitric acid), specifically, for cold sprayed copper (CS Cu) samples, there was enhanced preferential dissolution within particle-particle (P-P) interfaces (Dobkowska et al. 2021). Although aggressive DGR conditions are nowhere near as aggressive as those in this experimental program, and are very short-lived, with respect to the DGR lifetime, the results are insightful with respect to understanding the

copper reactivity. A series of experiments was additionally conducted to determine the effect of oxygen content on the extent of corrosion on CS Cu samples that were fabricated with a known amount of oxygen. The results suggested the extent of corrosion increased with increasing the amount of oxygen in CS Cu samples. This work showed the maximum depth of preferential corrosion measured by Micro-CT is around 120 µm for CS Cu with highest amount of oxygen (~700 ppm). To ensure not exceeding the localized corrosion allowance of 100 µm (Hall et al. 2021) the maximum oxygen content of 400 ppm is, therefore, suggested for copper coating specification for the current design of UFC.
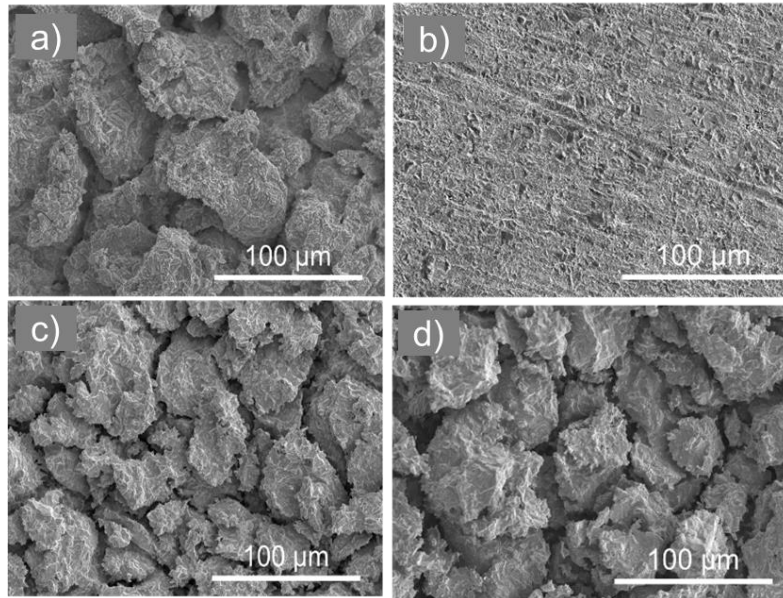
Figure 4-13: SEM Characterization for Representative Surface Morphologies Following Sample Immersion in Naturally Aerated 0.1 M HNO₃ for 24 h for a) and b) Low O CS Cu; c) Medium O CS Cu; d) High O CS Cu all Exhibiting Severe Preferential Corrosion, as well as Comparisons for a) and b) Low O CS Cu Exhibiting Mild and No Preferential Corrosion, Respectively.

4.2.1.4 Corrosion of Copper in Radiolytic Environment

The copper coated UFC will be exposed to a continuous flux of γ-radiation emitted from the decay of radionuclides in the used fuel. Although the γ-radiation does not affect the metal directly, any trapped water or humid air near the UFC will decompose to produce redox-active and acidic species that can affect the corrosion of the copper coating. There have been a number of approaches to predicting the radiation induced corrosion of UFC and of the spent fuel itself (Eriksen et al. 2012). These approaches can be broadly classified as being either empirical or deterministic. Deterministic models are based on a prediction of the yield of radiolytic oxidants (and reductants) using some form of bulk radiolysis model. Deterministic models can be further classified as either coupled or uncoupled, with the primary distinction being the degree of coupling between the interfacial electrochemical processes and bulk radiolysis model. Uncoupled models are the more common, for which it is assumed that the yield of radiolytic oxidants is independent on the rate at which they are consumed in the interfacial corrosion reaction. NWMO has been developing such models lately (King and Behazin 2021) and is currently in the process of converting existing models and developing new coupled models using the commercial software package COMSOL Multiphysics. The code is designated the

Copper Corrosion Model for Radiation-induced Corrosion (CCM-RIC) and the first phase of the work has been submitted for publications (Behazin et al., *submitted*).

4.2.2 Microbial Studies

Following closure of the DGR, groundwater will slowly saturate the bentonite clay. While any oxygen present due to excavation will be consumed long before this, it is possible for hydrogen sulfide species, should they be present, to cause corrosion of the UFC. Since both remaining potential DGR host sites do not contain hydrogen sulfide in their groundwaters at DGR depths, the only potential source of the oxidant is due to microbiological activity. However, these microbiological species called sulfate-reducing bacteria (SRB) will only be viable should the environmental conditions allow for it. With respect to the DGR, the bentonite clay ensures that SRB will not be viable by maintaining a low water activity (i.e., <0.96) and constricting pore spaces if the emplacement dry density exceeds 1.4 g/cm^3. While the HCB and the GFM are expected to have emplacement dry densities of greater than 1.4 g/cm^3, work is being conducted to explore the viability of microbes in a range of dry densities to fully understand the nature of the microbes in clay. Of particular interest is the GFM which will have a lower dry density than the HCB.

Significant effort has been dedicated recently to optimizing the extraction and characterization of DNA held within the bentonite clay, as this genetic material is not abundant (Engel et al. 2019a, Vachon et al. 2021). Much of this work is conducted in concert with corrosion and bentonite programs, as well as within work that is performed at the underground research laboratories (Mont Terri and Grimsel) in Switzerland (Engel et al. 2019b).

To supplement the in-situ work being performed in underground labs, pressure vessels (Figure 4-13(a) and (b)) have also been designed, fabricated, and commissioned to perform many ex-situ experiments at Western University. In 2022, an initial set of scoping experiments were completed where GFM ranging from dry densities of 1.1 to 1.6 g/cm^3 were saturated with water for up to 18 months. Pressure cells were then disassembled and analyzed for microbiological taxonomy and cell abundance. Figure 4-14:(c) shows results for the starting material (i.e., time zero GFM) and GFM compacted to 1.25 and 1.6 g/cm^3. In all cases there is short term growth of aerobic bacteria which then become in active after about 12 months. For SRB at low densities some small growth is shown over short timescales while the higher density GFM supresses SRB growth over all timeframes. Results of this first campaign are currently under peer-review.

Following the initial scoping tests which occurred throughout 2020-2021 an anoxic testing campaign commenced which is currently underway. This work will confirm that the behaviour seen in the oxic campaign is also applicable to an anoxic environment which is representative of the long-term DGR environment.
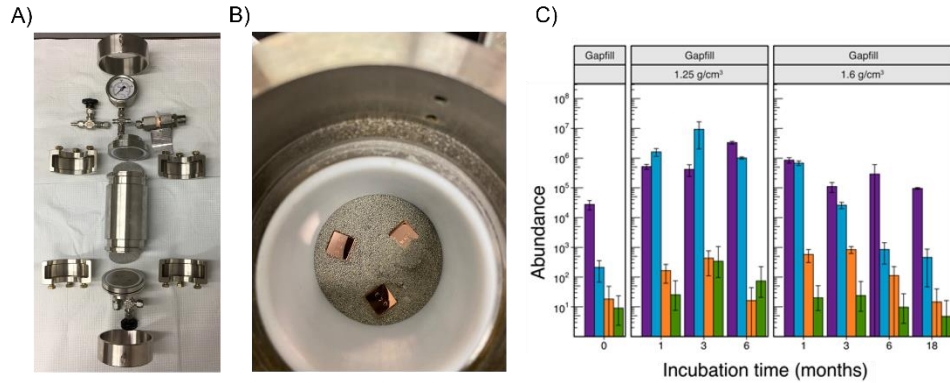
Figure 4-14: (a) Deconstructed Pressure Vessel for Ex-situ Microbiological and Corrosion Analyses; (b) View Diwn Inside a Pressure Cell Showing Copper Coupons and Bentonite (c) Abundances of Cultured Microorganisms from Pressure Cells Containing Uncompacted GFM and GFM with a Dry Density of 1.25 and 1.6 g/cm^3 versus Incubation Time.

4.2.2.1   Mont Terri HT (Hydrogen Transfer) Project

The Hydrogen Transfer project is a gas circulation experiment which occurs at the Mont Terri underground rock laboratory in Switzerland. This is an *in-situ* experiment with the aim of evaluating hydrogen consumption processes in a borehole and determining the role of microbial activity on these processes in an Opalinus Clay environment. Hydrogen is injected near the borehole mouth continuously and the seepage water is analyzed to track the generation/consumption of the hydrogen. To date, it has been seen that hydrogen consumption does occur within the borehole and this has been attributed to microbiological activity. Work developed in 2021 and published in 2022 outlines the numerical modelling efforts that have occurred to better understand the data acquired on the fate of hydrogen within the experiment (Damiani et al. 2022). Currently, the modelling supports the hypothesis that hydrogen in the borehole experiment is consumed by sulfate-reducing bacteria ultimately leading to a slight reduction in the water pH. However, this is counterbalanced by buffering species which naturally exist within the porewater. In the context of an NWMO DGR, the presence of bentonite is expected to supress any such behaviour of sulfate-reducing bacteria.

4.2.3   Field Deployments

To date, much work in the Engineered Barrier Science group has focused on laboratory-based experiments to elucidate the fundamental processes related to copper and bentonite integrity. Recently, greater attention is being paid to evaluating the synergistic behaviour of copper embedded in bentonite deployed in DGR-like environments. This work utilizes so-called "module experiments" based off designs created by Nagra the Swiss nuclear waste management organization. However, the NWMO has adapted these experimental methodologies and applied them in environments which more closely resemble potential Canadian DGR sites.

4.2.3.1   NWMO Ocean Module Deployments

In the summer of 2022, in partnership with Ocean Networks Canada (ONC) at the University of Victoria, the NWMO and academic partners at Western University and the University of Waterloo deployed 12 modules containing copper and bentonite compacted to various dry

densities on the floor of the Pacific Ocean (Figure 4-15). The modules were deployed to a depth of approximately 3000 m which applies a constant pressure of 30 MPa which is the range of the maximum expected pressure that the DGR would see during future ice ages. Additionally, this environment is highly saline, low in oxygen and microbiologically active which is a reasonable analogue for a DGR environment. The main goal of these experiments is to evaluate the effect, if any, of high pressure on the engineered barrier components over long timeframes. Modules will be retrieved every year for four years and analyzed for the corrosion and microbiological behaviour with the first set being retrieved in the summer of 2023.

Figure 4-15: Engineered Barrier Testing Modules Deployed on the Floor of the Pacific Ocean at the Endeavour Obseratory Operated by Ocean Networks Canada at About 3000 m Depth.

4.2.4   Corrosion Modelling

4.2.4.1   Uniform Corrosion Modelling

As with other components of the disposal system, it is necessary to make predictions of the long-term copper corrosion behaviour of the UFC including the uniform (general) corrosion in a deep geological repository (DGR).   The Copper Corrosion Model (CCM) predicts the uniform (general) corrosion behaviour of a copper-coated UFC in a deep geological repository (DGR). The model is generally applicable and is capable of describing the corrosion behaviour of copper in any O_2-containing Cl^- environment in which mass transport of species to and from the corroding surface occurs by diffusion. In its current form, the model is one-dimensional (1-D) which makes it robust and applicable to a range of container and DGR designs. The strength of the CCM is that it is mechanistically based and was developed in conjunction with an expensive experimental program of electrochemical and corrosion studies (King and Kolář 2000, 2006).

Recently, the custom-designed Copper Corrosion Model (CCM) developed by King and Kolàř (2000) has been converted to the commercial software called COMSOL Multiphysics to ensure that the model is available to future researchers and to provide a more-robust QA framework. A stepwise approach of increasing mechanistic complexity and model capability has been taken, with progress-to-date up to and including 1-D, 2-D time dependent implementations using the

full CCM mechanisms for an isothermal and saturated environment. Results of the Copper Corrosion Model – COMSOL (CCMC) model stepwise implementation, experimental validation, comparison to the previous CCM and initial findings are reported in King and Briggs (2022).

4.2.4.2   Localised Corrosion Modelling

The development of a mechanistic model of pitting under an Evans droplet during the early aerobic phase of the DGR including the hysteresis effects of the drying and re-wetting of the copper coated container was initiated in 2020 with work on-going in 2022. During this early aerobic, unsaturated phase in the DGR it is expected that the corrosion mechanisms are similar to atmospheric corrosion, involving the deliquescence of surface contaminants, droplet formation, secondary spreading and spatial separation of anodic and cathodic processes due to the geometry of the droplet.

Work being conducted at the University of Florida is developing a finite-element model with the means to predict, mechanistically the rate and extend of localized damage due to copper corrosion. Presentation of model development and early results were given at the 242th Electrochemical Society Meeting in 2022 (Chen et al. 2022).

4.2.4.3   Full Scale Emplacement – Gas (FE-G) Oxygen Modelling

Gas monitoring in FE-G was on-going in 2022 and included gas composition studies, numerical modelling, and complementary table-top experiments. The gas composition in the FE-G, like a potential DGR, is controlled by different bio-, geo, chemical and transport processes. Continued in 2022 was analysis of aerobic conditions after backfilling, gas advection through the tunnel EDZ and plug, gas exchange with the clay host rock and other bio-chemical processes. Composition of the bentonite pore-space has been monitored since construction in 2014 to capture long term behaviour of, for example, unsaturated transport of corrosive species (e.g., O_2 and H_2S) and gas generation (e.g., H_2).

4.3   PLACEMENT ROOM SEALS AND OTHERS

4.3.1   Reactive Transport Modelling of Concrete-Bentonite Interactions

The multi-component reactive transport code MIN3P-THCm (Mayer et al. 2002; Mayer and MacQuarrie 2010) has been developed at the University of British Columbia for simulation of geochemical processes during solute transport in groundwater. Prior reactive transport modelling work related to engineered barriers (e.g., bentonite) included the Äspö EBS TF-C benchmark work program (Xie et al. 2014), and simulations of geochemical evolution at the interface between clay and concrete (Marty et al. 2015).

In 2022, MIN3P-THCm was used to investigate long-term geochemical interactions driven by diffusion-dominated transport across interfaces between bentonite, concrete and host rock (limestone and granite) in the near field of a repository. Due to the relatively high pH of pore water in concrete, substantial mineral dissolution and precipitation has been predicted to occur at the bentonite/concrete and/or concrete/host rock interfaces, leading to porosity reduction or even pore clogging in close proximity (<1 cm) of the interfaces (Xie et al. 2022, 2021). The impact of altered interfaces on the migration of radionuclides (i.e., I-129) has also been numerically investigated. Depending on the rate of porosity reduction relative to the timing of

radionuclide release from a canister defect, the one-dimensional simulation results indicate that pore clogging could significantly inhibit radionuclide migration (Xie et al. 2022, 2021).

MIN3P-THCm was also applied to simulate the CI-D (tracer diffusion across 10-year old concrete-claystone interface) long-term diffusion experiment at the Mont Terri underground research laboratory. An anisotropic diffusion model for unstructured grids was implemented in MIN3P-THCm and verified against a three-dimensional analytical solution. The model was then applied to simulate the in-situ diffusion experiment in three spatial dimensions while honouring the complex geometry created by the vertical drill hole, the inclined test hole, the concrete-clay interface, the anisotropic Opalinus Clay (OPA), and the thin 'skin' layer between the concrete and the OPA. Simulation results show that long-term tracer diffusion is enhanced parallel to the bedding due to the anisotropic properties of OPA in comparison to the case without considering anisotropy (Su et al. 2022).

4.3.2   Gas-Permeable Seal Test (GAST)

Potential high gas pressure within the emplacement room due primarily to corrosion of metals and microbial degradation of organic materials is a significant safety concern for long term repository performance. To address this potential problem, Nagra initiated the GAST project at Grimsel Test Site, Switzerland in late 2010. The main objective of GAST is to demonstrate the feasibility of the Engineered Gas Transport System which enables a preferable flow path for gas at over-pressures below 20 bars where the transport capacity for water remains very limited. NWMO has been part of the GAST project since its inception.

GAST field experiment was delayed due to a major leak event occurring in 2014 followed by a very slow saturation process in the sand bentonite mixture. At the end of 2021, the long-lasting saturation process completed and preparation work for a full-scale gas flow test was underway immediately. In May 2022, the Gas Flow Test (GFT) was initiated with water-to-gas exchange. A few days later, gas flow through the sand/bentonite mixtures was confirmed by tracer detection, increase in storativity and TDR (time-domain reflectometer) data. Data evaluation and numerical investigations using TOUGH2 of the experiment are on-going.

In 2019, a smaller scale, well instrumented laboratory experiment - mini-GAST was initiated at UPC (Polytechnic University of Catalonia), Barcelona, Spain. The mini-GAST project aims to mimic the GAST experiment in a much better controlled fashion in the lab within a much shorter testing time frame. The mini-GAST experiment comprises of two semi-cylindrical shape mock-up tests, MU-A (50 cm in length and 30 cm in diameter) and MU-B (1/3 size of MU-A).

In 2022, the 2nd MU-B test (gas injection) was continued running after its initial tryout experiment in 2020. Meanwhile, more experiments with different materials using MU-A were under preparation in 2022. Before the lab experiment, Code Bright was used to perform 3D one-phase (liquid) and two-phase (liquid and gas) flow modelling to imitate the MU-A test conditions.

4.3.3   DECOVALEX Modelling

4.3.3.1   DECOVALEX 2023 Task C: Coupled THM Modelling of the FE Experiment

DECOVALEX is a multidisciplinary, cooperative international research effort in modelling coupled Thermal-Hydraulic-Mechanical-Chemical (THMC) processes in geological systems and addressing their role in Performance Assessment for radioactive waste storage (Birkholzer et

al., 2019). One of the projects in DECOVALEX-2023 is coupled thermal-hydraulic-mechanical modelling of the FE Experiment – Task C.

Task C of DECOVALEX-2023 ties into the FE experiment, with the aim of building models capable of representing the FE experiment and in particular pore pressure build-up in the Opalinus Clay associated with heating (Nagra, 2019). Similar work has been done before in other host rocks through DECOVALEX-2019 (Seyedi et al, 2021). The challenge here is in representing a large experiment in numerical codes and using the simulations to help analyse a large dataset from the experiment. Task C involves comparison of the models and methods used in coupled THM modelling of engineered materials. These models will also be used to investigate how engineering factors (e.g., shotcrete, tunnel shape) affect pore pressure safety margins in the repository.

NWMO participates in Task C modelling activity as one of the ten international modelling teams to validate the NWMO developed COMSOL THM model in application in the coupled THM modelling of the engineered materials used in the nuclear waste management programs.

The task is divided into three steps:

Step 0: Preparation phase: Benchmarking of the models against some simple, tightly defined test cases. It includes a 2D T simulation, a 2D TH+ vapour simulation, and a 2D THM simulation.

Step 1: FE heating phase: Modelling the change in pore pressure in the Opalinus Clay as a result of heating in the FE experiment. This requires 3D THM simulations with representation of partially saturated conditions. It includes three sub-steps: predication, analysis and calibration.

Step 2: FE ventilation phase: Modelling of absolute pressures in the Opalinus Clay, which will require representation of the ventilation of the FE tunnel prior to heating. Modelling teams can choose the complexity of the representation of excavation and EDZ development.

Step 3: Options for later parts of the task include:

- Consideration of more realistic geometry / additional materials etc
- Analysis of experiments on temperature dependent geomechanical properties
- Sensitivity analyses (e.g., considering the impact of higher temperatures)
- Anything else that comes from the comparison of models and data during Steps 1 and 2.

In the period of 2020-2021, Step 0 was finished. Ten modelling teams have performed the 2D thermal, coupled TH and coupled THM modelling FE experiment using different numerical modelling programs and the results are compered between different teams. The document for these comparisons between different teams is under preparation as an interim DECOVALEX report.

In 2021, Step 1 – prediction modelling of the FE experiment is on-going. In this step, all of the thermal, hydraulic and mechanical parameters and model geometry for the FE experiment are well defined and supplied to different modelling teams. The focus of 2022 work will be comparing results between different modelling teams and between numerical models and experiment measurements.

4.3.3.2   DECOVALEX 2023 Task F: Performance Assessment

The DECOVALEX program is interested in coupled processes (e.g., thermal, hydrological, mechanical, and chemical) relevant to deep geologic disposal of nuclear waste. Task F of DECOVALEX-2023 involves comparison of the models and methods used in post-closure performance assessment of deep geologic repositories.

Task F considers the generic reference case describing a repository for commercial spent nuclear fuel in a fractured crystalline host rock is proposed as the primary system for comparison. The NWMO is participating in the crystalline comparison. A second generic reference case describing a repository for commercial spent nuclear fuel in a salt formation (bedded or domal) is also a component of Task F however the NWMO is not participating in that component of task F.

The primary objectives of Task F are to build confidence in the models, methods, and software used for performance assessment of deep geologic repositories, and/or to bring to the fore additional research and development needed to improve performance assessment methodologies. The objectives will be accomplished through a staged comparison of the models and methods used by participating teams in their performance assessment frameworks, including: (1) coupled-process submodels (e.g., waste package corrosion, spent fuel dissolution, radionuclide transport) comprising the full performance assessment model; (2) deterministic simulation(s) of the entire performance assessment model for defined reference scenario(s); (3) probabilistic simulations of the entire performance assessment model; and (4) uncertainty quantification and sensitivity analysis methods/results for probabilistic simulations of defined reference scenario(s).

In 2022, Task F participants completed benchmarking of the various software programs and performance assessment tools used in Task F against hydrogeological flow and transport problem with known analytical solutions. The NWMO performed these benchmarks with the Integrated System Model (See Section 6.4.3.2.1) and its constituent codes COMSOL and HydroGeoSphere. Example results from select benchmark comparisons are shown in Figure 4-16 and Figure 4-17.
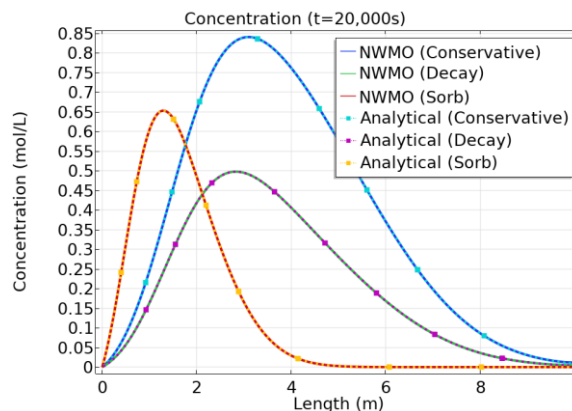
Figure 4-16: 1D Advective and Diffusive Transport Benchmark
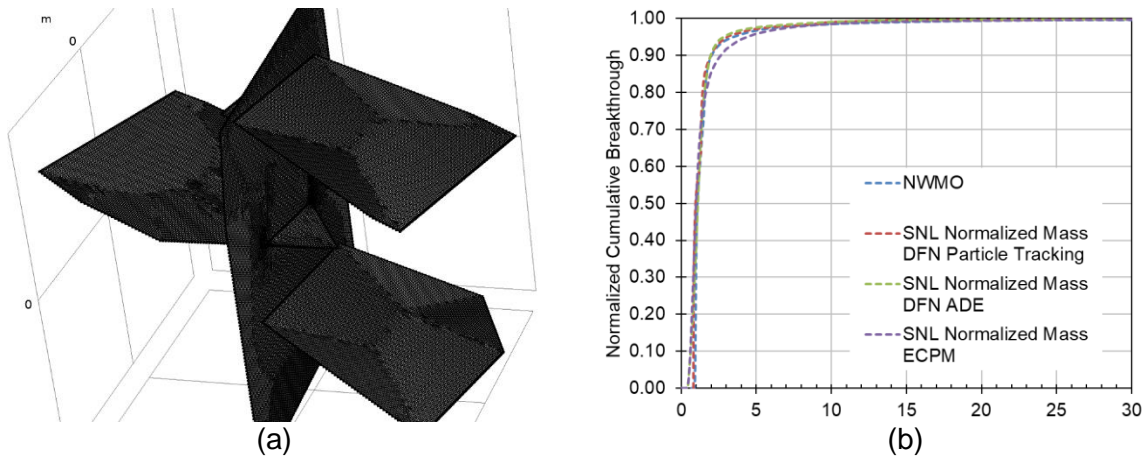
Figure 4-17: Task F - Four Fracture Benchmark (a) Geometry (b) Comparison with Sandia National Laboratory Results

In 2022, Task F participants finalized the definition of the generic crystalline rock assessment case and discrete fracture Network benchmarks. At present the generic crystalline rock site consists of a rectangular domain with a topographic high as one end of the site. The site rock and fracture characteristics are based on the Posiva characterization of Onkalo site and the hypothetical repository is based on the KBS-3 vertical in-floor disposal concept. The focus of the 2023 work will be finalizing and comparing results of the benchmark and generic crystalline site assessment across the various participants and producing documentation.

4.3.4   Shaft Seal Properties

In 2022, the NWMO completed the testing program that identified an optimized shaft seal mixture by evaluating the behavior of bentonite:sand blends having composition ratios other than 70:30. In this study, the use of a crushed limestone sand was examined in addition to granitic sand. Composition ratios of bentonite:sand of 50:50, 60:40, 70:30, 80:20 and 90:10 (by weight) were assessed by using two different salinity fluids, CR-10 (TDS 11 g/L) and SR-Sh (TDS 325 g/L), approximating groundwater conditions for crystalline and sedimentary sites, respectively.

The tests evaluated the following:
- Compaction/fabrication properties of the materials (to Modified and Standard Proctor density)
- Consistency limits (Atterberg Limits) and free swell tests
- Moisture content and density of fabricated material
- Mineralogical/chemical composition, including measurements of montmorillonite content
- Swelling pressure
- Saturated hydraulic conductivity
- Two-phase gas/water properties, specifically the capillary pressure function (or soil water characteristic curve, (SWCC)) and relative permeability function, measured over a range of saturations that include the fabricated and fully-saturated condition
- Mineralogical/chemical composition of the materials exposed to brine for an extended period of time

The test results indicate that for low salinity groundwater conditions (CR-10), compaction to 98% of the Standard Compaction Maximum Dry Density or 95% of Modified Maximum Dry

Density of the bentonite/sand mixtures studied will be sufficient to achieve the swelling pressure and hydraulic conductivity targets (>100 kPa and <10^{-10} m/s, respectively). There was no clear improvement in effective montmorillonite dry density (EMDD) once bentonite content exceeded 60%. Under high salinity conditions (SR-Sh), none of the materials compacted to 98% of Standard Compaction Maximum Dry Density met the Ps and k requirements for shaft backfill (<100 kPa and <1E-10 m/s). Materials compacted to 95% of Modified Compaction Maximum Dry Density achieved targeted Ps and k behaviour. There was no discernible effect of aggregate type on the hydraulic conductivity of any of the bentonite-sand blends examined in the study. However, it was observed that the swelling pressures with the crushed limestone at low density were slightly lower than those with the granitic sand. Since this was based on a very limited number of data points, it was not conclusively indicative. A larger database should be developed to confirm this phenomenon as it was not evident in the hydraulic conductivities measured for these same specimens.

In the study, discernible changes in the mineralogical or chemical composition of MX80 bentonite soaked in low salinity (CR10) and high salinity (SR-Sh) groundwaters were examined. Bentonite samples were analysed following 54 and 82 months of testing. There was no discernible change in the mineralogical composition and the chemical composition remains similarly unchanged except for elevated Ca and K and reduced Na contents that developed soon after soaking of clay was started. These changes are attributable to cation exchange on the montmorillonite clay surfaces with Na being lost to Ca and K being gained from the groundwater.

Soil water characteristic curves (SWCC) and gas permeability values were generated for potential shaft backfilling materials. These values will provide reference values for use in numerical modelling.

4.3.5   Bentonite-Low Heat High Performance Concrete

The NWMO reference concrete is Low Heat High Performance Concrete (LHHPC). The LHHPC mixture was optimized and its properties were measured from 2019 to 2021. Details in the optimization and material property are provided in NWMO-TR-2021-20 (NWMO, 2021a).

Upon completion of the LHHPC testing program, a new testing program was initiated in 2022 to assess the long-term interaction between the bentonite-based materials and LHHPC. As part of the NWMO placement concept, the LHHPC will be in contact with the bentonite-based materials and begin to evolve as soon as it is saturated with groundwater from the geological formation. That will likely modify the bentonite's geochemistry, mineralogy and texture near the concrete/bentonite interface. Consequently, this modification will affect the performance of the bentonite-based materials in the placement room.

In 2022, the scope of work was developed, and high-grade stainless-steel cells were designed for the testing program. A total of ten (10) cells will be manufactured and used for two reference waters (CR-10 and SR-290).

4.3.6 Thermo-Hydro-Mechanical Modelling of a NWMO Placement Room

In 2022, the NWMO continued to use fully coupled Thermo-Hydro-Mechanical (THM) CODE_BRIGHT models to study the unique NWMO placement concept. The previous numerical modelling was focused on the evolution of the bentonite-based materials in the crystalline rock geosphere (CR-10). In this year, the effect of the sedimentary rock geosphere (SR-290) on the evolution of the materials was numerically assessed. The major change in the numerical modelling was an increase in groundwater salinity.

The results obtained from the numerical modelling of an emplacement room in sedimentary rock indicated faster saturation than that of a similar room in crystalline rock, as the increased salinity would increase the bentonite hydraulic conductivity. As shown in Figure 4-18, the computed density field for the sedimentary rock case was more heterogeneous than that for the crystalline rock case. The results also indicated that an increase in salinity would reduce swelling pressure of the bentonite and consequently, result in less homogenization of bentonite density.
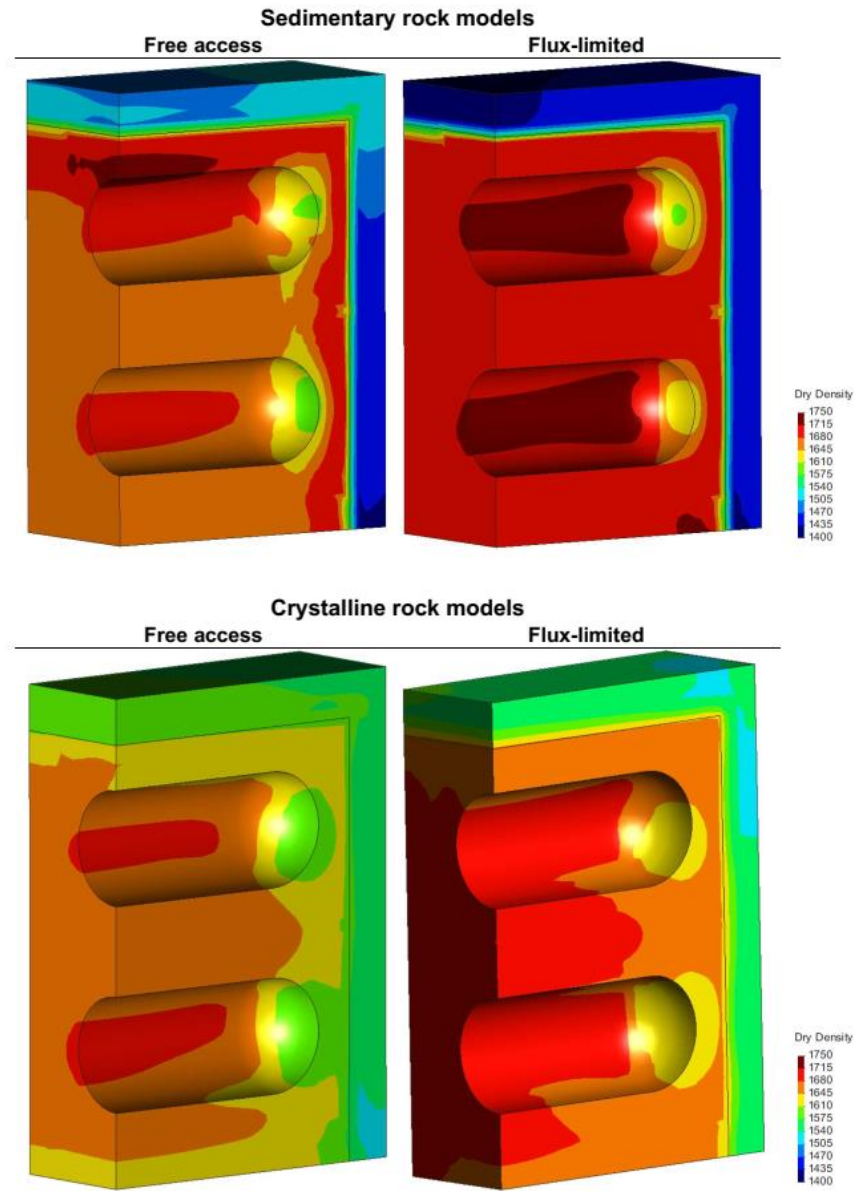
Figure 4-18: Comparison of Dry Density Fields of the Bentonite-based Materials for Sedimentary Rock (top) and Crystalline Rock (bottom) Models with Free Access to Water (left) and Flux-limited Access to Water (right)

4.3.7   Coupled Thermo-Hydro-Mechanical Benchtop Experiments

In late 2018, the NWMO and its contractor (the National Research Council of Canada) launched a work program to design and construct test cells to perform experiments examining the Thermal-Hydro-Mechanical (THM) response of HCB and GFM for use as a component in the Engineered Barrier System of the multibarrier concept. Results of the experiments will provide useful information for advancing the design of seals and will be compared against numerical THM models such as COMSOL or CODE_BRIGHT.

Two cylindrical experimental cells were manufactured; one to measure the THM response of HCB and GFM when exposed to a temperature boundary condition (called T apparatus) and the other to measure the THM response when exposed to both temperature and hydraulic boundary conditions (called THM apparatus). Figure 4-19 shows a representative schematic of the T and THM apparatuses.

In 2022, modification of the sensor layout and the heater design was completed, and sensors of moisture content and relative humidity were calibrated with different densities of HCB and GFM. A water delivery system for the THM test was developed and tested in this year.
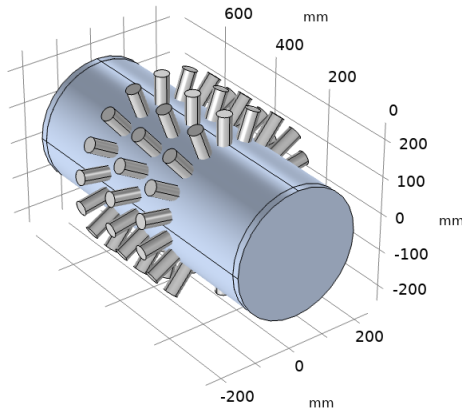
(a) 3D isometric view of the T apparatus
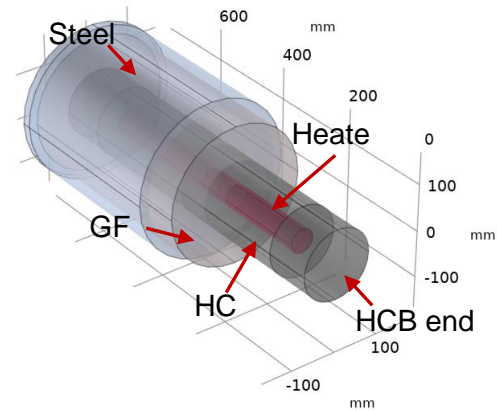
(b) 3D schematic of the T apparatus
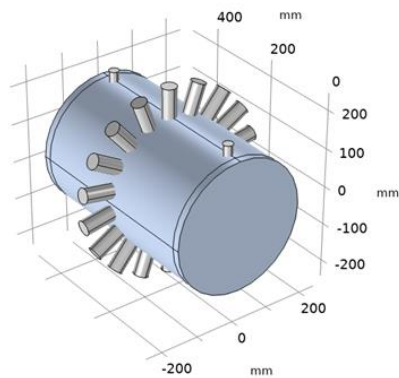
(c) 3D isometric view of the THM apparatus
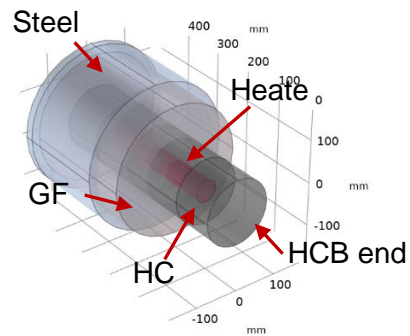
(d) 3D schematic of the THM apparatus

Figure 4-19: Representative Schematic of the T and THM Test Apparatuses

5 GEOSCIENCE

5.1 GEOSPHERE PROPERTIES

5.1.1 Geological Setting and Structure

5.1.1.1 Lithostratigraphic Framework for the Paleozoic Bedrock of Southern Ontario

The subsurface of southern Ontario has traditionally been the purview of the petroleum and salt industries. There are however, numerous other potential users of the subsurface geology and the pore space, for example CO2 storage, compressed air storage, nuclear waste disposal, heat storage and exchange, liquid waste disposal, etc. Subsurface data originating from the petroleum industry is managed by the Oil, Gas and Salt Resources Library (OGSRL). For this multiscale modelling study of the Paleozoic bedrock geology of southern Ontario additional data was also incorporated from the Ontario Geological Survey (OGS), and Nuclear Waste Management Organization (NWMO). Initial model development was focused on the lithostratigraphy of the 1500 m thick Cambrian to Devonian stratigraphic succession using nearly 300,000 borehole formation top picks from 20,836 petroleum wells, supplemented by measured sections, stratigraphic test data and 30 control points. Fortunately, given the near 100-year timespan of data collection the OGSRL had an existing Quality Assurance and Quality Control (QA/QC) protocol that was incorporated into the model development process. Lithostratigraphic boundaries were verified and, in some cases, added for intervals not previously considered significant to the petroleum industry. All QA/QC work was incorporated into the OGSRL database for the benefit of future users. The resulting bedrock model comprises 53 layers representing 70 formations for the 110,000 km^2 area of southern Ontario from the margin of outcropping Canadian Shield to the frontier with the USA. An updated digital subcrop geology map was constructed and combined with the digital bedrock topography to adhere interpolated layer surfaces to mapped bedrock geology. An independent confidence model was developed based on location, elevation, formation top picks, and data density.

A 14-layer hydrostratigraphic model was developed from the lithostratigraphic model with integration of shallow karst mapping, knowledge of contact zone aquifers, and addition of hydrochemical zonation from surface to depth of potable, brackish and saline formation waters. A preliminary version of the hydrostatigraphic model was subsequently used to support a regional finite element fully integrated groundwater–surface-water model by Aquanty Inc. The hydrostratigraphic model includes 3-D oil and gas pools and salt mine locations and extents. Included in the model are static level surfaces for the Cambrian, Guelph and Lucas-Dundee aquifers. This work has advanced at the core and pore scale through conversion of laboratory data from analogue form to digital.   Over 50 years of laboratory analysis representing approximately 50,000 porosity and permeability analyses were captured and a preliminary assessment for regional porosity variation was completed for the Lockport Group along with integration into an enhanced lithofacies framework. To further enhance the understanding of pore types and connections, select core from the Guelph Formation and A-1 Carbonate Unit were analyzed with a medical CT-scanner and a full 3-D image of the porosity distribution developed. Ongoing research involves the digital conversion of analogue downhole geophysical logs and analysis of porosity from neutron, density and sonic logs. This latest research will support the infill the data gaps for mapping the regional variation of porosity in the Lockport Group and A-1 Carbonate which is currently focused on core data that is predominantly located within oil and gas pools. Further research is also underway to model dolomitization patterns within the Salina A-1 Carbonate and A-2 Carbonate units.

To extend communication beyond the science and technology community a range of activities involving 3-D printing of the model layers, augmented and virtual reality initiatives, and university teaching support through ongoing collaboration are in progress. This numeric geoscience framework for southern Ontario is currently the most extensive and highest resolution of any jurisdiction in the Great Lakes basin. The framework is ideally suited to support continual evolution and development of multidisciplinary land use and pore-space management challenges of the region. It is also suitable for incorporation of additional datasets that can be attributed in a 3-D environment.
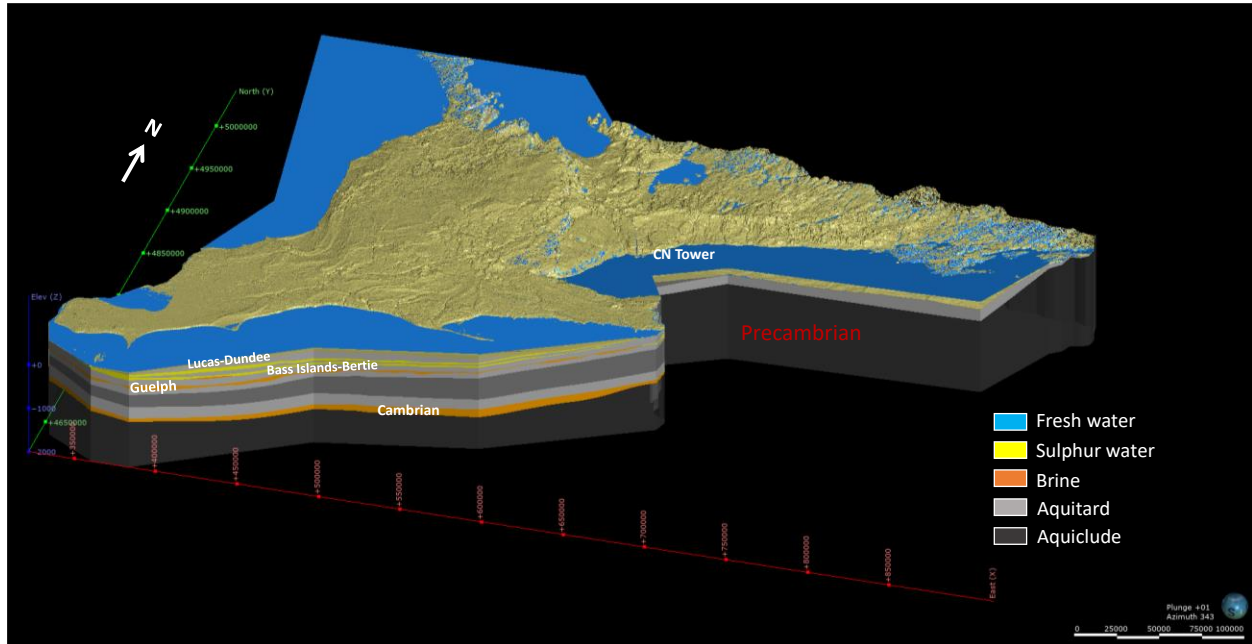
Figure 5-1: 3D Hydrostratigraphic model for Southern Ontario (Carter et al., 2021b)

5.1.1.2 Mont Terri Seismic Imaging (SI-B) experiment

During 2020, the NWMO joined as a partner in the SI-A Experiment (Seismic Imaging Ahead of and Around Underground Infrastructure) to investigate the applicability of high-frequency seismic impact or vibration sources, combined with three-component geophones integrated in rock bolts, for transmission and reflection imaging in an argillaceous environment to allow imaging of faults and fractures. The experiment is a high-resolution exploration test with resolution in the dm- to m-scale and within an observation range of several decameters to a few hundreds of meters. In 2020, seismic measurements were completed in Ga08, Ga04 and Niche CO2. In 2021, the focus was on acquisition of a seismic profile along the safety gallery, crossing both the upper and lower boundaries of the Opalinus Clay. Measurement was performed along a 400 m-long section within the safety gallery, using a 120 m-long land streamer with 120 geophones and a vibration source with a sweep of 30-120Hz. Previous experience indicated that imaging structures at larger distance from the tunnel is significantly enhanced when wavefield acquisition in deep boreholes (several 10s of meters) is performed.

In 2022 they continued the next phase of the project (SI-B), Seismic Imaging of Structures Below the Mont Terri Tunnel and Rock Laboratory, to investigate the deeper structures below

the tunnel (Figure 5-2). Previous seismic field tests have investigated relatively small source systems which are inappropriate for illuminating structures beyond ~100 m distance from the acquisition setup in claystone. It is the objective of this experiment to image geological structure down to the main thrust plane of the Mont Terri anticline at ~500 m – 1000 m depth below the tunnel. The wavefield will be recorded using receiver arrays in the safety gallery and additional borehole receiver arrays using available boreholes of ~80 m depth. During 2022, the installation of the receiver was completed, but the acquisition of the data (vibration at the shot points) was not completed due to personal health issues. The acquisition is postponed to 2023.
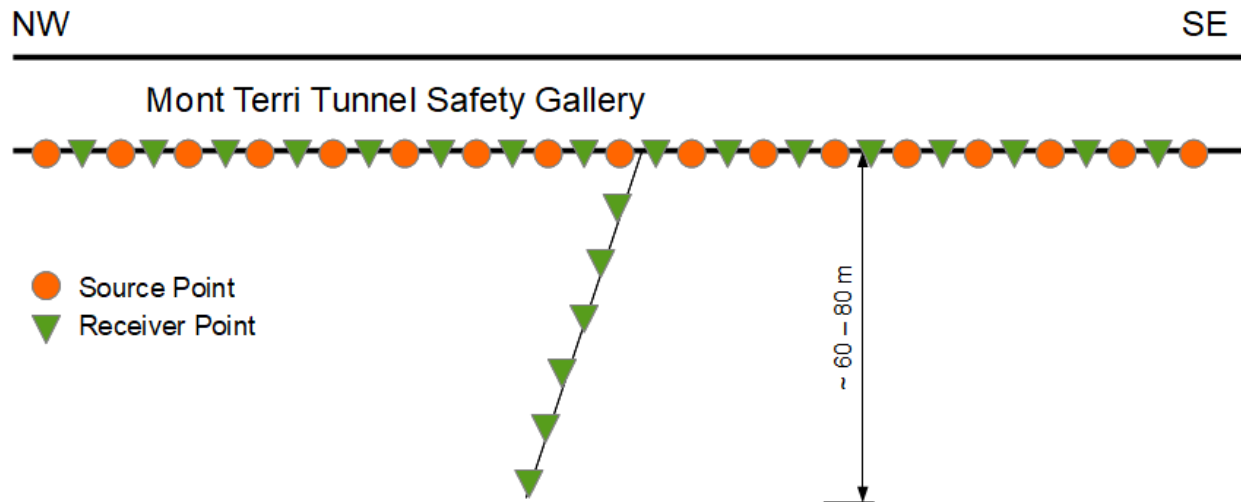
Figure 5-2: Conceptual Sketch of Seismic Acquisition Along the Safety Gallery in the Mont Terri Tunnel (cross-section, not to scale).

5.1.1.3 Metamorphic, Hydrothermal, and Diagenetic Alteration

5.1.1.3.1 Carbonate Paleogenesis

Based on the results of an ongoing regional study, conducted over the last decade exploring the origin of dolomite diagenesis in southern Ontario (Al Aasm et al 2021). It is proposed that the two deep boreholes drilled at South Bruce for the DGR Project will be sampled and the results added to this study.

This study will conduct a similar sampling program to the ones previously conducted at the Bruce Nuclear site and the OGSRL. Core samples are to be taken from the two deep boreholes at South Bruce and will be analyzed for petrographic, stable and Sr isotopes, fluid inclusion microthermometry and major, minor, trace and rare-earth elements (REE). The program will aim to further constrain the temperature of dolomite formation and fluid evolution within the Ordovician, Silurian and Devonian formations of southern Ontario.

The results will be synthesized with the existing data to demonstrate that South Bruce can be reconciled within the regional model to provide useful insights into the nature of dolomitization, and the evolution of diagenetic pore fluids in this part of southern Ontario.
Key Areas of Study:

1. Continue to enhance knowledge of diagenetic fluid history by differentiating between basinal (regional) and hydrothermal (local) sources of diagenesis. Recent work suggest

that the Silurian/Devonian systems have a separate and more recent fluid history. Further samples are needed to determine the number of fluid events and their relative timing.
2. Determination of Rare Earth Elements (REE) in both previously examined samples and new samples to be collected as part of this new work scope. REE's are applied to distinguish between a meteoric, basinal and/or hydrothermal source fluid for the dolomitized carbonates and siliciclastics in South Bruce site.
3. Peer review of earlier fluid inclusion work undertaken at the South Bruce site by the British Geological Survey.
4. Results will be in the form of a report to the NWMO with a paper (s) to be published.

5.1.1.3.2 Clumped Isotope Paleothermometer for Dolomite

A research project was initiated in 2021 with the GSC and NRCan that aims to use a new approach to assess fluid longevity within carbonate sedimentary rock mass. The clumped-isotope thermometer is a relatively new geothermometer which functions on the principle that rare 'heavy' isotopologues in a molecule prefer to bond together, with a dependence on the temperature of the system. Specifically, ^{13}C and ^{18}O in a carbonate mineral are thermodynamically ordered or 'clumped' depending on the temperature of the depositional environment. Determining the abundance of clumped isotopes in carbonate (Δ_{47}) then allows constraints to be placed on the formation temperatures.

This approach has the advantage of being able to directly infer the isotopic composition of the parent fluid, which is often difficult to reconstruct given 1) the prevalence of diagenesis in buried sedimentary successions and 2) the formation of secondary minerals over a wide range of temperatures. Using clumped isotopes analysis of carbonates as a tool, and with the objective of establishing a new paleothermometer for dolomite as well, key aims of the research program will be to reappraise the evolution of the Ordovician limestone sedimentary units in Southern Ontario and provide additional insights on the origin of mineralising fluids and post-depositional modifications to these rocks.

During 2021, the first step of work included hiring of an experienced staff member to help lead this project. This was completed by mid-2021. Several key tasks were initiated to ensure that: 1) the GSC instrumentation was optimized, 2) the required dolomite temperature calibration anchors were produced, 3) a data standardization scheme for dolomite was established.

In 2022, the following tasks were accomplished: 1) standardisation work on the instrumentation to ensure data accuracy and consistency with community accepted recommendations, 2) the analysis of temperature calibration anchors to produce calcite-specific and dolomite-specific clumped-isotope geothermometers, 3) preparation of a manuscript for publication in a scientific journal, and 4) selection and drilling of samples from the Bruce Site for analysis. Sample analyses were initiated late in 2022 and will continue in 2023.

5.1.2 Hydrogeological Properties

5.1.2.1 Hydraulic Properties of Fractured Crystalline Rock

5.1.2.1.1 Advances in Defining Hydraulic Properties of Crystalline Rock

Research at the University of Waterloo is being undertaken to develop improved approaches to characterize the hydraulic behaviour and evolution of groundwater systems in Canadian Shield settings. Snowdon et al. (2021) provided an extensive compilation of hydraulic properties in crystalline rocks of the Canadian Shield. Data were drawn from technical documents developed by Atomic Energy of Canada Ltd between 1975 and 1996 and includes 620 permeability estimates from sites across the Canadian Shield. During 2022, the database of hydraulic properties was expanded to include data on total dissolved solids concentrations, porosity, and tortuosity from sites across the Canadian Shield. A journal publication on these data, as well as their application in representative groundwater models for density-dependent flow was prepared. In addition to expansion of the reference dataset of hydraulic properties for Canadian Shield settings, research was performed on developing methods for generation stochastic correlated random fields for both equivalent porous media rock mass and discrete fracture zones that are conditioned to known data. The stochastic generation of conditioned correlated random fields was also linked to methods for correlating variability in fracture zone properties, including fracture size, orientation, degree of openness, to the assigned transmissivities. These methods are planned to be applied to site-specific groundwater modelling for the Revell Site.

5.1.2.1.2 HM Coupling of Rock Mass Stress and Permeability

In 2020, new research was initiated to evaluate the impact of the stress on the equivalent hydraulic conductivity of fractured rock masses and how this impact is also dependent on the fracture system in-situ properties (geometrical and hydraulic properties). To address these issues, intensive numerical simulations with the software DFN.lab are conducted, and an analytical framework is developed. In this case, a constitutive law to relate equivalent hydraulic conductivity to in-situ stresses with a parametrization based on the Discrete Fracture Network (DFN) properties is required. The "permecability" concept is a simplified hydromechanical coupling at the scale of the fractures with a transmissivity-stress relationship.

During 2022, sensitivity analyses were completed that include cases ranging from examining sensitivity to the parameters of the transmissivity-stress law (range of variation between residual and maximum hydraulic aperture), to simplified stress variation scenarios such as depth dependency or glaciation cycles and to the generation seed for DFN realization generation. Building of an analytical framework was also further investigated, and can be summarized as:

$$K(\theta) \sim p^{\wedge *}(\theta) \cdot <T\_(\theta)>\_g$$

In this equation, $K(\theta)$ is the rock mass equivalent permeability in any direction (θ), $p^{\wedge *}(\theta)$ is the effective connectivity of the DFN structure in the direction θ, and $<T\_(\theta)>\_g$ is an averaging term over the transmissivity distribution, also dependant on the direction g. The numerical set-up of DFN.lab was also used to evaluate the analytical framework for configurations of increasing complexity (from single or fracture pairs configurations to the realistic DFN models used as reference model in the sensitivity analyses). During 2022, a journal article on the research findings were progressed.

5.1.2.1.3 Äspö Task Force – Task 10

SKB originally initiated the Äspö Task Force on Modelling of Groundwater Flow and Transport of Solutes (the Task Force) in 1992 to enhance the understanding and increase the ability to model problems of interest in the field of groundwater flow and solute transport. In 2020, NWMO re-joined the Äspö Task Force to participate in Task 10 which is dedicated to building confidence in and "validating" models of flow and transport in fractured rock. The objective of this task is to develop pragmatic approaches to model validation. Task 10.2 which focusses on the single fracture scale and channelling will be undertaken first and will include validation of both flow and solute transport. Subsequent tasks will consider networks of fractures at larger scales.

Flow channelling in fractured rock is a phenomenon that occurs on different scales and can have a range of safety related implications. For example, channelling is relevant to:

- Characterization and interpretation of groundwater flow and transport in a fractured host rock,
- Assessing the potential for migration of meteoric water from the near surface to repository depths and subsequently radionuclide transport from the repository in the unlikely event of breached canisters,
- Inflows of groundwaters into deposition holes or emplacement rooms during buffer saturation and later flow within a deposition hole/emplacement room in the unlikely event of a breached canister.

Challenges when attempting to characterize flow channelling at a repository site include 1) most often, only a limited amount of data is available; and 2) the effects of channelling on mass transport on the scale of deposition holes/emplacement rooms needs to be "upscaled" to be used in larger scale groundwater flow and mass transport models.

5.1.2.2 Hydraulic Properties of Sedimentary Rock

5.1.2.2.1 Anomalous Pressures – United States Geological Survey

Research by the United States Geological Survey (USGS) will build on prior efforts to characterize the role, if any, of gas-phase methane on fluid pressure evolution at the Bruce site. Research will focus on (1) potential mechanisms by which the hydrogeologic system at the Bruce site could have reached its current (pre-drilling) state with gas-phase methane present in situ, and (2) the effects that gas phase has on field-based pressure measurements. These topics will be investigated through a series of multiphase hydromechanical simulations performed on a simplified 1D representation of the site that builds on previous hydromechanical investigations (e.g., Nasir, 2011 and others), and account for up to ~100 thousand years of simulated time. The 100 thousand-year timeframe is sufficiently long to fully capture the most recent glacial cycle (Stuhne and Peltier, 2015), but is also sufficiently brief to assume that the regional stress orientation was unaffected by major tectonic events and changes to it were therefore dominated by the glacial cycle (NWMO and AECOM 2011).

1D approximations of the site are justified because the hydraulic gradients observed within the same horizon between boreholes (lateral gradients) have far smaller magnitudes than the vertical hydraulic gradients (toward the underpressures and away from the overpressures) that are consistently observed in all of the boreholes at the site (NWMO 2011). In previous NWMO-

funded USGS studies (Neuzil and Provost 2014; Plampin 2019; Plampin and Neuzil 2018), simplified 1D representations of the system have effectively isolated fundamental system components and demonstrated controlling processes without obfuscation by 2D or 3D conceptualizations that would inherently be less well constrained than the obvious head gradient anisotropy. Most recently, Plampin (2019) reconciled the theoretical formulation behind the 1D hydromechanical coupling scheme that is incorporated into iTOUGH2 with a fully coupled 3D hydromechanical formulation and provided a preliminary demonstration of its utility to the Bruce problem. However, important characteristics of the site were excluded from this previous analysis, and a better match of the modeling results to the field data could be obtained by incorporating a more complexity into the 1D model.

A paper discussing the findings of the modeling was published in 2022 (Plamplin et al., 2022).

5.1.3   Hydrogeochemical Conditions

Chemical and isotopic compositions of groundwater and porewater within the rock matrix provide information on residence times and evolution of deep flow systems. Information on major ion compositions of the waters, pH, and redox conditions, as well as characterization of microbial populations, support calculations of radionuclide solubility and transport, and are also relevant to assessments of the stability (i.e., performance) of engineered barrier materials such as shaft seals.

5.1.3.1   Microbial Characterization – Waters & Rocks

In general, microbiological life in the subsurface is limited due to severe shortages of electron donors/acceptors and microbially degradable organic carbon sources. However, life is still possible in deep aquifer system or hydrocarbon reservoirs. While such features will not be in the immediate vicinity of the DGR, they will exist remotely and could impact the DGR. For example, if sulfate-reducing bacteria (SRB) are viable they can produce corrosive sulfide species which could migrate toward used fuel containers and cause corrosion. Such corrosion is currently accounted for in the NWMO's copper corrosion allowance, but it is important to include site-specific data to ensure that the corrosion allowance is well justified and conservative in nature.

As part of NWMO's site characterization activities, samples of rock core, groundwater and porewater have been collected at various depths from NWMO boreholes in the WLON-Ignace and the SON-South Bruce area. Each sample is being analyzed using methods developed through applied research at multiple Canadian universities (Waterloo, Toronto and McMaster). Researchers from these institutions apply DNA, RNA, PLFA and NMR-based techniques to determine the type of organisms present, the activity of these organisms, and the potential for the organisms to grow in the rock or in groundwater. Analysis of these samples is ongoing but some initial results, published by Beaver et al. in 2021, have concluded that no microbiological life was detectable in the crystalline rock sampled from the Revell site down to 500 m depth. Currently, samples of core from approximately 500 – 750 m depth from a borehole in the South Bruce area are being processed along with water samples taken from a borehole in the Ignace area. Initial PLFA data suggest that SRB are not present in either case. Therefore, from current data the impact of microbes on the DGR is expected to be insignificant. However, more work in this area is required and is ongoing.

5.1.3.2 Groundwater and Porewater Chemistry in Crystalline Rock (State of Science)

New research was initiated in 2021 with the University of Waterloo that aims to provide a comprehensive review and summary of current knowledge of the chemical and isotopic compositions of fluids (groundwaters, porewaters, and gases) in deep crystalline rock settings, as well as the associated understanding regarding fluid evolution. An important emphasis of this study is on any available data from plutonic/batholith environments. The objectives are to develop a comprehensive fluid geochemistry database for relevant environs from the Canadian Shield and publication of the summary data and findings in journal articles over the course of the project. Relevant data from Canada and around the world will be considered to build a robust data collection which can be used to understand key hydrogeochemical characteristics and processes occurring in deep crystalline environs, and to compare with site-specific data from the WLON-Ignace area.

Over the course of 2021 and 2022, building of the reference library for the Canadian Shield was advanced, and recruitment of a post-doctoral fellow to join the database and publication team at the University of Waterloo was accomplished. In 2022, the Canadian Shield component of the database was advanced (including thousands of data points), and a Canadian Shield fluids draft technical report is near completion and was submitted for NWMO review in December of 2022. A journal article documenting new observations arising from the compilation of the database will be submitted for publication early in 2023 and the final database (containing data from the Canadian Shield as well as international analogues) will be published as a distinct compilation in a scientific journal in 2023.

5.1.3.3 Measuring pH in Saline Groundwaters and Porewater Extraction by Paper Absorption

Hydrogeochemical research, whether it is lab- or field-based, commonly requires knowledge of the master variable, pH. pH measurements are commonly done potentiometrically, with electrodes, which is very challenging in high ionic strength (I) systems, such as the brines that make up the porewater and deep groundwaters in the Michigan Basin (up to I = 8M). Spectroscopic methods offer an alternative approach for pH measurement in brines. This involves calibration of the spectroscopic properties of colorimetric indicators using specially-prepared buffer solutions, with the pH of the buffers determined by geochemical modelling. Initial work was completed using a single indicator (phenol red) in the measurement range of pH ≈ 7 - 9. Over 2019-2020, the method was extended over a wider range of pH (~ 3 - 9) using a multi-indicator solution. The results demonstrate that the technique is most applicable up to I = 4M, but at higher ionic strength the sensitivity of the multi-indicator solution declines. This work was concluded in 2022.

A novel method has been under development for several years to extract porewater from rock cores into cellulosic papers for subsequent analysis of the porewater composition (Paper Absorption or PA method). Recent work (2021 and 2022) focused on testing the PA method using samples of the Opalinus Clay from a collaborative experiment at the Mont Terri underground laboratory in Switzerland. The data from these tests demonstrate excellent correspondence with the best available cation and anion data reported in the literature (Wersin et al. 2022).

5.1.3.4 Porewater Extraction Method Development

A significant area of research historically has been on development of techniques to extract porewater from the very low porosity crystalline and sedimentary rocks relevant to the Canadian program. There has been significant progress and several methods are now in use or have been recently applied as part of site characterization activities. However, techniques and approaches for the analysis and interpretation of results from porewater extraction experiments continues to be an active area of research - due to the indirect nature of these extraction procedures, as described in the following sections.

5.1.3.4.1 Porewater Extraction – Crystalline Rocks

A principal research activity has been developing a whole-core technique for extraction of porewaters from crystalline rocks using vacuum distillation. Vacuum distillation was established as a reliable method to extract porewater from low-permeability sedimentary rocks (Clark et al. 2013; Al et al. 2015) as an alternative to classical methods (e.g., centrifugation) that can be unsuccessful when attempted on rock samples of low water content.

The objectives of the current research are to: 1) develop and optimize a method to fully extract porewater from intact crystalline core samples, and 2) benchmark the approach using suitable core material saturated with water of known isotopic composition. Through repeated re-saturation and extraction experiments, it became clear that extraction of porewaters from low-permeability and low water content crystalline cores was possible without fractionation, but that artifacts of the re-saturation process caused isotopic depletion in the re-saturation porewaters. Over the past two years, a mechanism to fully re-saturate the cores for benchmarking was developed, such that the re-saturated porewaters were not accompanied by fractionation during the re-saturation process.

Testing of several different approaches to re-saturate core determined that re-saturation using a combination of high vacuum (45 mTorr), followed by heating (120°C) at elevated pressure (15 PSI), for long durations, produced high levels of saturation with no significant isotope fractionation, as shown in Figure 5-3.
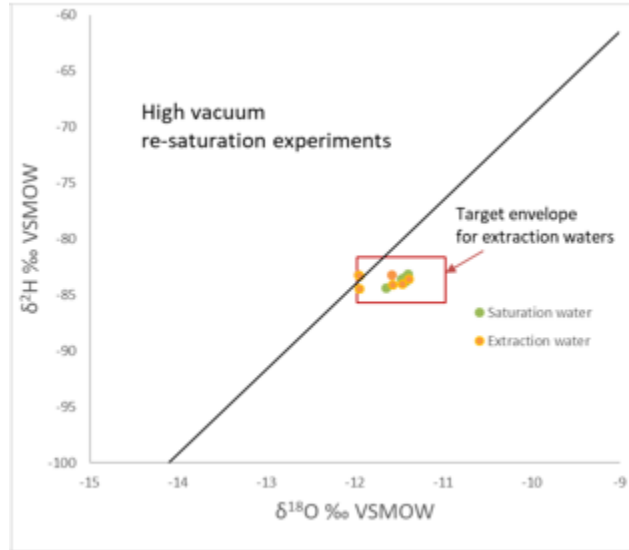
Figure 5-3: Isotopic Composition of Porewaters Extracted from Crystalline Rock Using Re-Saturation Protocols that Produce Porewaters Essentially Free of Re-saturation Artifacts

For porewater extraction experiments using this protocol, close to 100% of the re-saturated water mass could be recovered by distillation at 150°C (with overnight extraction under vacuum for saturated cores). Extended porewater extractions can be undertaken in two stages, assuring 100% yield for fully saturated cores, and has resulted in successful benchmarking of the method. Using the same approach, additional experiments were carried out to test the efficiency of porewater extraction at 120°C. The advantage of using the lower extraction temperature is to prevent the possible release of fluid-inclusions, which may otherwise influence the interpretation of the isotopic composition of the porewater. Extractions carried out at 120°C yielded comparable porewater recoveries to those carried out at 150°C ($100\pm1.55\%$, n=5 vs. $99.70\pm0.54\%$, n=9, respectively). Figure 5-4 shows $\delta^{18}O$ vs. δ^2H of the porewaters extracted at 120°C (Figure 5-4A) and 150°C (Figure 5-4B) plotted with respect to the local meteoric water line for Ottawa. As was previously observed with experiments carried out at 150°C (Figure 5-4B), the $\delta^{18}O$ and δ^2H of the recovered porewaters at 120°C fall within the acceptable error range of ±0.5 and $\pm2\permil$ for the isotopes, respectively (Figure 5-4). Therefore, a temperature of 120°C can be used to fully recover porewaters from crystalline whole-core samples without artifacts or isotope fractionation.
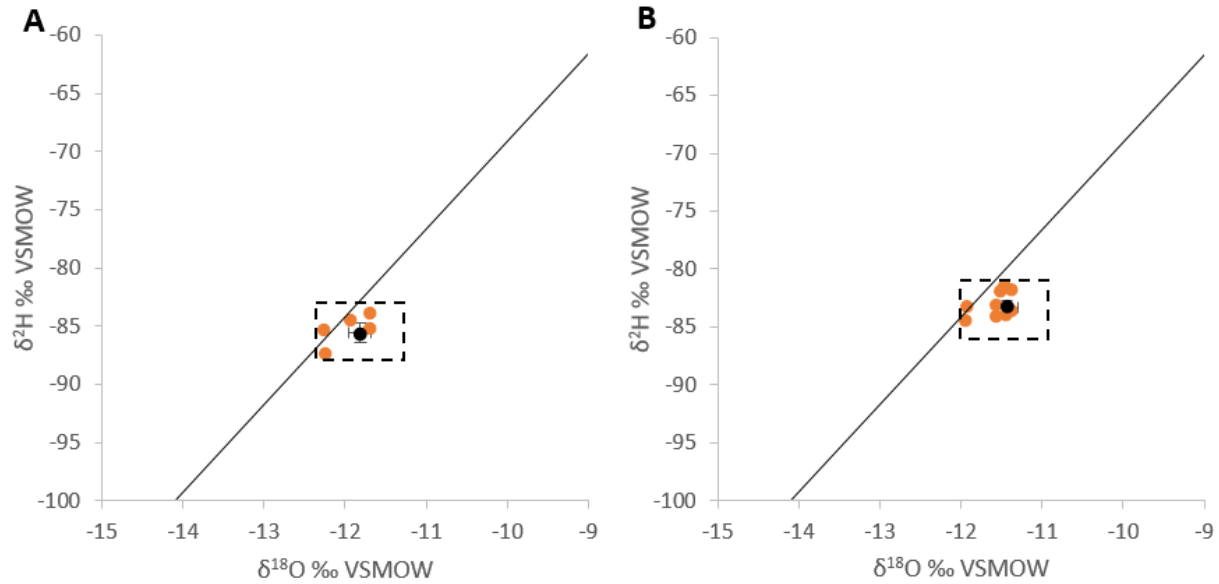
Notes: Left chart (A): Extraction Experiments Carried Out at 120 °C. Right Chart (B): Extraction Experiments Carried Out at 150 °C. Each Orange Data Point Corresponds to a Single Experiment. Black Points with Error Bars Correspond to the Average of $\delta^{18}O$ vs. δ^2H of the Saturating Water (± Standard Deviation). The Dashed Square Represents the Target Acceptable Envelope for Extraction Waters. The Solid Line Represents the Local Meteoric Water Line (LMWL) for Ottawa, Ontario, Canada.

Figure 5-4: δ18O vs. δ2H of Porewater Extracted from Whole-Core Samples

The success of the developed methodologies to saturate and fully extract porewater from whole-core samples, without isotopic fractionation, allowed for further testing using a synthetic saltwater solution (SSW, 1 mole/L NaCl and 0.05 mole/L KBr, 2x relative to seawater) to saturate whole-core samples. This approach allows for (1) determining the impact of ions/salts on the recovery of porewater, and (2) whether it is possible to reconstruct the geochemistry of the recovered porewater. The latter was investigated by submerging a whole core from post-vacuum distillation into a known amount of de-ionized water and allowing the ions to diffuse out until the electrical conductivity of the leachate has reached a plateau. Subsequently, once the concentrations of the desired ions in the leachate are known, the concentrations can be normalized by the original mass of water recovered from a core and compared to the composition of the saturating SSW.

The results thus far have revealed that saturating crystalline whole-cores with SSW did not influence the extraction efficiency with vacuum-distillation, as 97-100% of the water was recovered. Post-extraction, whole cores were leached for a period of 2-4 months in de-ionized water at room temperature (~22°C). Table 5-1 shows the concentration of Na, K, Cl, and Br in the leachates normalized to the amount of porewater extracted from cores that were initially saturated with SSW (1 mole/L NaCl, 0.05 mole/L KBr). Na, K, Cl, and Br are not expected to exchange onto mineral surfaces in these rocks, thereby providing an assessment of the leaching method. The normalized concentrations of the solutes were slightly above that of the original saturating synthetic saltwater solution (for core CT-05, Table 5-1). Nonetheless, the ratio of measured concentrations vs. the expected concentrations yields (M/E) values close to 100% indicating that the leaching method provides an acceptable estimate of the porewater chemistry in crystalline cores (cores CT-05 and C1-09). For the rest of the cores presented in

Table 5-1, though the ratio of M/E yields values close to 100% for the ions Na^+, Cl^-, and Br^-, the M/E ratio for K^+ fall below 100% (38-67%). The low M/E ratio for K^+ could be attributed to the duration of out-diffusion (1.8 months and 2 months vs. 4 months). A relationship can be observed between the M/E ratios for K^+ and the duration of out-diffusion, whereby the highest M/E ratio observed correspond to cores that were out-diffusing for ~4 months and vice-versa (Table 5-1). Therefore, it is possible that K^+ requires >2 months to fully out-diffuse into the leachate.

Table 5-1: Concentration of Na, K, Cl, and Br (mole/kgw) in the Core Leachates Normalized to the Amount of Porewater Extracted. M/E Corresponds to the Percentage of the Measured Concentration Relative to the Expected Concentration.

| Core ID | Ion | | | | | | | | Out-diffusion Duration |
	Na^+	M/E	K^+	M/E	Cl^-	M/E	Br^-	M/E	
CT-05	1.15	115	0.056	113	1.09	110	0.045	91	~4 months
C1-09	0.97	97	0.045	91	0.96	96	0.042	84	~4 months
CT-08	1.20	120	**0.03**	**67**	1.15	115	0.05	100	~2.5 months
CT-07	1.12	112	**0.02**	**47**	1.15	116	0.05	100	~2.5 months
CT-01	1.18	118	**0.02**	**39**	1.19	119	0.05	96	~1.8 moths
CT-02	1.18	118	**0.02**	**38**	1.23	123	0.05	99	~1.8 months

Therefore, porewaters from fresh, fully saturated crystalline cores can be fully extracted without artifacts using the extended extraction method. The isotope results indicate that this extraction procedure is quantitative and without isotope exchange or fractionation, providing an accurate measurement of the in-situ porewater isotope content in crystalline core samples. In addition, aqueous leaching of solutes from post-vacuum-distilled core samples can be confidently used to reconstruct the geochemistry of the porewaters.

Given the success in developing a methodology to fully extract porewater from whole-core crystalline samples, the method is now being applied to extract porewater from archived cores collected from Ignace, Ontario, Canada as a part of site selection activities.

5.1.3.4.2 Porewater Extraction – Sedimentary Rocks

Benchmarking the extraction of porewaters from the low water content and low permeability sediments of the Ordovician sequences of the Michigan basin continues to be a focus of research. Over the past year, work has continued using both gravel-size (2-4mm grains) and full-size cores from the Queenston, Georgian Bay and Blue Mountain formations.

The gravel-size fraction of samples from the Bruce Nuclear site (boreholes DGR-5/6) have been leaching in deionized water for ~10 years following their original analysis by 6-hour vacuum distillation at 150°C during the L&ILW DGR program (these are defined as 10-year gravels). In the current work, the majority of the 10-year gravel samples were extracted at 150°C for 6 hours, as well as at lower temperature (120°C for 6 hours). The purpose of the lower temperature extractions is to 1) test whether high-fidelity isotope measurements can be achieved at a lower temperature, and 2) further test whether any exchange between the clay hydroxyl groups and porewater might occur. Results at both temperatures show that no artefacts (enrichments or depletions in ^{18}O and ^2H with respect to the saturating water) were observed; extracted waters are within the range of the saturating fluid (0.5‰ for ^{18}O and 5‰ for ^2H). Some evidence of evaporation in the signatures are noted for both the saturating water and the extracted water, which is attributed to the 10 years of storage in plastic containers.

Full cores (whole cores) from the Bruce Nuclear site (DGR-4) equilibrated with a synthetic brine for just over 600 days were tested as part of a benchmarking exercise. In Figure 5-5, the $\delta^{18}O$ and δ^2H porewater values are plotted with the values measured for the saturating water (snowmelt from Ottawa), in addition to the values measured for equivalent-depth porewaters in DGR-5 core. The porewaters are close to the saturating snowmelt but form a trend towards the original DGR5 porewaters for these rocks. Also, a slight enrichment in deuterium exists such that the trendline falls above that of the saturating water. While geochemical exchange seems complete (measured to within about 5 percent), isotope exchange is incomplete for all samples. The trendline toward the initial value of the porewater is evidence of incomplete exchange.

The minor enrichment in deuterium is attributed to an additional incomplete exchange for deuterium with clay waters. This reservoir is likely sampled during extraction but is not considered to greatly alter the overall porewater value. The preexisting deuterium enrichment from original porewaters likely has not exchanged to equilibrium with the deuterium-depleted snowmelt water, yieding a slight enrichment. The much better agreement seen for the 10-year gravels suggests that, over time, this reservoir would also equilibrate with a different saturating solution. Note that were this to be an artifact of hydrogen contributions from clay minerals, the opposite effect would be observed, yielding a depletion in the porewaters.
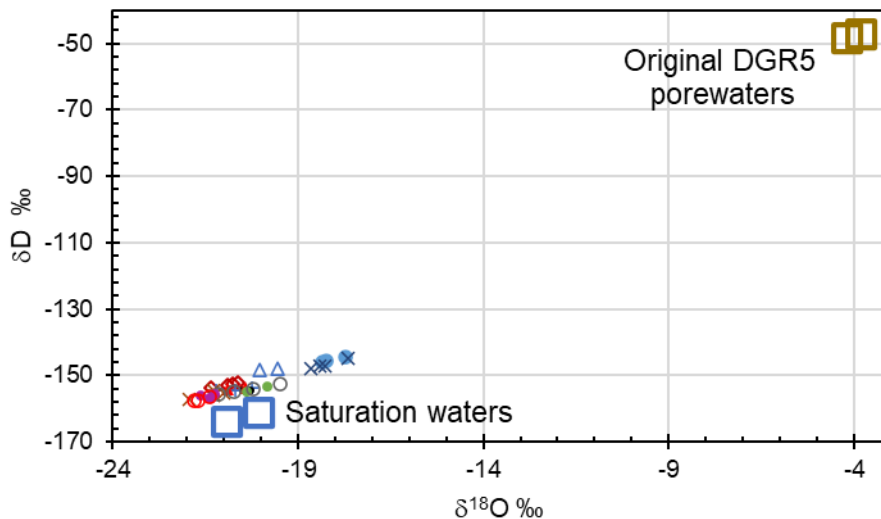
Figure 5-5: Out-diffusion was Run for 8 Weeks Before Measurements for Major Ion Chemistry Using Synthetic Porewater; Overall Concentration Ratios for Conservative Elements (Na, Cl) are Very Close to 1.0. For the Reactive Elements, Including Br (Organophilic), the Ratios were 1.11, 1.29 and 1.59 (Mg, Br, K).

Continuing work at the University of Ottawa focuses on the extraction of porewater from rock cores into cellulosic papers for analysis of the porewater composition (using the sedimentary cores that were saturated in the synthetic porewater for 600 days). Work focused on verification of the major-ion data, using core samples that have been equilibrated with a known synthetic porewater composition, are presented. The results are then benchmarked against the composition of the synthetic porewater. The experiments for verification of the porewater chemistry are complete and results are encouraging (see Table 5-2).

Table 5-2: Ratio of Ions Obtained from Aqueous Leaching Post Vacuum Distillation Relative to the Ions from Synthetic Porewater Initially Used to Saturate Sedimentary Whole-Core Samples (Rose 2018)

Ion	Na	K	Mg	Ca	Cl	Br	SO$_4$
Concentration ratio (mg/kgw)	0.93	1.59	1.11	0.92	1.02	1.29	214.15
Ratio Standard Deviation	0.07	0.16	0.16	0.21	0.07	0.05	234.53
Count				18			

The table presents the ratio of the ion concentrations obtained from aqeuous leaching relative to the ions from the original saturating synthetic porewater (within error) suggesting agreement. One exception is the sulfate anion, in which case the concentration of sulfate obtained from the aqueous leachates far exceeded the concentration from the original synthetic porewater (Table 5-2). This can be attributed to the oxidation of sulfide minerals during the leaching of the gravels using oxic H_2O.

5.1.3.5 Stable Water Isotopes in Clay-bound Water

Reliable measurement of the hydrogen- (H) and oxygen- (O) isotope compositions of porewater entrapped in Paleozoic shales in southern Ontario presents a challenge because of the very low water-contents of these rocks and possible porewater interaction with clays and other minerals. There is potential for modification of original porewater H- and O-isotope compositions from: [1] exchange between porewater and structural H and O in clay minerals, and [2] H- and O-isotope fractionation between mobile and bound water, depending on the method of porewater analysis.

Research at Western University focuses on the H- and O-isotope compositions of clay minerals in Ordovician shales from the Bruce Nuclear Power Generating Station ("Bruce Site") to try to understand the impact of these processes. Previous key findings this work include: 1) abundances of illite > kaolinite > chlorite comprise the <2μm fraction of these shales; 2) the clay mineral H- and O-isotope compositions plot to the left of terrestrial clay weathering lines in H- and O-isotope space; 3) calculated water H- and O-isotope compositions in equilibrium with these clay minerals at maximum burial temperatures (~90°C) match porewater H- and O-isotope compositions measured by three techniques; and 4) apparent H-isotope clay mineral-water exchange (0.4-3%) occurred in 10-week experiments at 68°C. These preliminary data suggested that isotopic exchange with clay mineral structural H can modify porewater H-isotope compositions in low water-content shales.

In 2022, significant progress was made with regard to process. The analytical challenge of separating adsorbed water from structural hydrogen in clay minerals for purposes of hydrogen isotope analysis was solved (N. Kanik MSc thesis; Kanik et al., *Applied Clay Science* 216 [2022]), which makes evaluation of H-isotope exchange between porewater and structural H in swelling clay minerals, such as smectites, possible.

Experiments were completed that measured the amount of apparent H- and O-isotope exchange between isotopically labelled deionized water and Clay Mineral Society (CMS) standard illite, kaolinite, chlorite and smectite, and clay mineral assemblages from the Bruce Site, held at 90, 120 and 150°C for 8 weeks. Significant H-isotope exchange occurred; the amount of exchange varied with clay mineral type but always increased at higher temperatures. For K-saturated samples held at 150°C, the amount of H-isotope exchange was 30% for Fe-smectite, 15-20% for Al-smectite, ~10% for kaolinite, ~5-10% for Mg-smectite, ~5% for illite and

~5% for chlorite. Clay surface cation-type had little effect on the amount of exchange, except for Al-smectite, for which the Na^+-form showed 30% exchange. At the Bruce Site, the amount of H-isotope exchange affecting the clay mineral assemblage ranged from 5-10‰ at 90°C to 10-15% at 150°C. Significant apparent O-isotope exchange was also detected, which had not been predicted. For illite, there was 30% exchange of octahedral O at 90°C (5% total O), rising to 90% exchange of octahedral O at 150°C (15% total O). For kaolinite, there was 5% exchange of octahedral O at 90°C (~2% total O), rising to 55% exchange of octahedral O at 150°C (25% total O). For the clay assemblage at the Bruce Site, there was 25-35% exchange of octahedral O at 90°C (4-6% total O), rising to 185-280% exchange of *"octahedral"* O at 150°C (30-45% total O). The latter result suggests involvement of tetrahedral O in the isotopic exchange.

These results imply that H- and O-isotope exchange between the Ordovician clay mineral assemblage at the Bruce Site and shale porewater was likely at the maximum burial temperatures predicted for these rocks (90°C). Given their low water/rock ratios, such exchange has the potential to modify original porewater H-isotope compositions. Such effects, however, would be most pronounced in Al- and Fe-smectite-rich shales and mudstones and least pronounced in illite and kaolinite-dominated rocks, like those of the Bruce Site. Next steps include completion of the O-isotope analysis of the clay minerals, especially smectites, used in the 8-week experiments, longer duration exchange experiments (50 weeks), use of brine rather than fresh test waters in some exchange experiments, examination of the isotopic exchange characteristics of Bruce Site whole-rock powders rather than only the <2μm clay size-fraction, and microscopic characterization of the reaction products from the exchange experiments.

First steps towards addressing question [2] (see first paragraph) were possible in the latter half of 2022. In July 2021, a new thermogravimetric analyzer (TGA) funded by NWMO was installed and used to develop high resolution, bound water plus hydroxyl group weight loss profiles for CMS standards illite, kaolinite and chlorite, and <2μm size-fractions of the Ordovician shales from the Bruce Site. In July 2022, a new laser-based water-isotope analyzer (CRDS) (50% funded by NWMO) was acquired, assembled, and work initiated to interface this unit with the TGA. The TGA-CRDS system under development (first in Canada, third in the world) is a sophisticated effort to release bound water from minerals or rocks using a TGA and sweep this water vapour directly to a CRDS for H- and O-isotope measurements. Such data should make possible determination of bound water–mobile water H- and O-isotope fractionations.

In September 2022, a TGA-CRDS interface prototype was constructed, and transfer of water released from the TGA to the CRDS attempted. The material tested was calcium oxalate hydrate ($CaC_2O_4 \cdot H_2O$), a common TGA calibration standard. Stoichiometrically accurate amounts of water were transferred from the TGA to the CRDS, and consistent but uncalibrated H- and O-isotope compositions were obtained for the water. Efforts continue to calibrate the TGA-CRDS system to the international standard (VSMOW) for water H- and O-isotope compositions. Next steps will then be to extract and isotopically analyze water from a range of standard clay minerals using the TGA-CRDS system and develop methods to benchmark this technique.

5.1.3.6 Binding State of Porewaters – NEA CLAYWAT Project

The CLAYWAT project, launched by the NEA Clay Club, is targeted at an improved understanding of the binding state of water in the nanometric pore space of argillaceous media. In addition to a literature review of methods of potential use in this context, the project included

an experimental programme on samples received from the Clay Club membership. A suite of measurements and experiments were performed by a number of laboratories, including differential thermogravimetry (TGA), differential scanning calorimetry (DSC), evolved gas analysis (EGA), mass loss upon heating to steady state at different temperatures, ad- and desorption isotherms for H_2O, N_2 and CO_2, and others. Further, nuclear magnetic resonance (NMR) relaxometry and imaging were applied to quantify porosity, pore-size distribution, to identify the relevant 1H reservoirs in the rock, to quantify diffusion coefficients for H_2O as well as to image the degree of heterogeneity of the 1H distribution in the samples.

Two abstracts were presented at the 2022 Clay Conference on work completed as a part of the project. In addition, the final draft of the NEA CLAYWAT Project report was provided to all Clay Club members for review in 2022.

5.1.3.7 Porewater Gases - Mont Terri PC-D Experiment

The NWMO is currently leading the Porewater Gas Characterization Methods (Non-inert and Noble Gases): Field and Laboratory Methods Comparison (PC-D) Experiment at the Mont Terri URL. The objectives of the experiment are to: 1) compare results obtained for gas concentrations and isotopes using different methods used by various nuclear waste management organizations to assess the comparability of different methods for homogeneous rock cores extracted from within the same shale unit (lower shale facies in the Opalinus Clay), and 2) assess the data from various approaches to determine if alternative (short-term or novel) methods can yield satisfactory results for site characterization needs in potentially less time than the current standard out-gassing approach employed by numerous researchers and laboratories around the globe for the purpose of gas characterization.

Over the course of 2020, due to delays associated with the global COVID-19 pandemic, emphasis was placed on experimental planning and establishing a drilling contract for an experiment-specific borehole. In September 2021, the PC-D borehole (BPC-D1) was drilled, parallel to being in the lower shale facies, with five regularly spaced sampling intervals over its 20-m length. Samples for noble and non-inert gases were collected adjacent to one another in each sampling interval for the three participating laboratories (Hydroisotop GmbH, University of Ottawa and GFZ Helmholtz – supported by BGR), as well as complementary samples for porewater chemistry analytics (to be run using the absorptive paper method). Over the course of 2022, the laboratory analytics began, and several analyses (short-term) were completed. Long-term samples are still running at select laboratories and these data will be collected early in 2023. The analytics, data compilation (including review and comparison of previous noble and non-inert gas data from within the lower shale facies in other experiments at the Mont Terri URL) and overall findings of the comparison study are anticipated to be ready for publication in a Mont Terri Technical Report in 2024.

5.1.3.8 Mont Terri Geochemical Data (GD) Experiment

The NWMO is a partner in the Geochemical Data (GD) Experiment at the Mont Terri Underground Research Laboratory (URL) in Switzerland. The GD Experiment aims to collect and evaluate data from various activities in the URL, in terms of assessing coherence with the established porewater conceptual model for system evolution. Open questions that are identified in the model(s) or in the understanding of behaviour often become targeted research projects within GD (e.g., lab investigations, in-situ measurements and/or modelling activities). In 2022, work as a part of GD was focused on the following key projects: 1) carbonates in clay

rocks, 2) redox and the role of Fe-containing minerals in controlling system E_h, and 3) assessment of trace elements in porewaters.

5.1.4 Transport Properties of the Rock Matrix

Near-field performance, safety assessment and groundwater transport/evolution models require knowledge of groundwater and porewater geochemical compositions, as well as petrophysical and solute transport properties, to provide representative estimations of long-term system behaviour. The following research programs contribute to the NWMO's technical capabilities in the context of assessing long-term solute mobility and retention.

5.1.4.1 Permeability

Recent research at McGill University focused on the estimation of the permeability of cuboidal blocks of granite obtained from Lac du Bonnet (western flank of the Canadian Shield) and from Stanstead (eastern flank of the Canadian Shield).

5.1.4.1.1 Permeability Characteristics of the LdBG

A technique for measuring the effective permeability of a large cuboidal specimen of Indiana limestone measuring 450 mm was developed by Selvadurai and Selvadurai (2010). The procedure involves measurement of surface permeability at nine locations of all six faces of the cuboid and extending the surface data to the interior of the cuboid using a kriging technique. The methodology enables the estimation the spatial distribution of permeability of the rock and this data is combined with a finite element technique to estimate the effective permeability in three orthogonal directions. These estimates are used to determine the geometric mean of the permeability for the cuboidal region. This procedure was adopted to determine the effective permeability of a cuboid of the LdBG measuring 300 mm. The data are reported in Selvadurai et al. (2020) and the estimates for the geometric mean-based permeability of the LdBG varied between $0.84 \times 10^{-19}\,m^2$ to $1.09 \times 10^{-19}\,m^2$. The permeability estimates for the LdBG obtained from small sample testing and in situ testing range from $34 \times 10^{-19}\,m^2$ to $53 \times 10^{-19}\,m^2$.

The nearly an order of magnitude difference between these studies need to be further investigated. In this regard, the work in the EGL focused on the permeability testing of a cylindrical sample of LdBG measuring 150 mm in diameter and 300 mm long containing a co-axial cylindrical cavity of diameter 10 mm and depth 50 mm. Steady state permeability tests were used to determine the permeability of the LdBG. The details of the investigation are in preparation for publication. The estimated permeabilities range from $0.67 \times 10^{-19}\,m^2$ to $0.88 \times 10^{-19}\,m^2$. These estimates for the permeability obtained from the cavity permeability tests are close to the values obtained by Selvadurai et al (2020) from surface permeability testing of the 300 mm cuboid. The discrepancies between the values reported in the literature therefore needs further investigation.

5.1.4.1.2 Permeabilities of Stressed Fractures in LdBG Specimens

Research activities have also been initiated into examining the fluid transport behaviour of a crack in a cylinder of the LdBG tested in the Obert-Hoek Cell. The samples tested in the Obert-Hoek Cell had dimensions of approximately 83 mm in diameter and 140 mm long and the longitudinal crack wea located approximately along a diametral plane. The initial average aperture of the fracture was measured using DEMEC gauges installed prior to the installation of

the fracture. The sample containing the crack was subjected to progressively increasing axial stresses and radial stresses maintaining the combined stress state in an isotropic condition. Steady state flow was initiated using the Quizix QX 6000 pump. The details of the experimental approach as applied to the stress-assisted permeability evolution in the Cobourg limestone is documented by Selvadurai and Głowacki (2017). The alterations in permeability can be calculated using the parallel plate model, only if the aperture changes with isotropic compression can be measured. In the Obert-Hoek cell arrangement, with the fracture in the diametral plane, there is no opportunity to measure the fracture aperture closure. Therefore, attention is directed to estimating the aperture closure using computational modelling. For this purpose, the fracture surfaces of the opened fracture are scanned using the CREAFORM HandiSCAN 307 (Figure 5-6). The future research will involve the incorporation of the scanned surface data to create a model of the fracture in the multi-physics code COMSOL. The aperture closure with stress will be examined using the computational model and fluid flow through the aperture will be modelled using three-dimensional representations of the aperture with contact zones subjected to either potential flow or Stokes' flow. This will enable the estimation of fracture permeability evolution with isotropic compression of the fracture (a journal manuscript is in preparation), The work will be extended to investigate the shear behaviour of planar diametral fracture tested in the Obert-Hoek cell under relative shear at a given radial compression (a journal manuscript is in preparation).
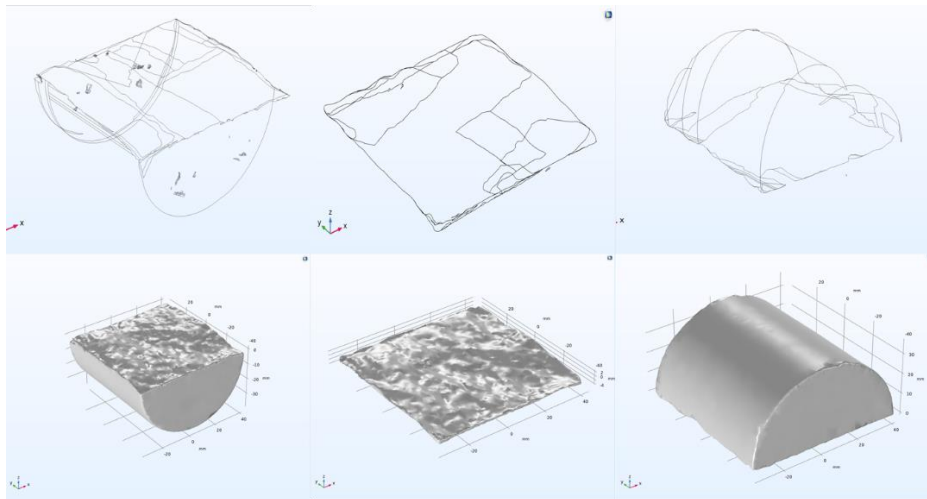
Figure 5-6: Surface Scans of Fractures Created in a Lac du Bonnet Granite Cylinder.

5.1.4.2 Diffusion Properties

5.1.4.2.1 Method Development – X-ray CT Imaging

The University of Ottawa acquired an X-ray CT system in 2016, and recent work has focused on optimizing measurement parameters for tracer experiments. The instrument has been modified to allow X-ray spectrometry, in order to minimize the effects of beam hardening and increase signal-to-noise ratios for improved tracer detection. The spectrometry system is operated in two modes, X-ray absorption in transmission mode and X-ray fluorescence. Both the X-ray absorption and fluorescence approaches have been successfully developed to monitor iodide and cesium diffusion in Queenston Fm shale and the data demonstrate that beam hardening effects are virtually eliminated. The X-ray fluorescence technique has potential for experimental monitoring of diffusion and reaction processes with a diverse range of tracers that are of interest

for evaluation of transport and attenuation properties in the near field. To date, X-ray measurement techniques have been developed using 2D and 3D imaging modes, radiography and computed tomography, respectively, and spectrometry mode (absorption and fluorescence).

5.1.4.2.2 Mont Terri Diffusion Experiments – DR-B, DR-E, CI, and CI-D

The NWMO is a partner in the DR-B long-term diffusion experiment in undisturbed Opalinus clay, the DR-E long-term diffusion experiment in the fault zone, the CI long-term cement-Opalinus clay interaction experiment, and the CI-D diffusion across 10-year-old concrete/claystone interface experiment at the Mont Terri URL.

The objectives of the DR-B experiment are i) to develop a means for the long-term monitoring (>10 years) of in-situ iodide diffusion process at a large scale in a clay formation; and ii) to validate the diffusion process understanding developed and transport parameters determined through previous experiments. The experimental setup consists of a central borehole and 3 surrounding observation boreholes. Sodium iodide (NaI) solution was injected in the central borehole in April 2017 and is expected to diffuse over time toward the observation boreholes. Starting in November 2018, a breakthrough of iodide in the observation borehole located closest to the injection borehole was observed. The iodide concentration in the observation boreholes has been measured regularly (Jaquenoud et al. 2021).

The DR-E experiment investigates tracer migration (including diffusion) in the main fault zone within Opalinus clay. The experimental setup includes two injection boreholes for multi-tracer solutions (including cations, anions, neutral species), one borehole will target the central part of the main fault zone, and the second one will target the upper boundary zone of the main fault zone. The objectives of the experiment are i) to investigate tracer migration (including diffusion) within the fault zone of Opalinus clay over long time period to provide effective transport properties of radionuclides for safety assessment calculations; ii) to determine if self-sealing and healing mechanisms of clay within fault zones apply as expect; and iii) to investigate if enhanced anisotropic permeabilities with respect to undisturbed shale zone are present.

The CI long-term (> 10 years) experiment is intended to complement the current knowledge on the influence of cement on Opalinus clay and bentonite. Three types of cement are used in the experiment: ordinary Portland cement (OPC) and two types of low-pH cement (LAC and ESDRED). The objectives of the CI-D experiment are i) to assess the impact of the long-term (10 years) cement-Opalinus clay interface reactions (CI experiment) on diffusion of solutes (^{3}H and ^{36}Cl); and ii) to provide in-situ data for reactive transport modelling. The CI-D experiment setup consists of a borehole filled in 2007 with three different types of concrete (OPC, LAC and ESDRED) and compacted bentonite (MX-80) (borehole for the CI experiment), an injection borehole, and monitoring boreholes. High pH fluid circulation started in July 2018, and tracer (^{3}H, ^{36}Cl) injection has started since May 2019. The CI-D experiment is expected to last for 3 – 4 years. An international joint CI/CI-D modelling team is modelling the alteration due to cement-clay interaction and the tracer transport across such interfaces with different reactive transport codes including MIN3P-THCm (e.g., Su et al. 2022; Prasianakis et al. 2022). A CI/CI-D modelling meeting was taken place in May 2022. The overcoring of the CI-D experiment is planned in 2023.

5.1.4.3 Sorption

Sorption is a mechanism for retarding sub-surface radionuclide transport from a DGR to the environment. The NWMO has initiated the development of a sorption distribution coefficient (K_d) database for elements of importance to the safety assessment of a DGR (Vilks 2011). This initial database was further developed to include sorption measurements for Canadian sedimentary rocks and bentonite in saline solutions (with ionic strength I = 0.23-7.2 M) including a reference porewater SR-270-PW brine solution (Na-Ca-Cl type with I = 6.0 M) (Vilks and Yang 2018).

Researchers at McMaster University continue to systematically study sorption properties of Se, Tc, U and Eu on limestone, shale, illite and bentonite (MX-80) in Na-Ca-Cl brine solutions including SR-270-PW, as well as on crystalline rocks and bentonite in Ca-Na-Cl solutions including a reference groundwater CR-10 (Ca-Na-Cl type with I = 0.24 M) under reducing conditions. The effects of ionic strength and pH on Se, Tc and Eu sorption on shale, illite, limestone, bentonite and crystalline rocks have been investigated (Walker et al. 2018, 2022; Racette et al. 2019; Yang et al. 2022). It was found that sorption of Se(-II) on illite and MX-80 showed little ionic strength dependency across the ionic strength range of 0.1-6 M. Sorption of Se(-II) on shale at low ionic strength (0.1 M and 0.5 M) were greater than those at higher ionic strength of 1-6 M. Sorption of Eu on bentonite was not affected by the ionic strength between 0.5 M and 6 M, while sorption at ionic strength 0.1 M is greater than those at ionic strength 0.5-6 M (Yang et al. 2022). Sorption of Se, Tc, Np, U and Eu were measured on crystalline rock samples biotite granodiorite tonalite, amphibolite and diabase dyke collected from three boreholes in the Ignace area in reference groundwaters CR-10, CR-10NF (CR-10 in equilibrium with bentonite and carbon-steel container) and CR-0 (Na-Ca-HCO$_3$ type water with I=0.007 M) under both oxidizing and reducing conditions.

A new research program was initiated in 2021 to study the sorption of Pd on biotite, quartz and feldspar in Ca-Na-Cl saline solution using batch experiments, sorption modeling and DFT (Density Function Theory) calculations. Quartz and feldspar are the main mineral components of granite, whereas biotite is a common but minor mineral component of granite which is considered to dominate the sorption of some radionuclides. The measured sorption K_d values will be used to update the NWMO sorption database for use in the safety assessment.

5.1.4.4 Surface Area & Cation Exchange Capacity

In 2018, the University of Bern completed research to characterize external surface area (BET) and cation exchange capacity (CEC) in sedimentary rock cores from the Bruce Nuclear site. Samples from the Queenston, Georgian Bay, Blue Mountain and Collingwood Member formations were evaluated (rock types included claystone, marl and limestone). The research focused on addressing the question of mineralogical fractionation induced by sieving to different grain sizes (i.e., can a specific fraction for geochemical experiments be used and the results considered representative of the whole rock?), as well as the effect of crushing on determined CEC values (e.g., does crushing create new mineral surfaces, and is it permissible to extrapolate geochemical data obtained on disintegrated or crushed material to the intact rock?). The main findings of this work were compiled into a Technical Report for the NWMO in 2019. A modified version of the final report is anticipated to published by the NWMO in 2023.

5.1.5 Geomechanical Properties

5.1.5.1 In-Situ Stress

The in-situ stress state is a fundamental parameter for the engineering design and safety assessment of a DGR. Obtaining reliable estimates of in-situ stress is important, however, this is often hindered by small numbers of field stress measurements as well as by variability arising from the geological environment. Bayesian data analysis applied to a multivariate model of in-situ stress can potentially overcome these problems and generate a multivariate stress tensor for a site. In 2020 together with SKB (Sweden), NWMO initiated a new research program at the University of Toronto to investigate the use of Bayesian data analysis in the statistical quantification of in-situ stress variability.

During 2022 further progress was made on developing and applying Bayesian linear regression of in situ stress, and development began on a Bayesian hierarchical Multivariate (MV) linear regression model for in situ stress. This latter model is capable of computing complete distributions of covariance matrices. Several analyses of extensive overcoring stress measurements from the SKB Forsmark site in Sweden were performed and presented to NWMO and SKB as part of project quarterly progress review meetings.

Two conference contributions on Bayesian linear regression of in situ stress were made during 2022 (Javaid et al., 2022a and 2022b). A paper on the use of Bayesian regression techniques and metrics to determine stress domains at the Forsmark site is being written for the ISRM Congress 2023. Furthermore, a poster that summarizes the research performed during the STRESSBAY project was presented at the NWMO Geoscience Seminar in June 2022.

5.1.5.2 Rock Properties from Laboratory Experiments

The focus of the research activities was primarily directed to preparing investigations of the experimental and computational approaches that can investigate the thermo-hydro-mechanical behaviour of both the intact and fractured Lac du Bonnet Granite (LdBG) from a quarry in Manitoba. In its supplied condition the blocks of the granite measuring 500 mm x 500 mm x 350 mm were competent and contained no observable surface defects. Coring was performed to extract samples of variable diameters and lengths for performing tests on the LDBG samples.

5.1.5.2.1 Elasticity Properties and the Biot Coefficient for the LdBG

The elasticity properties of the granite are an important input to any thermo-poroelastic model. The elasticity properties were determined using oven dried samples of the LdBG measuring either 100 mm dimeter and 200 mm long or 150 mm in diameter and 300 mm long. The results of these studies were reported in Selvadurai (2021). The Young's modulus was estimated to be in the range 70 GPa and Poisson's was in the range 0.21. These estimates compare favorably with values determined by other researchers that ranged from 68 GPa to 70GPa for the Young's modulus and 0.21 to 0.30 for the Poisson's ratio. More recently, Uniaxial tests were performed on LdBG samples measuring 83 mm in diameter and 140 mm long and the Young's modulus was estimated to be 71.4 GPa and the Poisson's ratio around 0.22. The experiments conducted at the Environmental Geomechanics Laboratory provided accurate estimates for the isotropic elasticity parameters for the LdBG, which can be confidently used in THM modelling.

The work was also extended to the estimation of the Biot coefficient for the LdBG. The skeletal elasticity properties were determined using the elasticity estimates for the oven dried rock determined in the laboratory. The estimation of the compressibility of the solid material composing the porous skeleton were determined using a multi-phasic approach that took into consideration the mineralogical compositions of the LdBG determined from X-Ray diffraction studies conducted at the McGill Institute for Advanced Materials, using the Bruker d8 Discovery X-ray Diffractometer. The mineralogical compositions are reported in Selvadurai (2021) and they compare favorably with estimates derived by other research groups. Using the multiphasic approach and the theoretical developments of Voigt, Reuss, Hill and Walpole, the bulk modulus for the skeletal solids was estimated to be between 53.3 GPa and 58.2 GPa. This enabled the calculation of the Biot coefficient for the LdBG which ranged from 0.30 to 0.31. The article by Selvadurai (2021) also provides a detailed record of estimates for the Biot coefficient for the LdBG. The estimates vary from 0.20 to 0.73. The wide variability of published data for the Biot coefficient for the LdBG needs further investigation. Additional research related to the estimation of the Biot coefficient for geomaterials was presented in a review article by Kasani and Selvadurai (*submitted*) and developments related to influence of grain contact processes and porosity on the estimation of the Biot coefficient are discussed by Selvadurai and Suvorov (2022).

5.1.5.3   Rock Properties from In-Situ and/or Large-Scale Experiments

5.1.5.3.1 POST Project

The activities in 2022 continued with testing rock joints at the intermediate scale, 70 × 100 mm, and at the large scale, 300 × 500 mm. Eleven more specimens of the intermediate scale were tested (which brings the total to twelve tested specimens in this program); where half of them had a natural rock joint and the other half had a tensile-induced rock joint. Six specimens were tested under constant normal stiffness (CNS) conditions and the other six specimens under constant normal load (CNL) conditions.

Four specimens were tested at the large scale using the novel large scale direct shear machine manufactured in this program Figure 5-7a). In total, four specimens with a natural rock joint and six specimens with a tensile induced rock joint have been tested in this program. Six specimens were tested under CNS conditions and four specimens were tested under CNL conditions. Figure 5-7b shows an exposed fracture surface of a specimen installed in the shear testing machine before testing.

The preparation of the tests of the small-scale specimens, 35 × 70 mm, have started, but the actual tests were put on hold until beginning of 2023.

Direct measurements of the relative displacement of the rock joints using an optical system were added to some the tests done at the intermediate scale. Acoustic emission measurements were carried out during the experiments of the intermediate and large-scale tests. The acoustic emission measurements, funded by RISE, are outside the POST project.

Results evaluations of the intermediate and large-scale experiments have started. The plan is to begin to release public reports from the project during 2023. An abstract to present experiments from the large-scale tests was submitted to the ISRM 2023 Congress in Salzburg, Austria.

The work on studying the quality assurance of producing replica samples of rock joints has continued within the associated PhD-project about scale effects, with partial funding from Swedish Rock Engineering Research Foundation (BeFo) resulting in two publications (Larsson et al., *submitted* a,b).

a)
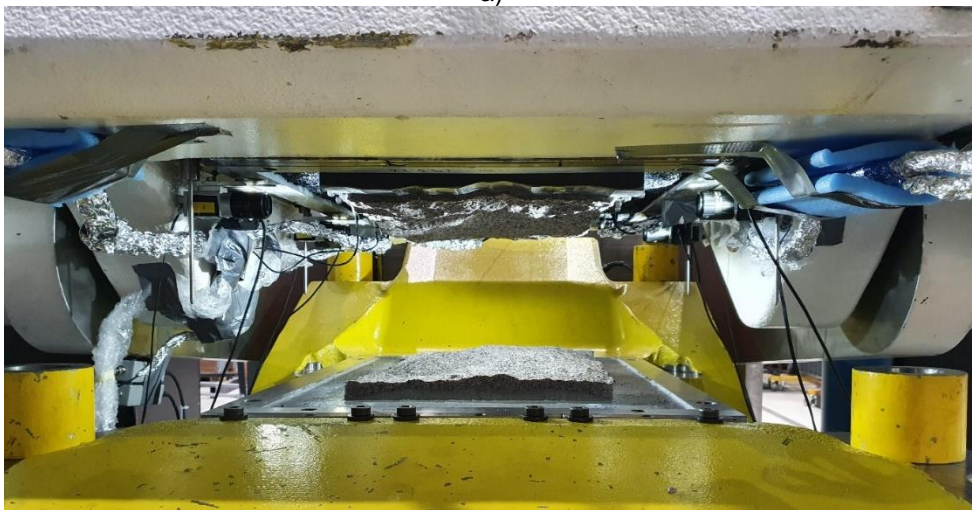
b)

Figure 5-7: POST Project: a) Large-scale Direct Shear Testing Machine Manufactured in this Program (Jacobsson et al 2021), and b) a 300 x 500 mm Specimen with a Tensile Induced Fracture Before Testing. Note that the Scale in Inset Figures a and b are not the Same.

5.1.5.3.2 Mont Terri FE-M Project

The FE-M experiment, long-term monitoring of the full-scale heater test, continues with the heating phase which commenced in December 2014. This experiment was designed to

demonstrate the feasibility of: (1) constructing a full-scale 50 m long and 3 m in diameter deposition tunnel using standard construction equipment; (2) heater emplacement and backfilling procedures; (3) early post-closure monitoring to investigate repository-induced coupled thermo-hydro-mechanical (THM) effects on the backfill material and the host rock (i.e., Opalinus Clay); and (4) validation of THM models.

Field measurements are on-going include temperature, pore-water pressure, humidity/water content and suction, thermal conductivity, deformations, and stresses. The program is currently focused on the long-term monitoring of the THM processes confirming the technical readiness of the conceptual modelling framework pertinent to assessment of the long-term performance in the near field scale. Nagra has established a THM modelling task force consisting of Technical University of Catalonia (UPC), the École Polytechnique Fédérale de Lausanne (EPFL), and BGR/TUBAF/UFZ. In 2022, modelling activities continued, which comprises code and calculation verification of TH and THM model results amongst the three teams which used Code_Bright, Code_Aster and OpenGeoSys, respectively.

5.1.5.3.3 Mont Terri GC-A Experiment

The main objective of this experiment is to understand the geomechanical in-situ response of the Opalinus clay during excavation at the transition from shaly to sandy facies. This experiment consisted of multiple components including:

- Monitoring of the excavation convergence and pore pressure response,
- Laboratory and field geophysical measurement of static and dynamic elastic properties of the Opalinus clay, and
- In-situ stress measurements.

5.1.5.3.4 Shear Induced Pore Pressure Around Underground Excavations

A new Ph.D. research project, co-funded by NWMO and Nagra, was initiated at the University of Alberta (UAlberta) in 2020. The overarching objective of this research is to advance the understanding of the coupled hydro-mechanical processes that occur during underground excavations in heavily overconsolidated clays and weak rock-like shale deposits.

Previous field tests completed at Mont Terri Underground Rock Laboratory (Mont Terri) established that deformations around underground openings in Opalinus Clay are highly dependent on the direction of the excavation relative to the materials bedding. Excavations completed in a direction parallel to the materials bedding have shown higher pore pressures, yielding at relatively small strains compared to laboratory results, and larger than predicted deformations. This research program examines these findings through two mine-by experiments completed at Mont Terri, one parallel and one perpendicular to the materials bedding, where instruments were strategically placed in front of and around the tunnel's excavation zone. The findings from these experiments will then be compared to the results of a laboratory testing program. The laboratory program utilizes a novel direct shear apparatus that is being developed at UAlberta. This apparatus will be the first to incorporate micro fibre optic pressure sensors (MFOPs) into a direct shear test to measure the pore pressure response along the shear zone of the sample while applying a strain-controlled boundary condition.

During 2022, research advances for laboratory work included 1) a successful triaxial testing program demonstrating the functionality of utilizing MFOP inside of clay samples; 2) a

successful testing program utilizing a one-dimensional consolidation device constructed specifically for this program at UAlberta. This device applies up to 20 MPa of force to a sample to create heavily overconsolidated samples for testing; 3) the design and partial construction of the aforementioned novel direct shear apparatus as shown on Figure 5-8 below. Advances for the field component includes the creation of two 3D anisotropic-elastic ubiquitous joint models of the mine-by experiments completed at the Mont Terri using the program FLAC3D. Initial processing of the models shows good correlation when comparing in-situ pore pressure measurements against the model's stress analysis converted to pore pressure through Skempton's parameters.
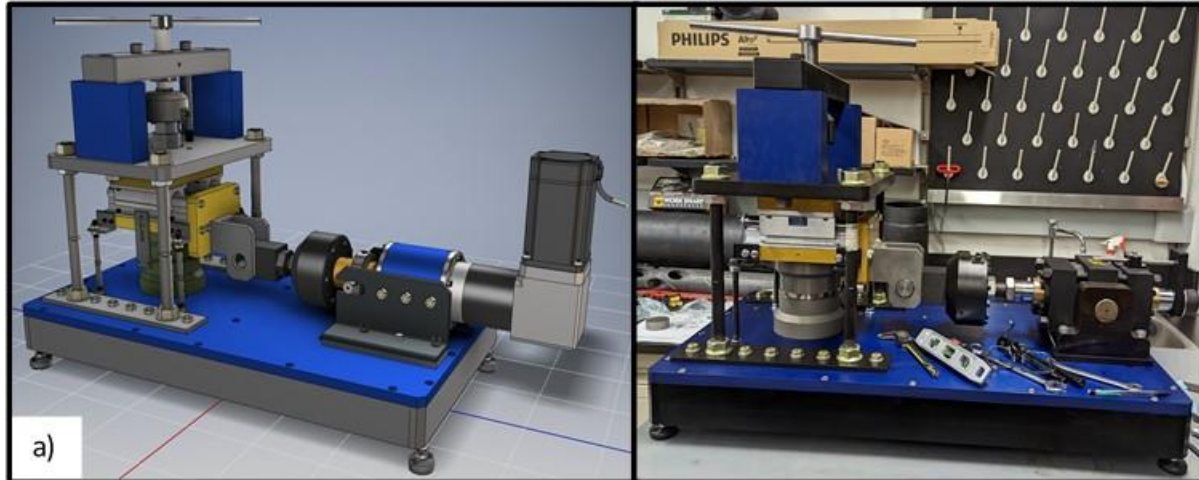
Figure 5-8: Novel Direct Shear Device Incorporating Fiber Optic Sensor Along Shear Plane of Sample. a) Original Design of Device for Planning and Construction Purposes. b) Device Under Construction in December 2022.

5.1.5.3.5 Field Trials of a New Tool for In-Situ Stress Measurements: Reservoir Geomechanics Pressuremeter

In 2021, NWMO joined with Nagra to provide support for their field trial of the University of Alberta's Reservoir Geomechanical Pressuremeter (RGP), a novel new tool for determining in-situ stresses and shear stiffness in sedimentary formations. Nagra's field trial was completed in December 2021. Nagra and NWMO are sharing information on the field campaign, including experience gained, testing results, and comparisons of the RGP results to results from other field tests (e.g., Hydrofracturing) and/or laboratory tests conducted by Nagra and used to verify the RGP measurements. This research agreement also includes the participation of Nagra personnel and information sharing for a field trial of the RGP by NWMO.

5.1.5.4 Numerical Modelling of Geomechanics

5.1.5.4.1 Rock Mass Effective Properties

This study aims at quantifying the rock mass effective mechanical properties from a DFN approach. The present phase of the project has started in 2020. During 2022, we carried out a synthesis work of the stress fluctuations analyses initiated in 2021, to elaborate the plan for a journal paper. With this work we have established the relationship between the stress dispersion coefficients (Gao and Harrison 2016, 2018a,b) and the DFN parameters. The journal paper is in

prep and planned to be submitted in Q1 or Q2 2023. These results were also presented at two conferences, the NWMO Geosciences Seminar in June in Toronto (Davy et al. 2022) and the Eurock conference in September in Helsinki (Lavoine et al. 2022).

In parallel, the Task 2 of the project started. The purpose of the task is to investigate the link between DFN properties and equivalent rock mass strength. The selected approach is similar to the one used in Task 1 for the stress fluctuations, it is based on numerical modeling of Synthetic Rock Mass (SRM) samples. The numerical set-up previously used is adapted to allow progressive failure in the rock around the fractures of the SRM when loaded under tensile or compressive conditions. The set-up is still developed with 3DEC. The Bonded Block Model (BBM) is selected for the representation of the rock surrounding the fractures. In this configuration, a SRM sampled is made as an assemblage of bonded polyhedral blocks which are deformable through zoning (defining sub-contacts) and which can fail at their sub-contacts. The characteristic size of these blocks is much smaller than the characteristic size of the fractures of the DFN. The block sub-contacts hence represent a network of small defects in the rock, which can fail (e.g., based on a Coulomb slip model). During a loading test, local failure of individual sub-contacts between blocks increases until the entire SRM failure occurs (peak strength).

A large number of tests (following the workflow illustrated in Figure 5-9) is performed to first test of the sensitivity of the results to the numerical parameters of the set-up and then to test the dependency of the micro and macro failure to a wide range of DFN models and realizations, both in tensile and compressive conditions. At the end of 2022 all the planned tensile tests and about half of the planned compressive tests are completed. Analyses are still in progress.
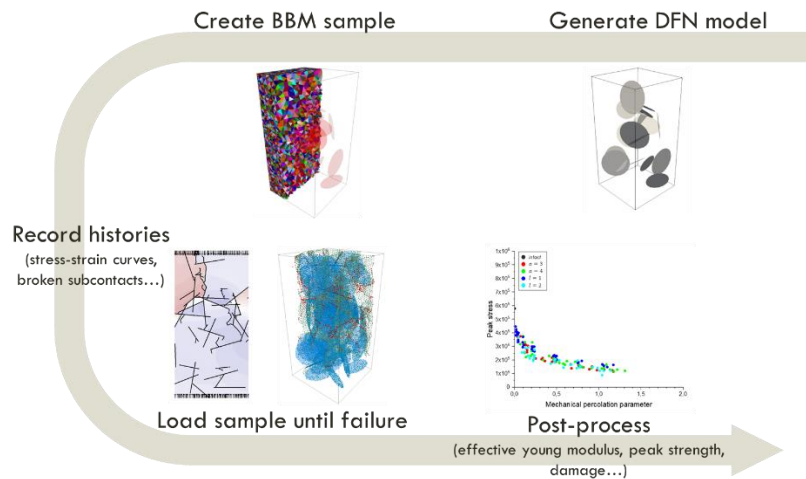
Figure 5-9: Illustration of the Modeling Workflow for the Testing of Synthetic Rockmass Model Samples with Various DFN Models and DFN Realizations

5.1.5.4.2   Determination of Biot and Skempton Hydromechanical coefficients for fractured rock masses (BIKE)

This study aims at defining equivalent Biot and Skempton coefficients for fractured rock masses, following a Discrete Fracture Network (DFN) approach to describe the rock mass.

The project began at the end of 2021 with a bibliographic review to support the formalization of the coupled Hydro-Mechanical (HM) behavior at the single fracture scale. The outcome of this task was to propose a way to estimate Biot's and Skempton's coefficients for a single fracture.

In 2022, the methodology was built-up to estimate the Biot and Skempton coefficients at the fractured rock mass scale. The proposed formal expressions for the equivalent Biot and Skempton coefficients, $\overline{\alpha}$ and $\overline{B}$, are given in the equation below. The rock mass is seen as the assembly of a rock into which discrete fractures are embedded, the rock and the fractures being the components of the rock mass, both linearly elastic. Acknowledging the assumption of no interaction, each component deforms according with its own mechanical properties, leading to the following expression:

$$\overline{\alpha} = \frac{\gamma^r \alpha^r + \sum_f \gamma^f \alpha^f}{\gamma^r + \sum_f \theta^f \gamma^f} \quad ; \qquad \overline{B} = \frac{\gamma^r \alpha^r B^r + \sum_f \theta^f \gamma^f \alpha^f B^f}{\gamma^r \alpha^r + \sum_f \gamma^f \alpha^f}$$

Where α^f and B^f are each fracture f Biot's and Skempton's coefficient, respectively; θ_f is the ratio is defined for each fracture as the ratio between the component of the applied stress that act normal to the fracture and the average applied stress; α^r is the rock Biot's coefficient, B^r is the rock Skempton's coefficient; and γ^i is the contribution of each component i (fracture f or rock r) to the total rock mass volume variation.

The validity of the proposed analytical expression was validated against estimations from numerical HM simulations performed in 3DEC7.0 (Itasca 2020).

Overall, during 2022, simplified expressions to quantify equivalent Biot and Skempton coefficients of a fractured rock mass were validated. They were then used to identify the impact of the DFN geometrical and mechanical properties on the rock mass behaviour. We have shown that the two coefficients strongly depend on the orientation of fractures with respect to the applied stresses and on the fracture stiffness. It is also evident that the impact of fractures increases with fracture density. More analyses are ongoing to apply the methodology to realistic in-situ fracturing conditions.

The results of the work were presented at two conferences, the NWMO Geosciences Seminar in June in Toronto (Davy et al. 2022) and the Coufrac conference in November in Berkeley (De Simone et al. 2022). One journal paper is currently submitted and a second is in prep.

5.1.5.5   NSERC Energi Simulation Industrial Research Chair Program in Reservoir Geomechanics

In 2019 NWMO joined the renewal of a multi-sponsor NSERC/Energi Simulation Industrial Research Chair (IRC) and Collaborative Research and Development (CRD) grant program in Reservoir Geomechanics at the University of Alberta. This IRC chair aims to advance experimental and numerical methods, as well as field studies, to help mitigate operation risks and to optimize reservoir management as they pertain to the coupled processes in oil and gas

reservoirs. Some of the findings are expected to be also applicable to sedimentary and crystalline rock settings for the geological disposal of used nuclear fuel.

Overall, participation in this multi-faceted IRC-CRD program is expected to advance our understanding of how intact rock and fractures at various scales respond to thermal-hydro-mechanical processes associated with a DGR. The first annual research symposium was held in February 2021 followed by the second symposium in May 2022. These symposiums provided sponsors with progress updates on all key research areas underway as part of the program.

5.2 LONG-TERM GEOSPHERE STABILITY

5.2.1 Long-Term Climate Change Glaciation

5.2.1.1 Surface Boundary Conditions

Glaciation associated with long-term climate change is considered the strongest external perturbation to the geosphere at potential repository depths. Potential impacts of glacial cycles on a deep geological repository include: 1) increased stress at repository depth, caused by glacial loading; 2) penetration of permafrost to repository depth; 3) recharge of oxygenated glacial meltwater to repository depth; and 4) the generation of seismic events and reactivation of faults induced by glacial rebound following ice-sheet retreat. The ability to adequately predict surface boundary conditions during glaciation is an essential element in determining the full impact of glaciation on the safety and stability of a DGR site and will be a necessary component supporting site characterization activities. For the NWMO's studies into the impact of glaciation, such boundary conditions have been defined based on the University of Toronto's Glacial Systems Model (GSM) predictions. The GSM is a state-of-the-art model used to describe the advance and retreat of the Laurentide icesheet over the North American continent during the Late Quaternary Period of Earth history.

Following the update to the GSM methodology and subsequent validation, a new phase of research is in progress with the goal of refining the representation of the evolution of paleolakes and surface drainage basins within the model, as well as further analyses of fits to relative sea-level data in Southeastern Hudson's Bay region. Additional modelling capabilities to University of Toronto GSM are currently being developed to deliver improvements to simulations of Laurentide ice sheet evolution.

During 2022, the incorporation of the latest PISM (Winkelmann 2011) based ice-dynamical core with coupled proglacial lakes, as well as approaches for representing surface drainage was refined, with a focus upon deglaciation and meltwater outflow in the St. Lawrence River area. The two main advances in the development of GSM were:

1) Incorporation of latest PISM-based ice dynamical core, with fully coupled proglacial lakes.
2) Development of graphical and postprocessing scripts for representing surface drainage results.

In addition, results from research conducted investigating the possible contributions from the Fennoscandian or British Isles ice sheets to a Henrich event (H3) which is known to have originated in Hudson Strait were published by Velay-Vitow et al. (2021).

5.2.1.2 Crustal Rebound Stresses

A new project to calculate the isostatic rebound (vertical rebound stress) at both sites was initiated in 2022 with the Swedish Land Survey (Lantmäteriet). The objective of this work program is to estimate the maximum glacially induced transient horizontal and vertical stresses for a range of depths at discrete intervals from the surface to below the deep geologic repository (DGR) horizon (down to several kilometers) around both the Ignace and South Bruce sites. The depths currently being examined for a deep geological repository at Ignace are 500 m, 650 m, or 800 m. In South Bruce, the host rock formation (Cobourg limestone) occurs at a depth of approximately 650 m. Stresses will be calculated with models that describe glacially induced lithospheric flexure and relaxation of the mantle over a time scale representing at least one full glacial cycle based on a new ice model for North America. The knowledge acquired through this work program will be used as input to long-term geomechanical stability analyses for both sites and will support safety assessments conducted by the NWMO. The calculated rebound stress components, when superimposed on the more contemporary lithostatic and tectonic stresses, will form the "total stress" of the in-situ stress regime.

The study makes use of updated boundary condition datasets from the ICE-7G models from the University of Toronto Glacial Systems Model (GSM) to calculate the maximum horizontal and vertical glacially induced stresses for a glacial cycle (using the timesteps from ICE-7G) in the areas of the two sites involved in NWMO's site selection process, i.e. Ignace and South Bruce. Elements of the work plan include:

1. Test of model resolution for most accurate stress determination and simultaneously efficient use of computation time
2. A brief review of the current knowledge of the subsurface structure in continental Canada and the regions surrounding the sites of interest.
3. Construction of stratified and three-dimensional complex GIA models.
4. Computation of the spatial and temporal evolution of the total glacially induced stress field which is a summation of the contributions from the evolving weight of the glacier ice, the melted ice water, and the oceans. The stress field also includes bending/fiber stresses and the migration of stress from the mantle to the lithosphere due to the loading. The faults before the onset of glaciation are assumed to be near equilibrium.
5. Investigation of sensitivity effects due to mantle viscosity, surface and mid-crustal weaknesses, and lateral heterogeneity in crust, lithosphere, and mantle.
6. Identification of areas for future research related to the understanding of faulting induced by glacial loading and unloading.

5.2.1.3 Glacial Erosion – Dalhousie University

The previous scope of work included two objectives. A state-of-the-science review of published information relating to glacial erosion in crystalline bedrock settings. A paper was submitted to Nature Geoscience (Norris et al, *submitted a*) and a revised version is expected to be accepted in 2023. A second, more comprehensive manuscript for submission to *Earth Science Reviews* will be competed in early 2023 (Norris et al., *submitted b*).

Starting In 2022 research focussed on four separate methodologies that will help the NWMO assess rates of erosion at the proposed sites. These are:

- Testing of the muogenic nuclide *paleotopometry method.*
- Testing of the muogenic nuclide *paleotopometry method* on the Canadian shield.
- Relative erosion efficacy under different ice sheet velocities.
- Stratigraphic chronology required to determine why some regions escape ice sheet erosion.

This work has been broken down into 5 tasks:

1. Muon Paleotopometry.
2. Collection of underground samples to test muon flux methodology.
3. GIS, sampling, and mapping of Newfoundland Ice Sheet (NIS) ice dynamics.
4. Sample processing - St. James Lowlands erosion.
5. Subsampling of selected pre-Wisconsinan tills in Alberta.

The Muon paleotopometry work (tasks 1-2), which will incorporate samples taken from the Alps in 2022 and new samples taken from the Copper Cliffs mine in Sudbury, is largely complete and two papers from this study are currently in preparation. Tasks 3-5 are anticipated to be completed by Q4 2023 with papers for 2024.

5.2.1.4 Final Borehole Sampling for Greenland Analogue Project (GAP)

Greenland Analogue Project (GAP) is a collaborative research project conducted by SKB, Posiva and NWMO between 2008 and 2013. The primary objectives of the original GAP were to enhance scientific understanding of glacial processes and their influence on both surface and subsurface environments relevant to the performance of DGRs for used nuclear fuel in crystalline shield rock settings. SKB is planning to terminate the field monitoring and maintenance in Greenland and hand over the GAP boreholes to Danish Technical University (DTU) in 2022. Before the termination and handover to DTU, NWMO jointly with SKB supported the final borehole sampling campaign which involves the withdrawal of high-quality water samples from one of the deep boreholes drilled during the GAP to study how groundwater flow and chemistry at depths equivalent to repository depth. Figure 5-10 is a photo taken in 2022 at the sampling borehole during the water sampling campaign in Greenland.
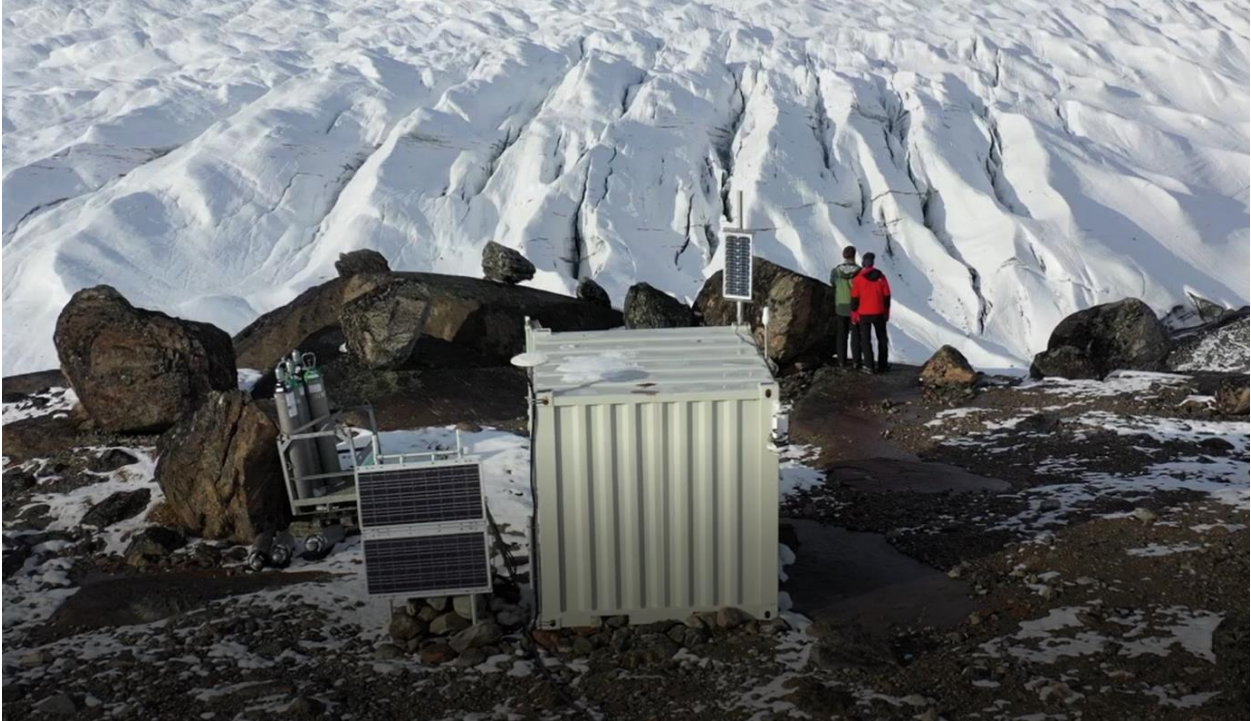
Figure 5-10: The Well-head Container of Borehole DH-GAP04 (Photo by Lillemor Claesson Liljedahl)

5.2.1.5 Glacial and Proglacial Environment – Numerical Modelling

5.2.1.5.1 CatchNet Project

CatchNet (Catchment Transport and Cryo-hydrology Network) is a joint international program formed by international nuclear waste organizations and cold region hydrology researchers (URL: https://www.skb.se/catchnet/). It was established in 2019 to advance our understanding of hydrological and biogeochemical transport processes for a range of cold-climate conditions in the context of long-term, deep geological disposal of used nuclear fuel. CatchNet has identified three research packages (RP) to address important knowledge gaps:

- RP1: connecting the glacial and sub-glacial hydrology with the periglacial hydrological system on landscape scale;
- RP2: permafrost transition periods;
- RP3: biogeochemical cycling.

With BGE and BMWK joining the CatchNet program in 2022, CatchNet has four full members (SKB, NWMO, RWM and BGE) and two supporting members (COVRA and BMWK). Each full member funds a PhD student or postdoctoral fellow to work on a research topic related to cold-climate conditions.

5.2.1.5.2 McGill University

As a full member of CatchNet, NWMO is supporting a PhD student based at McGill University. This PhD program started in September 2020 and the research topic is to examine the impacts of permafrost transition on surface and subsurface hydrologic processes.

In 2022, a working FEFLOW groundwater flow model was developed for Wolf Creek Research Basin (~ 195 km^2) in the southern mountainous headwaters of the Yukon River Basin in the subarctic region of northwestern Canada, Yukon. This model is used to investigate the effect of permafrost distribution on groundwater travel.

5.2.1.5.3 University of Montana – Joint Research with SKB

In 2019, NWMO and SKB initiated a project to support researchers at the University of Montana (USA) to study coupled ice sheet, groundwater, and surface water hydrological processes through new data analysis and numerical modeling. This modelling study uses the field data previously collected from two international projects (GAP and GRASP) in the Kangerlussuaq area of western Greenland. This joint project has focused on the following two main areas:

- Evolution of the thermal state of the ice sheet bed;
- Ice-sheet processes influencing the ice sheet - bedrock boundary and underlying groundwater pressures near the ice sheet margin.

The researchers work closely with the CatchNet program, participating in the CatchNet annual meeting and other activities regularly. In particular, the results of this study will be used as boundary conditions by CatchNet RP1.

In 2022, all data analyses were completed and two more journal articles documenting the results were published (Stansberry et al. 2022; Saito et al. 2022).

5.2.1.5.4 University of Laval

In 2022, a PhD program supported by NWMO was initiated at the University of Laval. The research program will be focused on numerical modelling of permafrost-impacted groundwater flow systems, aiming to deepen our understanding of the effect of permafrost growth and decay cycles on the thermal regime and groundwater flow field within the near and far-field environment of a DGR. This program will take advantage of the long-term field data collected from two well-characterized permafrost sites maintained by the University of Laval: Salluit (continuous) and Umiujaq (discontinuous). See Figure 5-11 for locations and permafrost conditions of these two field sites.
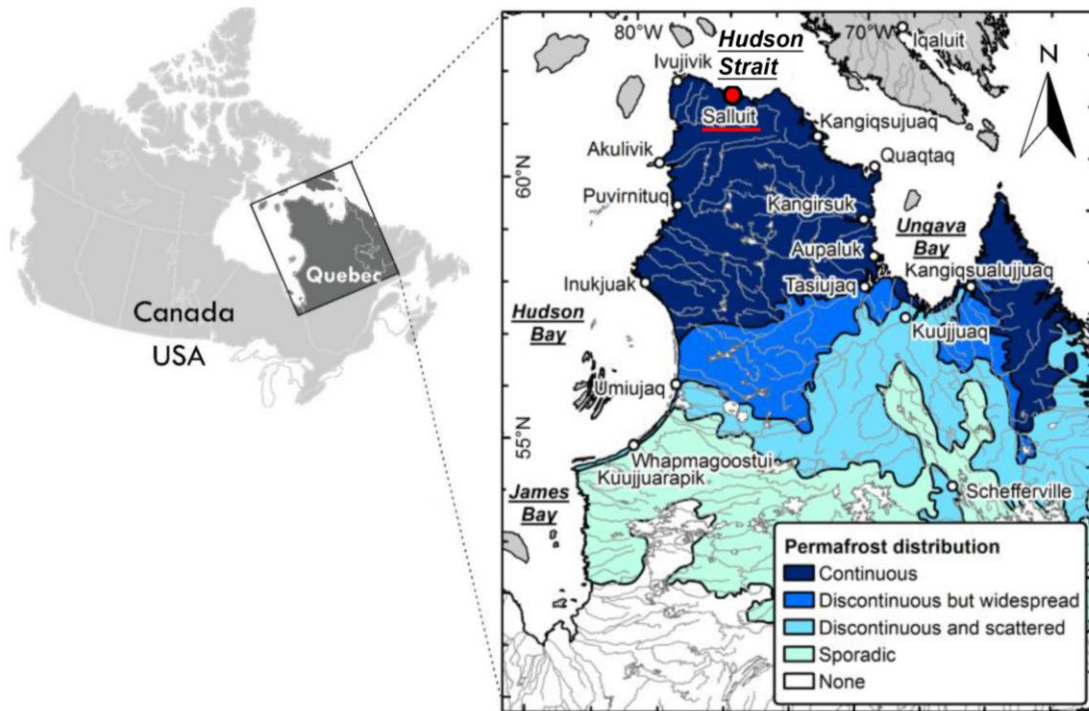
Figure 5-11: Location of Existing Research Sites at Salluit and Umiujaq, Nunavik, Québec (after Lemieux et al. 2020)

5.2.2   Groundwater System Stability and Evolutions

5.2.2.1   Numerical Modelling Approaches

Reactive transport modelling is a useful approach for assessing long-term geochemical stability in geological formations. Reactive transport modelling is used to assess: 1) the degree to which dissolved oxygen in recharging waters may be attenuated within the proposed host rock; 2) how geochemical reactions (e.g., dissolution-precipitation, oxidation-reduction, and ion exchange reactions) may affect groundwater salinity (density) and composition along flow paths; and 3) how diffusive transport of reactive solutes may evolve in low-permeability geological formations.

Unstructured grid capabilities were recently implemented into the multi-component reactive transport code MIN3P-THCm for 3-dimensional (3D) systems, including the parallelization of the unstructured grid functions (Su et al. 2022a; Su et al. 2021; Su et al. 2020). A 3D demonstration simulation based on a hypothetical sedimentary basin has been performed to evaluate the code capabilities for large-scale flow and reactive transport simulations using unstructured meshes. The new code capabilities allowed to evaluate the effect of dimensionality (2D versus 3D) and ice sheet geometry on the development of flow patterns and solute transport in sedimentary basins during a glaciation cycle. The numerical experiments indicate that a 3D analysis will give more comprehensive results for flow patterns and reactive solute transport subjected to glaciation/deglaciation cycles in the case of a narrow ice lobe, but also suggest that a 2D approach might provide an adequate representation for the case of a relatively wide ice sheet (Su et al. 2022b).

The impact of paleo-glaciation on the formation and distribution of elevated dissolved sulfide is also being investigated through reactive transport simulations. MIN3P-THCm was previously applied to investigate the mechanisms responsible for elevated dissolved sulfide observed in the Michigan Basin (Xie et al. 2018). These simulations have recently been updated using a more complete and realistic geochemical network including ferrous and ferric iron and associated redox and mineral dissolution/precipitation reactions. Simulation results show improved agreement with the available field data. The results of this research will be published in a journal paper.

5.2.2.2   MICA – Michigan International Copper Analogue project

The Michigan International Copper Analogue (MICA) project was initiated in early 2021 and originally involved NWMO, RWM, SKB, Nagra and the Geological Survey of Finland (GTK). In July of 2021, BGE signed on as full partners for Phase I. The purpose of the MICA project is to provide evidence of the behaviour of metallic copper on geological timescales. The internationally renowned copper deposits of the Keweenaw peninsula, USA, will be studied to ascertain both genesis and evolution - and by extension stability - in response to changing conditions such as Eh, pH, groundwater chemistry, temperature, presence/absence of oxygen, etc. The knowledge gained could be considered subsequently by waste management organizations in relation to the stability of copper on long timescales. The project may also enhance the robustness of a safety case that considers a disposal concept that uses metallic copper as part of the engineered barrier system, concerning, for example, the persistence of metallic copper under certain geochemical conditions that could be experienced by an evolving deep geological repository in certain environments. Such knowledge could be used in subsequent work to evolve the disposal concept, or to initiate further research activities. This project is managed by the Geological Survey of Finland (GTK) and various technical experts.

Phase I of the MICA project concluded in September 2022, with the technical report expected to be completed in Q1 2023. Phase I involved a comprehensive, state-of-the-science review, including a description of the known geologic history of each sample, information on environment(s) of exposure (including timing and length(s)), identification and planning of analytical research and some preliminary analyses as proof of concept. Through the Phase I work, 12 types of copper analogues were identified and described, and samples have been identified for each analogue, which will undergo testing in Phase II. Phase I also included testing the capability of GTK to carry out analytical testing to study metallic copper samples as part of Phase II. This process showed good capability regarding physical, mineralogical, geochemical and isotopic analysis and resulted in the development of methodologies to describe the properties of unaltered samples and corrosion/alteration phenomena.

In 2022, member of the MICA project team conducted a field excursion to the Keweenaw Peninsula to view the geological setting of the natural copper analogues. In 2021, the MICA project plan was presented at the safeND conference in Germany (Liebscher et al., 2021). The MICA project is anticipated to comprise at least 2 phases. Phase II will be the main research phase on selected Keweenaw-based natural analogues from Phase I; specific testing will be decided after Phase I is complete.

5.2.3   Seismicity

5.2.3.1   Regional Seismic Monitoring

The Canadian Hazards Information Service (CHIS), a part of the Geological Survey of Canada (GSC), continues to conduct a seismic monitoring program in the northern Ontario and eastern Manitoba portions of the Canadian Shield. This program has been ongoing since 1982 and is currently supported by a number of organizations, including the NWMO. CHIS now provide monitoring of both northern Ontario and southern Ontario. All the stations are operated by CHIS and transmit digital data in real-time via satellite to a central acquisition hub in Ottawa. CHIS-staff in Ottawa integrate the data from these stations with those of the Canadian National Seismograph Network and provide monthly reports of the seismic activity in these regions.

A technical report submitted to NWMO in late 2022 summarizes operational statistics and additions to the earthquake catalogue for the year 2020 and was published at the end of 2022 (Boucher et al. 2022). During 2020, 108 earthquakes were located in the northern Ontario study area (Figure 5-12), ranging in magnitude from 1.4 to 3.6 m_N. The pattern of seismicity generally conformed to that of previous years. The largest earthquake was an event at 3.5 km depth, north of Kapuskasing.
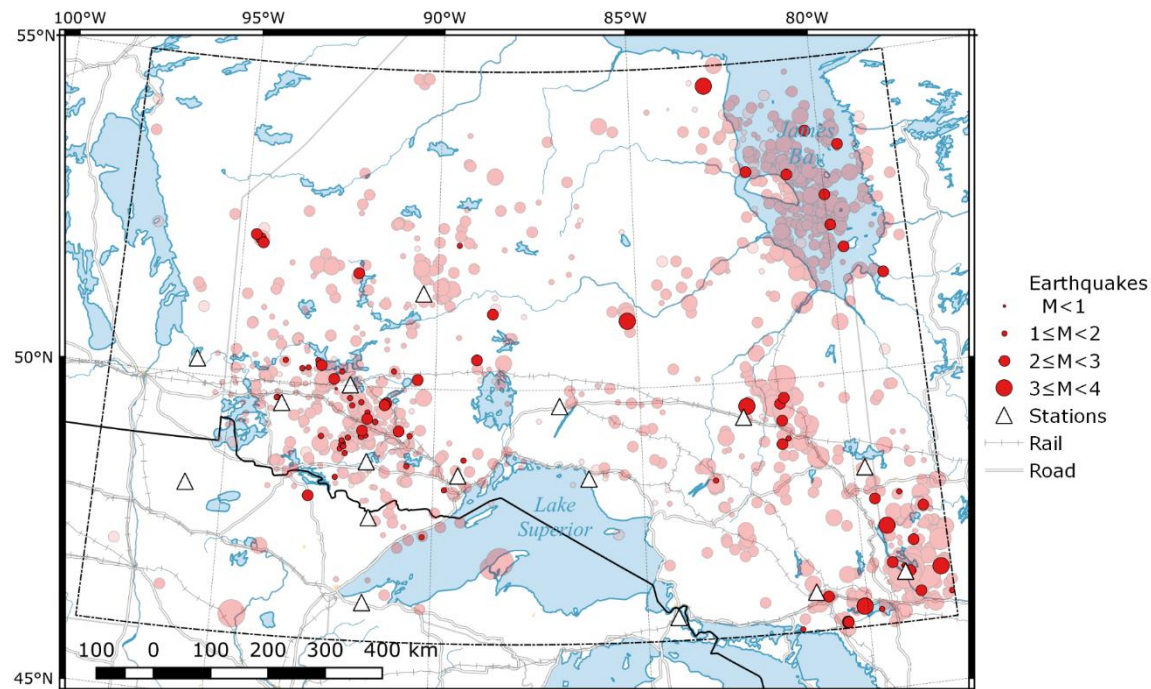
Notes: Events in 2020-2021 have black outlines, while events from 1900–2020 are plotted semi-transparently and have grey outlines. Events and stations are plotted in the study area only. The study area is outlined with a dash-dotted line. Only stations with data available in 2020-2021 are shown.

Figure 5-12: Earthquakes in Northern Ontario, 2020–2021.

Within Southern Ontario in 2020, the seismograph stations (Figure 5-13) detected three earthquakes occurred within 150 km of the Bruce nuclear site, all less than m_N 2. A group of earthquakes 275 km southeast of the site, near Niagara Falls, included the largest in the region used for earthquake-recurrence estimation. This was a 2.9 m_N for which the depth was

estimated to be 6.0 km based on regional depth phase modeling (RDPM). In all, 41 earthquakes have been catalogued within 150 km of the site since 1952.
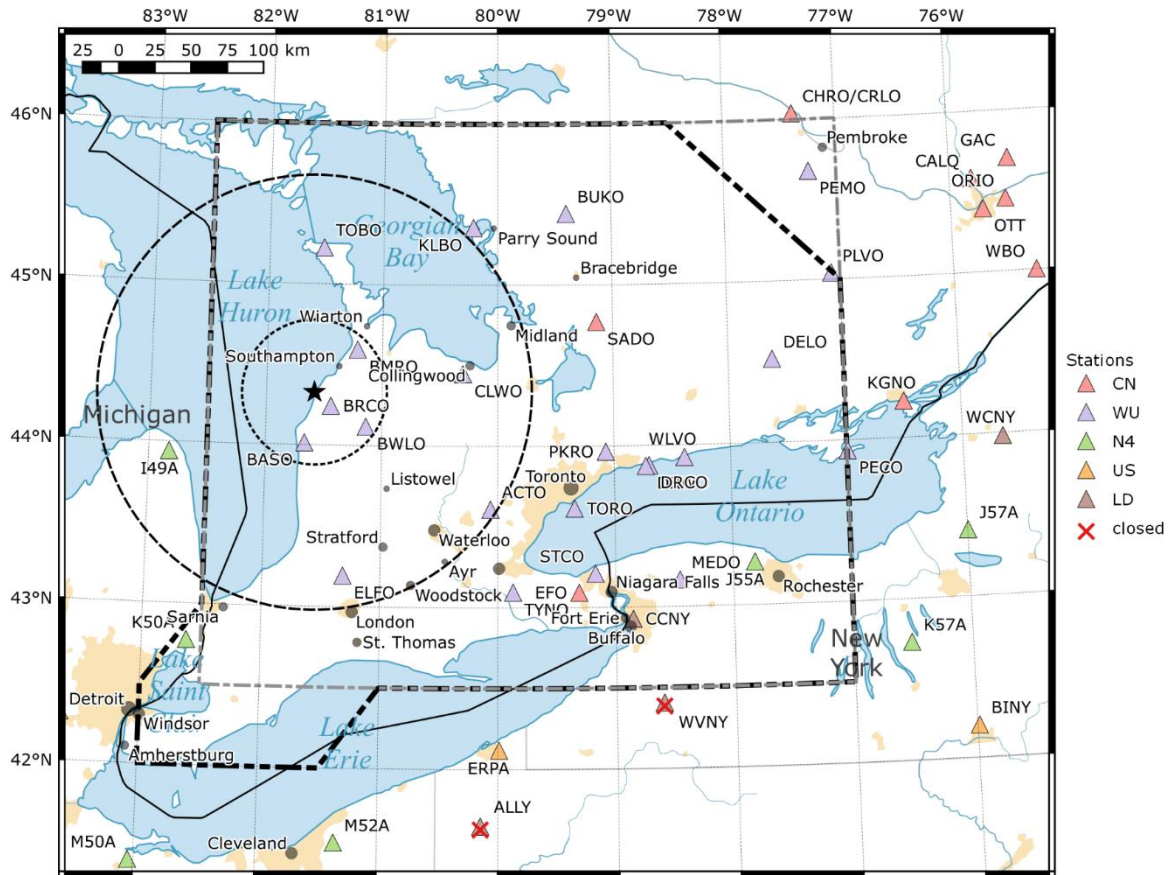
Notes: The Bruce nuclear site is indicated with a black star, and dashed circles are approximately 50 and 150 km radii around this site. The grey rectangular (dash-dotted) and black polygonal (dash-dot-dotted) outlines are two areas used for recurrence calculations. Triangles are operational stations, coloured by network code. Stations that closed during 2020 are marked with an X. Urban areas (Schneider et al., 2003) are marked in pale yellow.

Figure 5-13: Seismograph Stations in Southern Ontario, 2019–2020.

5.2.3.2   Mont Terri Nanoseismic Monitoring (SM-C) Experiment

The NWMO is involved in the Mont Terri Nanoseismic Monitoring (SM-C) Experiment, which serves as a comparative tool for the NWMO microseismic monitoring program. During 2022, upgrades were completed and all tiltmeters have now been digitized.
These tiltmeters are used in several experiments for long-term and short-termed events such as CO_2 injection tests that commenced in November. The results of previous injection experiments are published in Guglielmi et al. 2021 and Zapone et al. 2020.

5.2.3.3 Paleoseismicity

Due to the long-life cycle of a repository, potential perturbations from ground motions associated with rare strong earthquakes requires consideration. No such earthquakes have occurred in Ontario in human-recorded history. However, the NWMO is carrying out research to look for evidence, or absence of evidence, of such events in the past as described below.

During 2020, new research project with the Geological Survey of Canada in Ottawa was initiated focusing on i) developing criteria to objectively distinguish between neotectonic and glaciotectonic faulted sediments; and ii) assessing the inferred neotectonic origin of the Timiskaming East Shore fault. Similar reconnaissance profiling was also carried out in Tee and Kipawa lakes, Quebec. This research continues to build on work that began in 2012 and is aimed at providing an understanding of seismicity over time frames dating over the Holocene. Additional results from this earlier phase of research were published (Brooks et al., 2021) on a mass transport deposit, interbedded within glaciolacustrine deposits of Lake Ojibway which was discovered using a sub-bottom profile survey at Frederick House Lake, Ontario.

Surveys in summer 2022 were conducted to the east and south of the Kipawa Lake at Auboin, McLachlin, Grindstone, Smith, Otter, Petit Beauchene, and West Beauchene lakes (Figure 5-14). Gordon (aka Truile) Lake, located adjacent to Lake Temiscaming, was also surveyed. The survey locations on a given lake focused on deep (>30 m), steep-sided sub-basins, as identified from available fishing bathymetric maps and local word-of-mouth. Experience from the 2019 and 2021 surveys indicates that these characteristics are the most promising to locate subaqueous landslides.
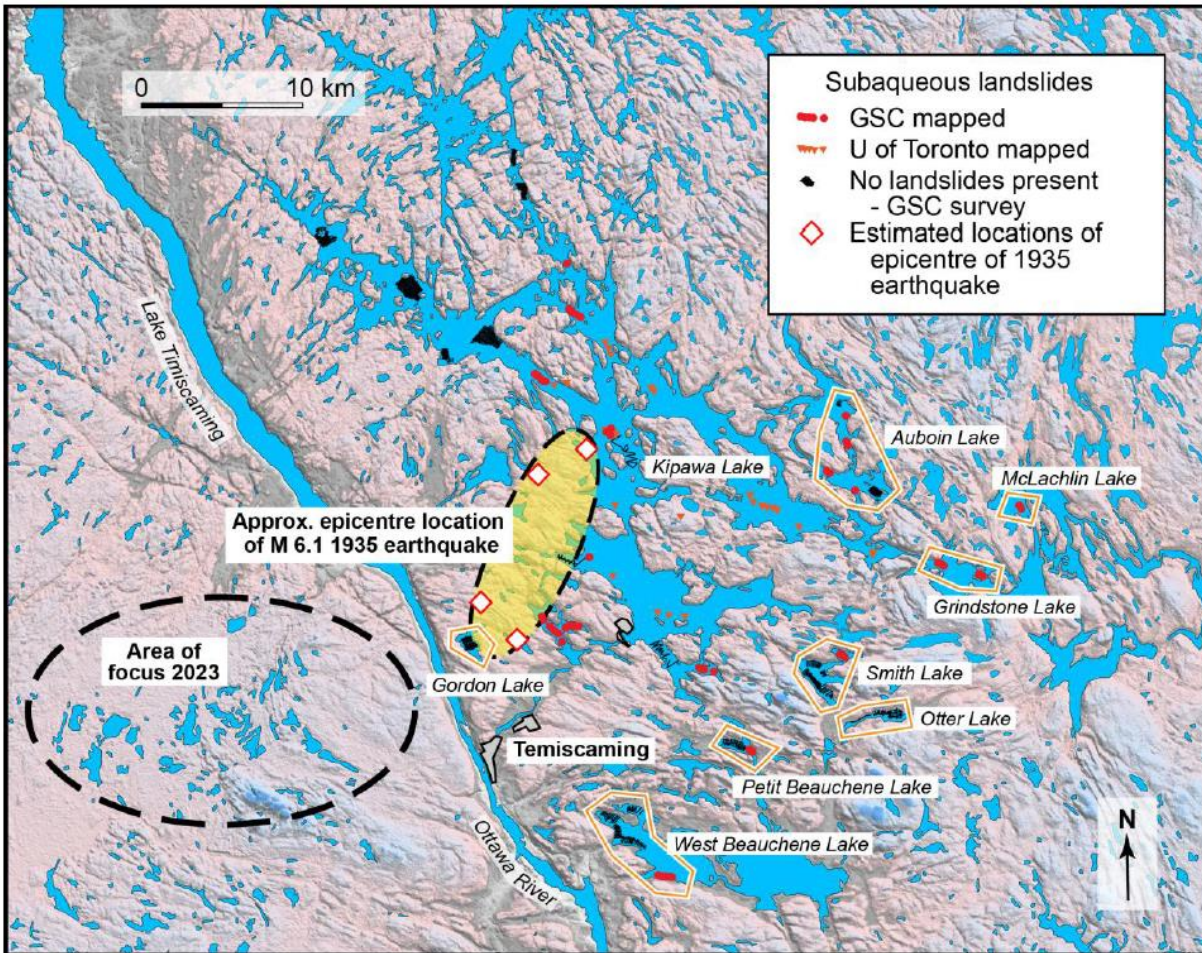
Notes: Young subaqueous landslides identified in sub-bottom acoustic surveys (red circles – GSC unpublished data; orange triangles – after Doughty et al., 2010). The locations surveyed in August 2022 are outlined by orange polygons and labeled by lake name. The deposits are inferred to be associated with failures triggered by the 1935 Temiscaming earthquake. Also shown is the area west of Temiscaming where surveying is planned for 2023. A yellow-shaded oval encompasses the area within which the 1935 earthquake epicentre is estimated to be located (data from Adams and Vonk, 2009).

Figure 5-14: Preliminary Map of the Young, Subaqueous Landslides Identified in Sub-bottom Acoustic Surveys in the Temiscaming Area.

5.2.4 Geomechanical Stability of the Repository

5.2.4.1 Excavation Damaged Zones

The Queen's Geomechanics and Geohazards Group, QGGG, has been developing predictive tools for Excavation Damage Zone (EDZ) evolution around deep geological repositories in sedimentary and crystalline rock. Past research focussed on fundamental mechanics of EDZ, damage threshold definition and prediction and assessment of EDZ using advanced numerical simulation. In the past few years, Queen's research has also focussed on updated conventional testing and investigation tools and developed new protocols for characterization, bringing the

level of investigation in line with the power of modern simulation tools (Gagnon and Day 2022, Innocente et al., 2022, Packulak et al, 2022).

The team has been investigating the effect of confining stress, boundary conditions and sample damage on sonic velocities in rock – leading to a better understanding of the discrepancies between lab- and field-derived elastic properties (Figure 5-15. left). Significant advances in understanding of multi-stage shear testing for rock joints have been made. Identical samples were made using 3D photoscans of real joints, 3D printed casting molds producing hardened cement grout jointed core samples for testing (Figure 5-15. middle). Another highlight of research in 2022 include advancements in the determination of true tensile strength, TTS, a key parameter for brittle damage simulation. While the Brazilian Indirect Tension Test (BTS) is the most convenient and universally applied test method, the resulting strength value overpredicts the true tensile strength. Using strain measurement to detect the formation of the first crack in the sample, the true tensile strength can be obtained. 2D digital image correlation or DIC techniques have been refined to detect very small strains prior to sample failure (Figure 5-15. right). 3D versions of this technique will be used on tensile and compressive samples to understand the role that anisotropy and rock fabric play in pre-failure deformation, damage evolution and strength behaviour of rock (Packulak et al., 2022, Packulak and Day, *submitted*).

An exhaustive study has been completed to develop a more robust approach for the determination of EDZ damage parameters (Crack Initiation stress or CI and Crack Damage stress or CD). This work has been utilized by Fischer and Diederichs (2023)to develop and mechanically calibrate discrete fracture networks within brittle rock to simulate the interaction of EDZ development in intact rock and geological structure.
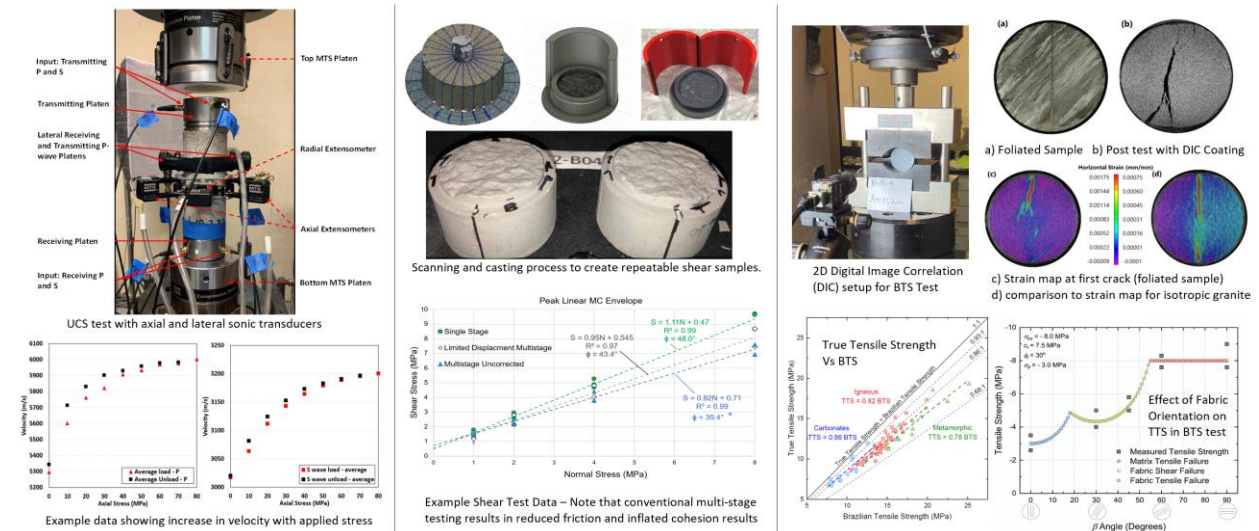
Figure 5-15: Highlights of Research Progress in 2022 by Queen's Geomechanics and Geohazards Group.

5.2.4.2 Repository Design Considerations

5.2.4.2.1 Analysis of Shaft and Cavern Stability

The excavation of the underground openings (i.e., including placement rooms, shafts) for a repository, and the subsequent backfilling with heat-emitting UFCs as well as the buffer material, will induce coupled THM processes in-situ. NWMO has been conducting numerical analyses at near- and far-field scales to enhance our understanding of the response of the rock mass to hypothetical Canadian DGR configurations in both sedimentary and crystalline settings (ITASCA 2015). These studies considered perturbations induced by the repository as well as the natural processes expected during a 1 Ma period. In the study by ITASCA (2015), the THM processes were one-way coupled, whereas a recent THM modelling study (also by ITASCA) employed fully coupled THM analyses using refined input parameters. The sensitivity of the model predictions to some uncertain model input parameters (e.g., block-to-contact stiffness ratio for discontinuum modelling, poroelastic properties, and rock mass permeability) were also investigated. NWMO's review of the final technical report on this research was on-going during 2022. Two journal papers have been produced from this study (Radakovic-Guzina et al 2022 and *submitted*).

5.2.4.2.2 Fault Rupturing

ITASCA has completed a research project with NWMO to numerically simulate a sizable seismic event resulting in the mobilization of surrounding fracture networks. Rupture of a seismogenic fault and its effect on the deformation of the off-fault fractures were examined. The purpose of the analysis was to determine the off-fault fracture displacements to inform the selection of respect distance within the repository horizon in crystalline rock.

Three different models were constructed to accommodate the fault size for moment magnitudes (Mw) of 6.1, 6.6 and 6.9 seismic events occurring at the end of the glacial cycle when the vertical stress due to ice sheet is zero but glacially-induced horizontal stresses still remain. This base case analysis was conducted for five DFN realizations developed from the structural geology of Forsmark, Sweden. The modelling results revealed that for an earthquake with a moment magnitude, Mw of 6.1 and a dip angle of 40° (base case), the fault average shear displacement during the slip is about 1.6 m and the maximum shear displacement along the fault is 3.4 m. No DFN fractures slip more than 5 cm were observed in all DFN realizations except for a fault dip angle of 30°. Increasing the event magnitude while maintaining a dip angle of 40° (base case) resulted in a greater number of off-fault fractures with slippage over the 5 cm criterion and an increase in the distance to the fractures with such large displacements. NWMO's review of the final technical report on this research was on-going during 2022. The results of this study have been published in a journal paper (Blanksma et al 2022).

6   REPOSITORY SAFETY

The objective of the repository safety program is to evaluate the operational and long-term safety of the candidate deep geological repository. In the near-term, during site selection, this objective is addressed through preliminary site-based studies, incorporating progressively more site details.

The NWMO has completed generic studies that provide a technical summary of information on the safety of repositories located in a hypothetical crystalline Canadian Shield setting (NWMO 2017) and the sedimentary rock of the Michigan Basin in southern Ontario (NWMO 2018). The reports summarized key aspects of the repository concept and explained why the repository concept is expected to be safe in these locations (see Table 6-1).

Table 6-1: Typical Physical Attributes Relevant to Long-term Safety

Repository depth provides isolation from human activities
Site low in natural resources
Durable wasteform
Robust container
Clay seals
Low-permeability host rock
Spatial extent and durability of host rock formation
Stable chemical and hydrological environment

6.1   WASTE INVENTORY

6.1.1   Physical Inventory

Currently there are about 3.2 million used CANDU fuel bundles. Based on the known plans for refurbishment and life extension of the existing reactor fleet, the total projected number of used fuel bundles produced to the end of life of the reactors is approximately 5.5 million used CANDU fuel bundles (about 106,000 Mg heavy metal) (Reilly 2022).

The CANDU fuel bundles are a mature product, with small design variations over the years primarily in the dimensions and the mass of each bundle, as well as variations in the number of elements per bundle by reactor type. The 37M bundle introduced in some stations has slightly different dimensions compared to the standard bundle.

In addition to the CANDU used fuel, AECL also has ~500 Mg of prototype and research reactor fuel fuels in storage at the Chalk River Laboratories and Whiteshell Research Laboratories. Most of this is UO_2 based fuel from the Nuclear Power Demonstration (NPD), Douglas Point and Gentilly-1 prototype reactors. AECL also holds a small amount (i.e., less than ~100 Mg) of various research fuel wastes with a variety of compositions and enrichments. There is also a very small amount of fuel still in service in low-power research reactors at McMaster University, Royal Military College of Canada and École Polytechnique de Montréal.

The Canadian used fuel inventory and forecast are updated annually by the NWMO (Reilly 2022).

6.1.2 Radionuclide Inventory

An update of the reference CANDU radionuclide inventory was completed in 2020. Calculations were carried out using the most recent Industry Standard Tool version of the ORIGEN-S code and the latest CANDU specific nuclear data (e.g., cross-sections, decay data, and fission product yields) for a range of used fuel burnups of interest to the safety assessment or design. A report documenting the updated inventory and thermal power as a function of decay time for a reference CANDU fuel bundle was published (Heckman and Edward 2020).

The radionuclide inventory depends on the fuel irradiation history. The NWMO maintains a statistical summary of the key parameters for the used CANDU fuel bundles: bundle type, source reactor, date of discharge, burnup and peak linear power. Burnup in particular is important for determining the radionuclide content of a fuel bundle. The burnup and peak linear power distributions for CANDU fuel discharged from the Bruce, Pickering and Darlington nuclear stations were determined up to 2019 (Lampman 2021). The median burnup of CANDU fuel ranges from about 130 to 220 MWh/kgU, depending on the station.

In 2021, a short-term leaching and dissolution study on a prototype used fuel bundle was completed, providing experimental data supporting NWMO's current CANDU fuel inventory and instant release fractions databases.

6.2 WASTEFORM DURABILITY

6.2.1 Used Fuel Dissolution

The first barrier to the release of radionuclides is the used fuel matrix. Most radionuclides are trapped within the UO_2 grains and are only released as the fuel itself dissolves (which in turn only occurs if the container fails). The rate of fuel dissolution is therefore an important parameter for assessing long-term safety.

UO_2 dissolves extremely slowly under reducing conditions similar to those that would be expected in a Canadian deep geological repository. However, in a failed container that has filled with groundwater, used fuel dissolution may be driven by oxidants, particularly hydrogen peroxide (H_2O_2) generated by the radiolysis of water.

A state-of-the-art review was conducted in 2022 to review the basic properties of unirradiated and in-reactor irradiated UO_2 fuel (Badley and Shoesmith 2022). The corrosion behaviour of fuel matrix and radionuclide release under disposal conditions, the suppression of fuel corrosion by redox scavengers (Fe^{2+} and H_2 produced by corrosion of steel vessel), fuel corrosion models, and chemical dissolution of UO_2 matrix under anoxic conditions have been reviewed. The review included studies conducted on natural UO_2 (pellet/powder), SIMFUELs (to replicate chemical changes due to in-reactor irradiation), alpha doped UO_2 (to simulate fuels of different ages after discharge from reactor) and spent fuel.

The mechanistic understanding of the corrosion of UO_2 under used fuel container conditions is important for long-term predictions of used fuel stability. Research on UO_2 dissolution continued at Western University to further understand the mechanisms of a number of key reactions, such as the influence of H_2O_2 decomposition and the reactions of the fuel with H_2 produced either radiolytically or by corrosion of the steel vessel (Liu et al. 2017a, 2017b, 2017c, 2018, 2019). A study on the kinetics of H_2O_2 decomposition on SIMFUELs (simulated spent nuclear fuels;

doped UO_2 specimens containing noble metal particles) has observed that > 98% of the H_2O_2 was consumed by H_2O_2 decomposition (Zhu et al. 2019). The study of the kinetics of H_2O_2 decomposition has been extended to the standard UO_2 pellets to investigate variations in fuel reactivity due to differences in the manufacturing process. The characteristics of a series of standard UO_2 pellets (1965-2017) have been investigated using electrical resistance measurements and Raman spectroscopy.

The kinetics of H_2O_2 reduction on SIMFUEL, RE^{III}-doped UO_2 and non-stoichiometric UO_2 have been conducted using standard electrochemical methods at rotating disk electrodes. It was found the rate of H_2O_2 reduction decreased in the order of SIMFUEL > Gd-doped UO_2 > Dy-doped UO_2 with the rate suppressed on the RE^{III}-doped UO_2. The slightly faster rate on the SIMFUEL may be attributable to the catalysis of reduction on the noble metal particles. The H_2O_2 reduction on all three specimens was found to be suppressed by the presence of the ground water anion HCO_3^-/CO_3^{2-} (Zhu et al. 2020, 2022).

The H_2 effect in suppressing the corrosion behavior of UO_2 (un-doped and RE^{III}-doped UO_2) without catalysis of noble metal particles has been studied by producing H radicals electrochemically and radiolytically to simulate radiation effects on UO_2 corrosion when H_2 is present (Liu et al. 2021). It was observed that the combination of gamma radiation and H_2 was required to reduce the UO_2 matrix, and the reduction of U^V was reversible for specimens close to stoichiometric (UO_{2+x} with x < 0.005) but only partially reversible for RE^{III}-doped UO_2 with a much higher U^V content. At high gamma dose rates and dissolved H_2 concentrations the matrix reduction appeared to be irreversible. Further investigation of the effect of H_2 on the corrosion of pre-oxidized and naturally corroding UO_2 (un-doped, unirradiated) is ongoing. This research will work towards expanding the established model for the α-radiolytic corrosion of used nuclear fuel.

6.2.2 Solubility

The maximum concentration of a radionuclide within or near a failed container will be limited by the radionuclide solubility. Radionuclide solubilities are calculated by geochemical modelling using thermodynamic data under relevant geochemical conditions. These data are compiled in quality-controlled thermodynamic datasets.

In 2022, the NWMO continued to support the joint international Nuclear Energy Agency (NEA) effort on developing thermodynamic databases for elements of importance in safety assessment (Mompeán and Wanner 2003). Phase VI of the NEA Thermochemical Database (TDB) project will provide a review of the chemical thermodynamics of lanthanides. The reviews of molybdenum thermodynamic data, ancillary data, the state-of-the-art reports on the thermodynamics of cement materials and high-ionic strength systems (Pitzer model) are underway.

The NEA TDB project provides high-quality datasets. This information is important, but is not sufficient on its own, as it does not address the full range of conditions of interest. For example, the NEA TDB project has focused on low and moderate salinity systems in which activity corrections are described using Specific Ion Interaction Theory (SIT) parameters. The SIT model is most useful in ionic strength up to 3.5 molal (Grenthe et al. 1992). Due to the high salinity of porewaters observed in some deep-seated sedimentary rock formations in Canada, a thermodynamic database including Pitzer ion interaction parameters is needed for radionuclide solubility calculations for sedimentary rock environment. The NEA state-of-the-art report on

high-ionic strength systems (Pitzer model) will be useful to identify the data gap for Pitzer ion interaction parameters.

The NWMO is also co-sponsoring the NSERC/UNENE Senior Industrial Research Chair in High Temperature Aqueous Chemistry at the University of Guelph, where there is capability to carry out various thermodynamic measurements at high temperatures and high salinities. This Chair program initiated in 2016. Progress has been made in several areas: (1) the equilibrium constants for uranyl complexes with sulfate at high salinities from 25 to 350 ºC have been determined by Raman spectroscopy approach (Alcorn 2019). These are the first measurements to be reported at 350 ºC; (2) the equilibrium constants for uranyl complexes with chloride at high salinities from 25 to 300 ºC have been determined by Raman spectroscopy approach; (3) the equilibrium constants and transport properties of lanthanum with chloride at high salinities from 25 to 250 ºC have been determined by Raman spectroscopy and conductivity approach (Persaud 2021); and (4) participating in the NEA TDB project to lead the state-of-the-art review of experimental methods and thermochemical databases for actinides, lanthanides and other selected elements at high temperature and pressure relevant to nuclear waste management (the initial report was completed in 2022). The results of the research on thermodynamic properties of uranyl chloride complexes will be published in a journal publication.

The NWMO updated the databases of radionuclide solubility for Canadian crystalline rock environment (Colàs et al. 2021) and Canadian sedimentary environment (Colàs et al. 2022). The radionuclide solubility limits were calculated in a reference groundwater CR-10 (Ca-Na-Cl type with TDS = 11 g/L) which simulates the groundwater geochemical conditions at the repository depth of Canadian crystalline rock, and in a reference groundwater SR-290-PW (Na-Ca-Cl type with TDS = 287 g/L) which simulates the groundwater geochemical conditions at the repository depth of Canadian sedimentary rocks. The radionuclide solubility calculations considered three scenarios: 1) groundwater directly enters the canister without interacting with the bentonite buffer or the canister materials; 2) groundwater interacts with the carbon-steel container prior to contacting the used nuclear fuel waste inside the container; and 3) groundwater interacts with both bentonite buffer and carbon-steel container prior to contacting the used nuclear fuel waste inside the container. The solubility calculation in SR-290-PW was carried out using a Pitzer database DGR_Pitzer_TDB which has been developed based on the Yucca Mountain Pitzer database data0.ypf.R2 (Jove-Colon et al. 2007) and modified with additional information from the THEREDA database (Altmaier et al. 2011) and the available Pitzer data from the literature.

6.3 BIOSPHERE

In the context of deep geologic repositories, biosphere models are developed to derive potential dose and non-radiological consequence by calculating constituent of potential concern (COPC) concentrations in the biosphere and considering dominant or representative pathways.

In 2022, the NWMO continued the development of its dynamic biosphere model, which is implemented using the AMBER software. The model simplifies the biosphere as a series of compartments which can each receive, accumulate, and transfer contaminants. Transfer between some compartments is dynamically modelled, while others are modelled by ratios that assume the compartments are in quasi-equilibrium over the time scales of interest. In the model, the calculated COPC environmental concentrations are then used to calculate the dose to stylised human receptors by applying dose coefficients and lifestyle-specific exposure rates. The model will continue to evolve in an iterative approach as the sites are characterized and the assessment objectives evolve.

6.3.1 Participation in BIOPROTA

BIOPROTA is an international collaborative forum created to address key uncertainties in long-term assessments of contaminant releases into the environment arising from radioactive waste disposal. Participation is aimed at national authorities and agencies with responsibility for achieving safe radioactive waste management practices. Overall, the intent of BIOPROTA is to make available the best sources of information to justify modelling assumptions made within radiological assessments constructed to support radioactive waste management.

In 2022, the NWMO continued to participate in this forum and to sponsor the Transport of C-14 in the Biosphere project, initiated in 2021. The primary objective of the project was to investigate the use of new conceptual models for the transport of C-14 releases from geological disposal facilities for solid radioactive wastes. The scope of the project included literature review, conceptual models, and preliminary mathematical models for terrestrial, freshwater, and marine environments. The literature review and the development of conceptual models were completed in 2021 and work progressed in 2022 on developing the report of the project. A final report is expected to be published in 2023.

6.4 SAFETY ASSESSMENT

6.4.1 Screening

Used nuclear fuel stored in the repository will contain hundreds of different isotopes arising from fission, neutron activation and decay processes. However, there is a large range in both the concentration and in the hazard of each of these various species (radionuclides or chemical elements). In 2022, the NWMO issued a minor revision to the radiotoxicity and screening analysis published in 2021 (Gobien et al. 2022). The purpose of this document is to quantify the hazard associated with used CANDU fuel and determine which radionuclides and chemically hazardous species in the fuel are of highest consequence for more detailed analyses.

Gobien et al. (2022) details the data supporting the hazard and screening assessments, the results of the hazard assessment as well as the methodology and results of the screening assessments. The hazard assessment considered the fuel activity and radiotoxicity, and the screening assessments identify radionuclides and chemically hazardous elements of consequence to pre-closure, post-closure, human intrusion, and non-human biota assessments.

The radionuclides and chemically hazardous elements identified in Gobien et al. (2022) will be considered in future safety assessments.

6.4.2 Pre-closure Safety

The pre-closure period includes site preparation, construction, operation, monitoring, decommissioning, and closure of the facility. Topics include normal operations safety (public and worker dose), and malfunctions and accidents. These topics were addressed for a generic site as part of AECL's Environmental Impact Statement (AECL 1994, OHN 1994), and reviewed as part of the NWMO options study (NWMO 2005). The NWMO is presently updating the analysis methodology and conducting initial site-based assessments; this work will be updated with more site-specific information and design once available.

6.4.2.1 Acceptance Criteria

Acceptance criteria for radiological and non-radiological contaminants applicable to pre-closure safety assessments are used to judge the acceptability of analysis results for the protection of humans and the environment. In 2022, the NWMO has advanced the work on developing preliminary pre-closure criteria for the protection of persons and the environment from radiological and non-radiological contaminants, consistent with the latest applicable national and international guidance.

6.4.2.2 Normal Operations

A preliminary dose assessment of the facility was carried out in 2014 to guide ALARA (As Low As Reasonable Achievable) development of the repository concepts (Reijonen et al. 2014).

An update to this preliminary study was initiated in 2022, to estimate the potential radiological impact to the public from normal operation of the DGR and its related surface processing facilities. A conceptual design of the DGR with potential site-specific surface facilities layouts were considered for these studies. During normal operations, airborne radioactivity could be released during handling of the used fuel from surface contamination that is generally present on used fuel bundles and from cladding failures in the fuel elements. Waterborne emissions could result from cell washdowns and decontamination of used fuel modules, used fuel transportation packages, and containers. The analysis considers potential facility emissions (airborne and waterborne) and external exposure (direct and skyshine). Simple conservative models are used to estimate the dispersion of airborne and waterborne emissions, and the external dose from the used fuel in the UFPP. The study assumes exposure to receptors at a few locations, including a potential fence line location. The preliminary normal operation analysis indicates that the potential public doses would be below the preliminary acceptance criterion. This preliminary analysis is continuing to incorporate site specific information and will inform the further development of the preliminary DGR design.

6.4.2.3 Abnormal Events and Accidents

A preliminary study was carried out in 2016 for a generic site to identify potential internal accident scenarios that may arise during the operations phase for the repository, based on a conceptual design of the UFPP and repository (Reijonen et al. 2016). In this preliminary study, a failure modes and effects analysis (FMEA) was used to identify potential internal hazards resulting from, for example, failure of equipment, failure of vehicles, failure of the shaft hoist system, loss of electric power, ventilation and filtration system failure, and human error. The estimates of the internal initiating event frequencies were obtained based on data from the nuclear industry and from earlier used fuel management studies (AECL 1994).

An update to this analysis was initiated in 2022, including assessing the potential public dose consequences for the accident scenarios identified in the 2016 hazard identification study (Reijonen et al. 2016). The analysis considers exposure to a person standing at various distances from the fence line under conservative generic atmospheric conditions. Atmospheric dispersion factors were derived based on the Gaussian dispersion model described in CSA N288.2-M91 (CSA 2003). The presence or absence of ventilation system High Efficiency Particulate Air filters is also considered in combination with specific accident scenarios. The preliminary analysis indicates that the potential public doses for inhalation, air immersion and ground exposure pathways would remain below the preliminary safety assessment acceptance

criteria for all accidents considered. This preliminary analysis is continuing to incorporate site specific information.

Potential external natural and human-induced hazard events are dependent on the site. In 2022, the NWMO initiated preliminary assessments to identify the external hazard hazards at the two DGR study areas in Ontario and to screen out hazards that are unlikely to lead to effects on systems, structures, and components at the site. The assessment followed the guidance of REGDOC-1.1.1 (CNSC 2018) and REGDOC-2.4.4 (CNSC 2022). These preliminary results will be updated with more site information as it becomes available.

6.4.2.4 Dose Rate Analysis

An accurate estimate of dose rates associated with different used fuel configurations is required to support the radiological characterization of used fuel during handling of the fuel. In 2022, the effective dose rate estimates have been updated to reflect the latest radionuclide inventory estimates (Heckman and Edward 2020) and the latest container design and to include a more detailed representation of the within-bundle source term spatial distribution.

Two geometry configurations were analysed, an unshielded single used fuel bundle and used fuel bundles inside a UFC. Dose rate locations up to 100 m from the source were considered, and calculations were performed for two burnup values (220 MWh/kgU and 290 MWh/kgU) and for decay times up to 10^7 years. The results of this work were published in a technical report (Ariani 2022a).

6.4.2.5 Climate Change Impacts and Flood Hazard Assessment Studies

A study was performed in 2018 to review anticipated climate change impacts on climate conditions (e.g., temperature and precipitation) and develop a methodology to incorporate these climate changes into probable maximum precipitation (PMP) estimation appropriate for the DGR study areas in Ontario. A report documenting the study was published in 2019 (Wood 2019).

The preferred method developed by Wood (2019) was subsequently applied to assess the climate change impacts on the PMP, Intensity-Duration-Frequency (IDF) curves, and snowpack accumulation projections for both the WLON-Ignace and the SON-South Bruce areas. The multimodel ensemble approach was used to describe the probable range of results and potential climate changes to PMP and IDF amounts expressed as percentiles, so that the level of acceptable risk can be selected by using the desired percentile. Both studies considered projected changes in climate over three time periods: mid-century (2041 to 2070); end-of-century (2071-2100); and beyond 2100. There is a level of inherent uncertainty when projecting future climate. To that end, the approach taken in these studies aims to address this uncertainty by relying on a multi-model ensemble and providing percentiles. The results of the studies were published in 2020 for both the WLON-Ignace (Schardong et al. 2020) and the SON-South Bruce (Breach et al. 2020) areas.

6.4.2.5.1 Preliminary Flood Hazard Assessments

A preliminary flood hazard assessment was initiated in 2020, to estimate the flood potentials and associated climate change impacts for the WLON-Ignace area using the PMP, IDF and snowpack accumulation values estimated by Schardong et al. (2020). The assessment was based on international guidance (IAEA 2011) and the flooding was quantitatively assessed for direct rainfall on-site and for upstream watershed flooding. The scenarios considered in the assessment were divided by time periods (current, mid-century, and end-of-century) and by climate change scenarios (three PMP risk projections). The results for the WLON-Ignace area were published in a technical report in 2021 (Rodriguez and Brown 2021).

A similar assessment was completed for the SON-South Bruce area and the results were published in 2022 (Rodriguez and Brown 2022). Figure 6-1 shows the simulated maximum flood levels under the End-of-Century PMP with 95% percentile. This is an extreme scenario in which 769 mm of rain falls in the area within a 24 hour period.
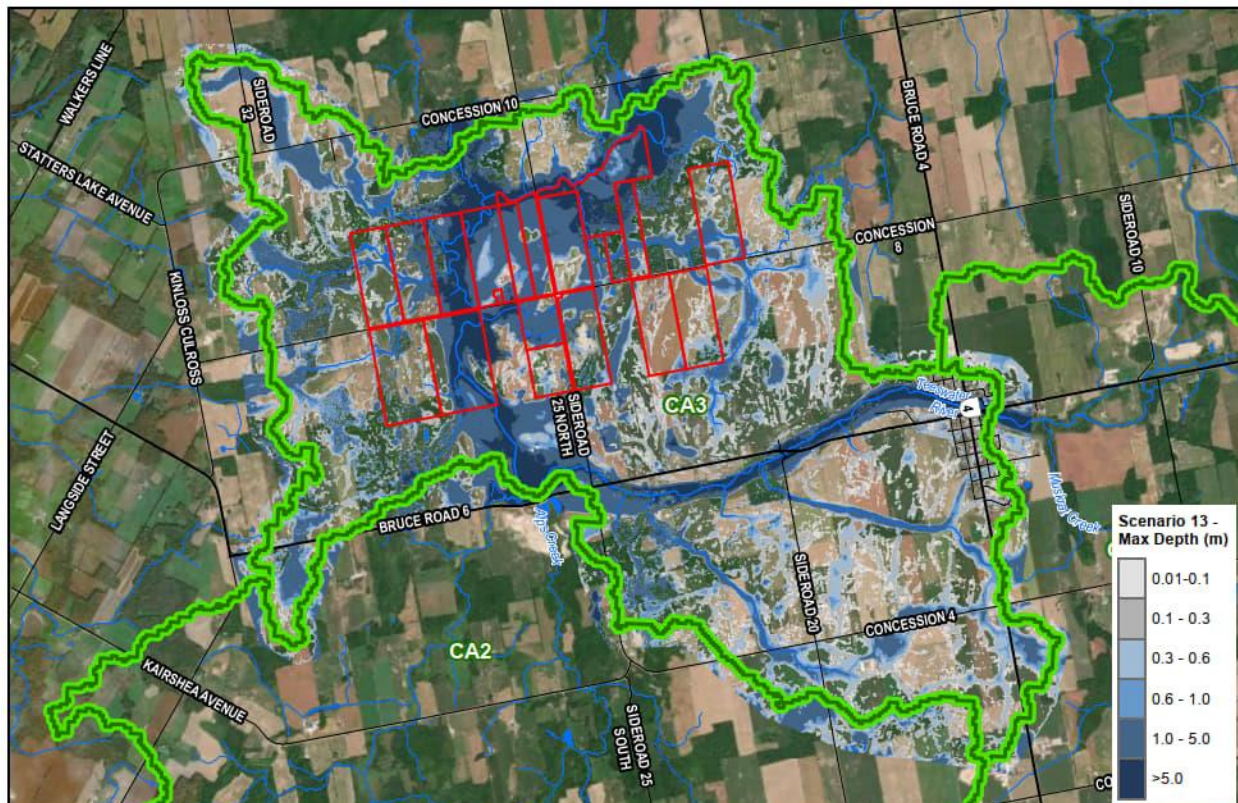
Note: red lines in the figure represent the South Bruce portion of the NWMO owned/optioned land.

Figure 6-1: Simulated Maximum Flood Levels under End-of-Century PMP with 95% Percentile for the SON-South Bruce Area (769 mm rainfall)

These preliminary assessments considered only existing conditions and did not consider any grading or ditch configurations which would form part of the civil design within the proposed study sites. That is, these results showed the effects of an extreme storm on the sites as it exists now, before any design. The preliminary results at both sites indicated that even under extreme precipitation (PMP) events with existing natural terrain conditions, the risk for flood hazards is likely small. As the preliminary design progresses for the proposed facilities at both

study sites, it is expected that site grading will modify some of the current floodplain delineations. It is also expected that site stormwater management measures such as ditches would further mitigate potential surface flooding impacts within the sites.

6.4.3   Post-closure Safety

The purpose of a post-closure safety assessment is to determine the potential effects of the repository on the health and safety of persons and the environment during the post-closure timeframe.

6.4.3.1   Acceptance Criteria

Acceptance criteria for radiological and non-radiological contaminants applicable to post-closure safety assessments are used to judge the acceptability of analysis results for the protection of humans and the environment. Preliminary acceptance criteria were used in NWMO's generic case studies (NWMO 2017, 2018). In 2022, the NWMO has advanced the work on developing the preliminary post-closure criteria for the protection of persons and the environment from radiological and non-radiological contaminants, consistent with the latest applicable national and international guidance.

6.4.3.2   Post-closure Safety Assessment Methods

The 2022 preliminary work towards site-specific assessments of post-closure safety included:

- Estimating general relationships between depth and rock permeability in the WLON-Ignace area, based on earlier results from literature surveys of measured rock permeabilities at varying depths for several sites across the Canadian Shield (Snowdon et al. 2021);
- Adapting the 3D geological model of Southern Ontario by Carter et al. (2021b) to calculate groundwater flow and transport in the SON-South Bruce area;
- Developing complementary methods for calculating hypothetical transport of assumed contaminant transport within the rock neighbouring the repository vault; and
- Developing groundwater flow and transport models, building on the approaches developed in previous case studies (e.g., Kremer et al. 2019).

Further effort was given to exploring additional metrics for assessing site suitability, including multiple types of water-supply wells, a broad set of lifestyles, and an expanded series of imagined repository failures.

The post-closure assessment methodology is based on guidance from REGDOC-2.11.1 volume III, version 2 (CNSC 2021).

6.4.3.2.1   Integrated System Model

The NWMO initiated in 2018 the development of a system modelling tool known as the Integrated System Model (ISM). The ISM consists of a connected series of models developed in commercially available codes each representing a specific portion of the repository system. The ISM-NF model was developed using COMSOL and contains the waste form, containers, engineered barrier system, and excavation damaged zone surrounding the placement room. It assumes the failure of some containers, degradation of the used fuel by water, and transport of

radionuclides and stable isotopes from the fuel, through the engineered barrier system and into the geosphere. The ISM-GEO model developed using HGS describes the movement of species from the repository via the groundwater through the rock mass and fractures, to the surface environment. The ISM-BIO model developed using AMBER determines the concentration of species in environmental media (e.g., surface water, groundwater, sediments, soils, air) and estimates the consequent radiological dose to a critical group living near the repository.

Initial versions (v1.0 and v1.0.1) of ISM were released in 2020. The theory of the component models of the initial ISM versions was described in Gobien and Medri (2019).

In 2021, the development of a data processing and linking tool known as paLINK was also completed. This tool manages data preprocessing, stochastic data sampling, model linking, and postprocessing of ISM data and models. Figure 6-2 shows the structure of the combined paLINK-ISM configuration.
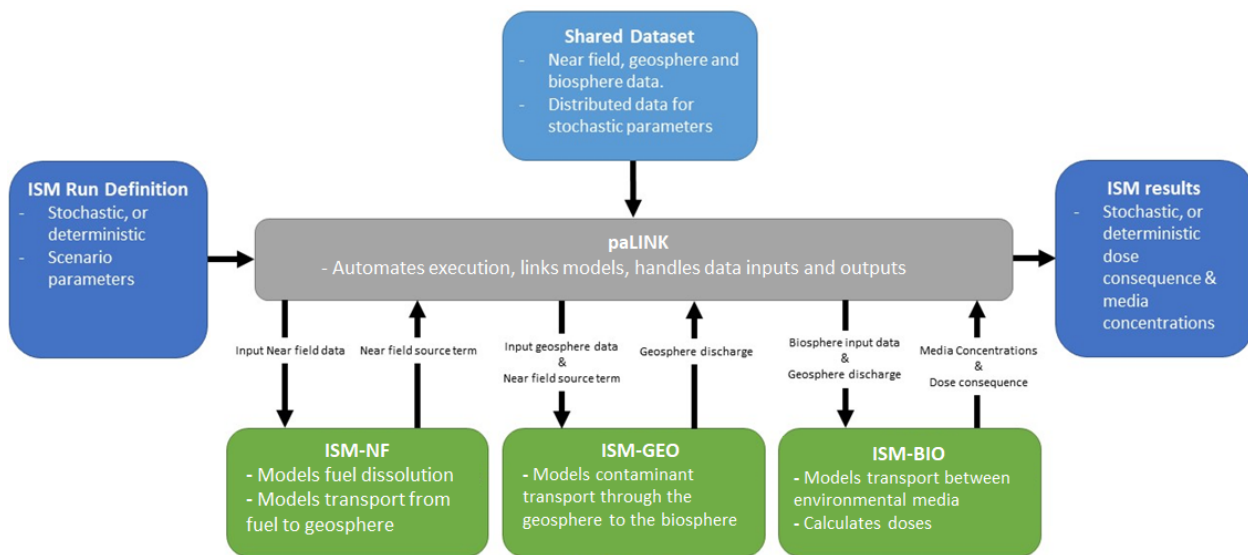
Figure 6-2: paLINK-ISM Configuration

In 2022, the ISM v1.2 was released, which further refined the site-specific nature of the ISM-GEO and ISM-BIO models for the Revell and South Bruce Sites. An updated theory manual applicable to ISM v1.2 and v1.1 is expected to be published in 2023.

The NWMO continues to develop and test the ISM in a manner consistent with NWMO technical computing software procedures, and with the CSA Standard N286.7-16 (CSA 2016). The next iteration, ISM v1.3, is planned to increase the site-specificity of the geosphere and biosphere models as well as to include several other minor changes and is expected to be released in 2023.

Validation of the ISM is an ongoing task, with further validation of specific process models or overall system-level comparisons performed when suitable opportunities arise (for example DECOVALEX Task F – see Section 4.3.3.2). A preliminary validation report is expected to be published in 2023.

6.4.3.3 Dose Rate Analysis

The used fuel container is a major engineered barrier that must be strong enough to withstand geological pressures, including the hydrostatic load of glaciation events, and chemically resistant to long-term corrosion. In the event of the failure of a fuel container, groundwater could enter the container and contact the fuel. Consequently, estimates of alpha, beta, gamma, and neutron dose rates in the water near the fuel container and fuel surfaces are required to support the assessment of the potential effects of the radiolysis of water on the integrity of the container and the used fuel.

The dose rate estimates were updated in 2022 using the latest used fuel inventories (Heckman and Edward 2020), container designs, and state-of-the-art computational method. The dose rate calculations included contributions from alpha, beta, gamma, and neutron sources in the used CANDU fuel. Dose rates were estimated for decay times up to 10 million years, for two burnup values (220 MWh/kgU and 290 MWh/kgU), and for various used CANDU fuel configurations (i.e., single fuel bundle immersed in water, UFC immersed in water, breached and water-filled container, and a placement room). The results were published in a technical report (Ariani 2022b).

6.5   CONFIDENCE IN SAFETY

In 2022, Confidence in Safety reports were produced for each site (NWMO 2022b, NWMO 2022c). The purpose of these reports was to summarize the results as of early 2022 indicating why each site would be suitable from a technical perspective for hosting a repository. They are intended to support public discussion around site selection.

The NWMO's assessment of the suitability of the South Bruce Site described in NWMO (2022b), was based on both intrinsic characteristics of the multiple-barrier approach, as well as regional geological information and South Bruce Site specific results acquired to date. The key points are as follows:
- The Cobourg Formation is the preferred rock formation, and boreholes confirmed it was at the expected depth of around 650 m at this site.
- The Cobourg Formation is surrounded by 100s of meters of strong rock.
- No inflowing groundwater into boreholes below 325 m.

The NWMO's assessment of the suitability of the Revell Site described in NWMO (2022c), was also based on both intrinsic characteristics of the multiple-barrier approach, plus the evidence of the suitability of the rock at the Revell Site from recent studies. The key points are as follows:
- The Revell Site is in a 2.7-billion-year-old, stable and strong granitic rock.
- Boreholes show that the rock is very uniform.
- It is consistent with other similar Canadian Shield rocks and with the types of rock at the Finland and Sweden repository sites.

These reports are part of a multi-year assessment process. In both cases, further work including detailed site characterization is planned, should the site be selected, in order to obtain the information needed for the regulatory licence application. Ongoing and future technical work will include further site studies, design development and safety analyses to confirm and extend the results to date. These would ultimately be presented to Canadian federal regulators for an Impact Assessment and a series of regulatory licence applications. This is a process that will take years before a final approval to construct could be received. During construction and operations, there

will be continued monitoring to ensure that the site is, and remains, suitable for long-term containment and isolation of used nuclear fuel.

6.6 MONITORING

6.6.1 Knowledge Management

The NEA established in 2019 the Working Party on Information, Data and Knowledge Management (WP-IDKM) to further explore potential standardized approaches to manage information, as well to preserve the information in the long term for radioactive waste disposal and decommissioning. The work under this international collaboration builds on outcomes and learnings from previously completed NEA projects such as the Repository Metadata (RepMet) Management (NEA 2018), and the Preservation of Records, Knowledge and Memory (RK&M) across Generations projects (NEA 2019a, 2019b, 2019c).

The NWMO participates in the WP-IDKM initiative and continues monitoring the international collaborations and research on knowledge management and long-term preservation of knowledge and records.

7 SITE ASSESSMENT

In 2022, we continued to assess the suitability of both potential sites: the WLON-Ignace area in northwestern Ontario, and the SON-South Bruce area in southern Ontario. The status of the geological and environmental studies underway in these regions is described below.

7.1 WABIGOON LAKE OJIBWAY NATION (WLON)-IGNACE AREA

7.1.1 Geological Investigation

By the end of 2022, the main Geoscience fieldwork activities for this phase of work were completed. These activities include the drilling, coring and testing of 6 kilometre-long boreholes, installation of a shallow groundwater monitoring network, and installation of microseismic monitoring network. As of the end of 2022, main fieldwork activities include ongoing maintenance, monitoring and groundwater sampling.

Figure 7-1: Installed shallow groundwater monitoring well in the WLON-Ignace area.

7.1.2   Environmental Program

There was a great deal of environmental field work in the WLON-Ignace area completed in 2022. Some of this work included year 2 environmental media baseline monitoring, continuation of Tier 1 biodiversity work, including further bat research. Ongoing engagement related to the environment program, and environmental monitoring of site investigation studies also continued. Details of the work completed in 2022 are described below.

7.1.2.1   Baseline Media Sampling and Biodiversity

A key piece of work completed in the Northwest for 2022 included the completion of baseline monitoring for both environmental media and biodiversity. To complete this work the NWMO contracted KGS Group as the environmental baseline data collection consultant. Baseline media work completed in 2022 included: surface water quality monitoring, hydrology, and soil quality monitoring. Surface water quality monitoring was completed; summer and fall campaigns were completed accounting for a total of 39 sites visited and 140 samples collected. The fall water monitoring campaign also included sediment and benthic invertebrate sampling at select sites. Hydrology monitoring was completed and included bathymetry and lake level monitoring (Figure 7-2) at 11 lake and pond sites and flow monitoring at 6 stream and river sites. Soil quality monitoring was completed and consisted of samples being collected at a total of 15 sites.

Baseline biodiversity work completed in 2022 included: aquatic eDNA sampling, terrestrial ecosystem/habitat suitability mapping and aquatic habitat mapping. Aquatic eDNA sampling was completed in partnership with Wabigoon Lake Ojibway Nation community members. Through summer and fall sample campaigns field crews visited 153 collection sites and collected a total of 467 aquatic eDNA samples. Terrestrial ecosystem/habitat suitability mapping surveys were completed. Throughout the summer and fall months these crews mapped a total of 600 sites which account for approximately two thirds of the Tier 1 program. Aquatic habitat mapping was completed and included the completion of surveys at a total of 287 sites (146 wetland, 13 pond, 32 lake and 86 stream/river sites).

The NWMO and the University of Guelph have partnered on a joint environmental DNA (eDNA) research program to further understand biodiversity conditions around the potential repository sites in the Wabigoon Lake Ojibway Nation-Ignace area and the Saugeen Ojibway Nation-South Bruce area. eDNA is a non-invasive technology to detect what species are present by looking at DNA that is naturally shed by animals and studying the collected DNA using metabarcoding technology. Once samples are collected in the field by NWMO's consultants, they are sent to the University of Guelph's Hanner Lab for analysis and interpretation to help understand what species are likely to be present in the local environment based on existing genetic sequence libraries. The data collected as part of NWMO's eDNA program will be shared with global databases so that future projects can benefit from our learnings.

Figure 7-2: Photo Showing Level Logger Observed Under High water.

7.1.2.2   Bat Research in Partnership with the Toronto Zoo

The NWMO has continued its partnership with the Toronto Zoo Native Bat Conservation Program in conducting research to close knowledge gaps in the ecology of Ontario's bat population. The goal of this work is to contribute to conservation efforts now and in the future, which starts with studies to better understand bat populations and trends. Work completed in the Northwest for 2022 included continued passive acoustic monitoring of bats at three new locations on and around the Revell, and six nights of mist netting surveys to capture bats.

Capture surveys yielded 14 captured bats of three species across two sites: three endangered little brown myotis, nine silver-haired bats and one eastern red bat.

Youth engagement was also a large factor included in the bat program work in 2022. Workshops were conducted where youth from Ignace and Wabigoon Lake Ojibway Nation joined Toronto Zoo Native Bat Conservation program representatives and NWMO staff to learn about the importance of bats in the ecosystem followed by an evening walk to listen for bats in the area. The youth attending these workshops also constructed bat boxes for installation around each community to provide roosting areas for the bats.

Figure 7-3: Photos from an Evening Field Monitoring Session Near in the WLON-Ignace area. The Left Image Shows a Silver-haired Bat. The Eastern Red Bat (right) is Displaying Typical Behaviour when Handled by Opening its Mouth to Echolocate and Gain an Understanding of What is Going On.

7.1.2.3 Engagement

Engagement related to the environmental program is ongoing in the Northwest. In 2022 this included representation at community events such as open houses and providing information and updates to community groups such as the ICNLC and other interest groups. Environmental day camps were also held for youth in the Ignace community. Participants accompanied an NWMO staff person in the field and spent the day identifying trees, plants, birds, and other wildlife. Participants also participated in other activities including building bird houses, planting a seed to grow on their own, and learning about the different uses for edible and medicinal vegetation found in the area.

Figure 7-4: NWMO Staff at the Environmental Baseline Monitoring Open House

7.1.2.4 Planned 2023 Work

Going forward into 2023 the environmental team aims to continue monitoring and compliance initiatives for work completed in the Northwest, continue working with community members as part of the baseline monitoring program and continue executing the Environmental Baseline Monitoring Program as designed. Baseline media sampling for 2023 will include the launch of the Northwest Community Tissue Sampling Program for the tissue chemistry work of the baseline design. Additional work will also include atmospheric monitoring (air quality, noise, and light). Biodiversity baseline work anywhere that data gaps are identified by the designers of the program will be completed in 2023, completing the Tier 1 studies for aquatic eDNA, aquatic habitat mapping as well as terrestrial ecosystem/habitat suitability mapping, and no further sampling is planned for 2023 in the Northwest. Lastly, bat research will be ongoing with plans to completed further active and passive monitoring in partnership with the Toronto Zoo Native Bat Conservation Program.

7.2 SAUGEEN OJIBWAY NATION (SON)-SOUTH BRUCE AREA

7.2.1 Geological Investigation

In 2022, NWMO's geoscience work at the potential repository site in this area continued, and main fieldwork activities for this phase of work were completed. This includes fieldwork activities such as the drilling, coring and testing of 2 deep boreholes, completing a 3D seismic survey in the area, installing a microseismic monitoring network, and installation of a shallow groundwater monitoring well network. As of the end of 2022, main fieldwork activities include ongoing maintenance, monitoring and groundwater sampling.

Figure 7-5: Example of Core from South Bruce Borehole 1

7.2.2 Environmental Program

Environmental field work in the SON-South Bruce area completed in 2022 included the surface water and hydrology components of the Environmental Media Baseline Program (EMBP), aquatic habitat mapping, environmental DNA (eDNA) sampling, terrestrial ecosystem mapping, and significant wildlife habitat suitability components of the biodiversity impact studies baseline program design (BPD), private drinking water sampling, and bat studies. Ongoing engagement related to the environment program, and field level oversight also continued. Details of the work completed in 2022 are described below.

7.2.2.1 Surface Water Quality and Hydrology

The NWMO and Saugeen Valley Conservation Authority (SVCA) continued their joint program to further understand water resources in the SON-South Bruce and surrounding area.

As part of this program, the SVCA is undertaking the surface water quality component of the EMBP in the SON-South Bruce area. The SVCA completed the 2022 winter, spring, summer and fall surface water quality sampling campaigns throughout the Saugeen watershed (Figure 7-6). Fall 2022 marked the beginning of Year 2 for data collection, and field sampling was expanded to include sediment, phytoplankton, zooplankton, eDNA, and benthic invertebrates in addition to surface water sampling. This work will continue to be executed by the SVCA in 2023-2024, as designed in the Environmental Baseline Monitoring Program.

The SVCA also continued the Hydrology component of the EMBP, including monthly water level measurements; manual flow measurements; rating curve development; maintenance of two flow station along the Teeswater River; maintenance of a meteorological station in the Area of Interest (AOI); and a channel characterization survey along a 30 km stretch of the Teeswater River.

Figure 7-6: SVCA Staff Monitoring Water Levels and Sampling Surface Water at a Wetland Site, May 2022

7.2.2.2 Aquatic Habitat Mapping

As part of the NWMO's environmental baseline monitoring program, North/South Consultants (NSC) was contracted to complete the Aquatic Habitat Mapping and eDNA components of the BPD at stream, wetland, and lake sites (Figure 7-7). Land permissions were obtained before entry to private, Municipal, County, Conservation Authority, and NWMO owned/optioned lands. Between July and October, NSC and their sub-contractor assessed 198 plots. Work will resume in 2024 on newly accessible properties, and anywhere that data gaps are identified by the designers of the program, such as seasonally wet wetlands that were dry in the summer that will need to be evaluated during the spring freshet.

Figure 7-7: NSC Staff Performing Aquatic Habitat Mapping at a Stream Site, August 2022.

7.2.2.3 Environmental DNA

As part of the NWMO's environmental baseline monitoring program, North/South Consultants (NSC) was contracted to complete the Aquatic Habitat Mapping and eDNA components of the BPD at stream, wetland, and lake sites (Figure 7-8). Land permissions were obtained before entry to private, Municipal, County, Conservation Authority, and NWMO owned/optioned lands. NSC completed the summer and fall campaigns by sampling 104 and 159 plots, respectively. The number of plots increased during the fall campaign because permission was granted to access a greater number of properties. Work will resume in 2024 on newly accessible properties, and anywhere that data gaps are identified by the designers of the program, such as seasonally wet wetlands that were dry in the summer that will need to be sampled during the spring freshet.

As described in Section 7.1.2.1, this program was also part of the partnership between NWMO and the University of Guelph environmental DNA (eDNA) research program. eDNA is a non-invasive technology to detect what species are present by looking at DNA that is naturally shed by animals and studying the material using metabarcoding technology. Once samples were collected in the field by NSC, they are sent to the University of Guelph for analysis and determination of species presence. The data collected as part of NWMO's eDNA program will contribute to global genetic databases so that future projects can benefit from our learnings.

Figure 7-7: NSC Staff Collecting an Environmental DNA Sample at a Stream Site, October 2022.

7.2.2.4   Terrestrial Ecosystem Mapping and Significant Wildlife Habitat Suitability

As part of the NWMO's environmental baseline monitoring program, Tulloch Environmental was contracted to complete the Terrestrial Ecosystem Mapping (TEM) and Significant Wildlife Habitat Suitability (SWH) components of the BPD (Figure 7-9). Land permissions were obtained before entry to private, Municipal, County, Conservation Authority, and NWMO owned/optioned lands. Between July and September, Tulloch and their sub-contractors assessed 473 plots. Work will resume in 2024 on newly accessible properties, and anywhere that data gaps are identified by the designers of the program.

Figure 7-8: Tulloch's Sub-contractor from North/South Environmental Looking at a Soil Profile while Performing Terrestrial Ecosystem Mapping, September 2022.

7.2.2.5   Private Water Well Sampling

As part of the NWMO's environmental baseline monitoring program developed with the community, Tulloch Environmental was contracted to complete private water well sampling in the area near the potential repository site in the SON-South Bruce area (Figure 7-9). The program was voluntary and provided landowners an opportunity to find out their existing drinking water quality. A total of 14 wells were sampled in Fall 2022 and data was shared directly with the landowners. The program will continue in 2023.

PRELIMINARY WATER WELL SURVEY AREA
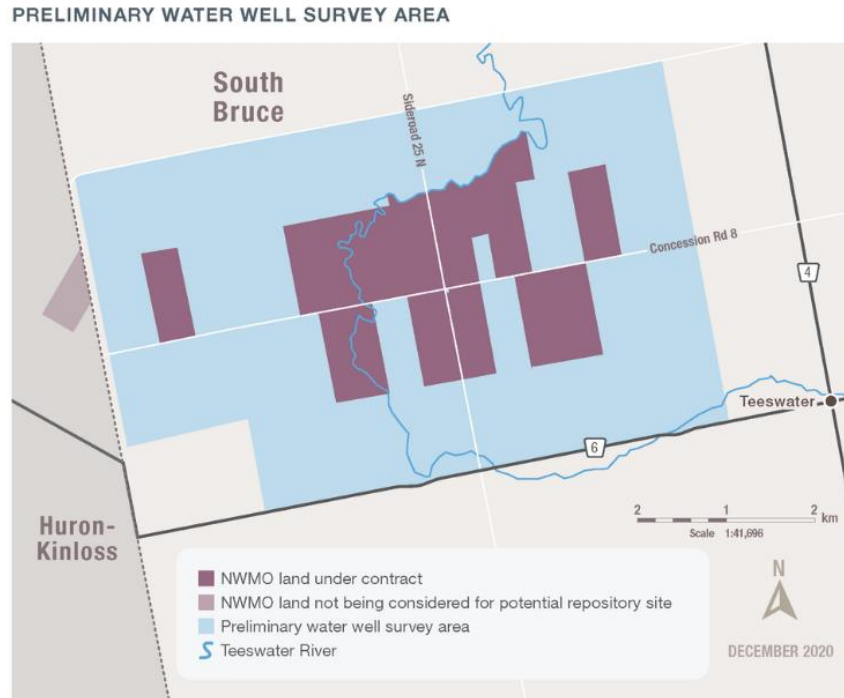
Figure 7-9: Map of the Area Where the 2022 Water Well Sampling Program was Offered to Property Owners near NWMO Acquired Lands

7.2.2.6   Bat Research in Partnership with the Toronto Zoo

Field studies of local bat populations and their trends near the SON-South Bruce area were completed as part of the Toronto Zoo's Native Bat Conservation Program in partnership with the Nuclear Waste Management Organization (NWMO). In 2022, data collection was focused on acoustic monitoring in areas that have previously been monitored, including locations around NWMO's Area of Interest and at local conservation authority properties with a known roost of endangered little brown myotis. These data will be used to develop future studies.

Several community activities were organized to support awareness of the program and facilitate community participation. Representatives from the Toronto Zoo Native Bat Conservation Program spent a day discussing ongoing research including long-term acoustic monitoring, trap and release studies and telemetry studies with families and children from the Saugeen First Nation and the Chippewas of Nawash First Nation. The discussion focused on the conservation program before switching to arts and crafts and building and decorating bat boxes.

The Toronto Zoo also completed another successful year of their community science program in the SON-South Bruce area, where members of the public collaborated with professional scientists to collect and analyze data related to local bat populations. Métis families across the Métis Nations of Ontario - Georgian Bay Traditional Territory as well as other local SON-South Bruce area residents participated in the Toronto Zoo Community Science Project to track bat populations in their backyards across the region. A total of 96 volunteers were engaged, and 102 monitoring sites were sampled to collect approximately 120,000 observations, a five-fold increase compared to the first year of the program.

7.2.2.7   Compliance and Monitoring

The NWMO Environmental Program team also provided environmental monitoring and compliance oversight to contractors completing work in/near the SON-South Bruce area throughout the year. In-field contract oversight and inspections by the NWMO contract administrator were completed. In-field observations by a peer review team were also completed in 2022.

7.2.2.8   Engagement

The NWMO Environmental Program team continues to engage the communities in and around the SON-South Bruce area about the Environmental Baseline Monitoring Program. This includes but is not limited to updates to the South Bruce community liaison committee (CLC), indigenous groups, community groups, and local municipal leaders. Additionally, the NWMO continues to engage with local property owners who allow property access for environmental baseline studies, and local residents who enquire about our baseline monitoring work throughout the year.

7.2.2.9   Planned 2023 Work

Going forward into 2023 the environmental team aims to continue monitoring and executing compliance initiatives for work completed in the SON-South Bruce area, engage with community members as part of the baseline monitoring program, and continue executing the Environmental Baseline Monitoring Program as designed. Baseline media sampling for 2023 is planned to include surface water sampling, hydrology, soil sampling, and the launch of the atmospheric monitoring program. Biodiversity work is planned to resume in 2024 and will include the continuation of eDNA, aquatic habitat mapping and terrestrial ecosystem mapping programs, which are heavily dependent on private land access. Lastly, bat research will be ongoing with plans to complete further active and passive monitoring in partnership with the Toronto Zoo Native Bat Conservation Program.

REFERENCES

Ackerley, N., V. Peci, J. Adams and S. Halchuk. 2021. Seismic Activity in the Northern Ontario Portion of the Canadian Shield: Annual Progress Report for the Period January 1 – December 31, 2019. Nuclear Waste Management Organization Technical Report, NWMO-TR-2021-10. Toronto, Canada.

Adams, J. and A. Vonk. 2009. The November 1, 1935, M 6.2 Timiskaming earthquake, its aftershocks, and subsequent seismicity, Open File 6207, Geological Survey of Canada, doi:10.4095/247644.

Ariani, I. 2022a. Dose Rate Analysis to Support Radiological Characterization of Used CANDU Fuel. Nuclear Waste Management Organization Technical Report NWMO-TR-2022-03. Toronto, Canada.

Ariani, I. 2022b. Dose Rate Analysis to Support Radiolysis Assessment of Used CANDU Fuel. Nuclear Waste Management Organization Technical Report NWMO-TR-2022-02. Toronto, Canada.

Birch, K. & Mielcarek M. (2016, September 11-14). The Use of Isostatic Compression to Produce Full-Scale Highly Compacted Bentonite Blocks. 3rd Canadian Conference on Nuclear Waste Management, Decommissioning and Environmental Restoration, Ottawa, ON, Canada.

AECL. 1994. Environmental Impact Statement on the concept for disposal of Canada's nuclear fuel waste. Atomic Energy of Canada Limited Report AECL-10711, COG-93-1. Chalk River, Canada.

Al, T., I. Clark, L. Kennell, M. Jensen and K. Raven. 2015. Geochemical evolution and residence time of porewater in low-permeability rock of the Michigan Basin, Southwest Ontario. Chemical Geology, 404, 1-17.

Al-Aasm I., R. Crowe and M. Tortola. 2021. Dolomitization of Paleozoic Successions, Huron Domain of Southern Ontario, Canada: Fluid Flow and Dolomite Evolution Water 13 (17), 2449.

Al-Aasm, I.S. and R. Crowe. 2018. Fluid compartmentalization and dolomitization in the Cambrian and Ordovician successions of the Huron Domain, Michigan Basin. Marine and Petroleum Geology, 92, 160-178.

Alcorn, C.D., J.S. Cox, L. Applegarth and P. Tremaine. 2019. Investigation of uranyl sulfate complexation under hydrothermal conditions by quantitative Raman spectroscopy and density functional theory, Journal of Physical Chemistry B 123, 7385-7409.

Altmaier, M., V. Brendler, C. Bube, V. Neck, C. Marquardt, H.C. Moog, A. Richter, T. Scharge, W. Voigt, S. Wilhelm, T. Willms and G. Wollmann. 2011. THEREDA Thermodynamische Referenz-Datenbasis. Abschlussbericht (dt. Vollversion).

Andersson, P., K. Beaugelin-Seiller, N.A. Beresford, D. Copplestone, C. Della Vedova, J. Garnier-Laplace, B. J. Howard, P. Howe, D.H. Oughton, C. Wells, P. Whitehouse. 2008. Deliverable 5: Numerical benchmarks for protecting biota from radiation in the

environment: proposed levels, underlying reasoning and recommendations. PROTECT. Stockholm, Sweden.

Aquanty Inc. 2018. HydroGeoSphere User Manual, Aquanty Inc., Waterloo, Canada.

Badley, M. and D.W. Shoesmith. 2022. The Corrosion/Dissolution of Used Nuclear Fuel in a Deep Geological Repository. Nuclear Waste Management Organization Technical Report NWMO-TR-2022-09. Toronto, Canada.

Bailey Geological Services Ltd. and Cochrane, R.O. 1984a. Evaluation of the conventional and potential oil and gas reserves of the Cambrian of Ontario. Ontario Geological Survey, Open File Report 5499. Ontario, Canada.

Bailey Geological Services Ltd. and Cochrane, R.O. 1984b. Evaluation of the conventional and potential oil and gas reserves of the Ordovician of Ontario. Ontario Geological Survey, Open File Report 5498. Ontario, Canada.

Bastola, S., L. Fava and M. Cai. 2015. Validation of MoFrac 2.0 using the Äspö dataset. Nuclear Waste Management Organization Technical Report NWMO-TR-2015-25. Toronto, Canada.

Beaver, R.C., K. Engel, W.J. Binns and J.D. Neufeld. 2021. Microbiology of barrier component analogues of a deep geological repository. Can. J. Microbiol. (99) 999, 1-18.

Birkholzer, J.T., C.F. Tsang, A.E Bond, J.A. Hudson, L. Jing and O. Stephansson. 2019. 25 years of DECOVALEX - Scientific advances and lessons learned from an international research collaboration in coupled subsurface processes. International Journal of Rock Mechanics and Mining Sciences; 122, 103995.

Blain-Coallier A. 2020. Surface permeability mapping of Stanstead and Lac du Bonnet granite, MEng Thesis, McGill University.

Blanksma, D., J. Hazzard, B. Damjanac, T. Lam, and H. A. Kasani. 2022. Effect of fault reactivation on deformation of off-fault fractures near a generic deep geological repository in crystalline rock in Canada. Journal of Seismology, 26:987–1002. doi: 10.1007/s10950-022-10096-7.

Boucher C., N. Ackerley, V. Peci. 2020. Seismic Activity in the Northern Ontario Portion of the Canadian Shield: Annual Progress Report for the Period January 01, 2020 – December 31, 2021. Nuclear Waste Management Organization Technical Report NWMO-TR-2022-23. Toronto, Canada.

Breach, P., J. Kelly and S. Capstick. 2020. Climate Change Impacts on Climate Variables for a Deep Geological Repository (South Bruce Study Area). Nuclear Waste Management Organization Technical Report NWMO-TR-2020-09. Toronto, Canada.

Briggs, S., C. Lilja and F. King. 2020a. Probabilistic model for pitting of copper canisters. Materials and Corrosion, 72(1-2). doi:10.1002/maco.202011784

Briggs, S., C. Lilja and F. King. 2020b. Probabilistic model for pitting of copper canisters under aerobic, saturated conditions. Svensk Kärnbränslehantering AB. SKB TR-20-01. Forsmark, Sweden.

Brooks, G. 2021. Insights into the Connaught sequence of the Timiskaming varve series from Frederick House Lake, northeastern Ontario. Canadian Journal of Earth Sciences, 58(12).

Carter, T.R., L.D. Fortner, H.A.J. Russell, M.E. Skuce, F.J. Longstaffe and S. Sun. 2021a. A Hydrostratigraphic Framework for the Paleozoic Bedrock of Southern Ontario. Geoscience Canada, 48, 23- 58.

Carter, T.R., C.E Logan, J.K. Clark, H.A.J Russell, F.R. Brunton, A. Cachunjua, M. D'Arienzo, C. Freckelton, H. Rzyszczak, S. Sun, and K.H. Yeung. 2021b. A three-dimensional geological model of the Paleozoic bedrock of southern Ontario—version 2; Geological Survey of Canada, Open File 8795, 1. doi.org/10.4095/328297.

Chen, Z., P. Hannigan, T. Carter, X. Liu, R. Crowe and M. Obermajer. 2021. A petroleum resource assessment of the Huron Domain. Nuclear Waste Management Organization Technical Report NWMO-TR-2019-20. Toronto, Canada.

Chen, J.D., A.H. Kerr, E.A. Hildebrandt, E.L. Bialas, H.G. Delany, K.M. Wasywich, and C.R. Frost. 1989. Radiochemical Analysis of CANDU Used Fuel Stored in Concrete Canisters in Moist Air at 150°C. Proceedings Second International Conference on CANDU Fuel. pp. 337 – 351. Pembroke, Canada, October 1-5, 1989 (Also available at https://inis.iaea.org).

Chen, J.D., P.A. Seeley, R. Taylor, D.C. Hartrick, N.L. Pshhyshlak, K.H. Wasywich, A. Rochon and K.I. Burns. 1986. Characterization of Corrosion Deposits and the Assessment of Fission Products Released from Used CANDU Fuel. Proceedings 2nd International Conference on Radioactive Waste Management. Winnipeg, Canada, 7-11 September 1986. Canadian Nuclear Society, Canada.

Chowdhury, F. et al. *submitted*. Measuring Key Parameters Governing Anion Transport Through Mx-80 Bentonite. Proceedings of the Canadian Society of Civil Engineering Annual Conference 2021, p. 547–558, Springer Nature Singapore.

Clark, I.D., T. Al, M. Jensen, L. Kennell, M. Mazurek, R. Mohapatra and K. Raven. 2013. Paleozoic-aged brine and authigenic helium preserved in an Ordovician shale aquiclude. Geology, 41, 9, 951-954.

CNSC. 2018. Reactor Facilities Site Evaluation and Site Preparation for New Reactor Facilities. Canadian Nuclear Safety Commission, REGDOC-1.1.1. Ottawa, Canada.

CNSC. 2021. Safety Case for the Disposal of Radioactive Waste, Version 2. Canadian Nuclear Safety Commission, REGDOC-2.11.1 Volume III, Version 2. Ottawa, Canada.

CNSC. 2022. Safety Analysis for Class IB Nuclear Facilities. Canadian Nuclear Safety Commission, REGDOC-2.4.4. Ottawa, Canada.

Colàs, E., A. Valls, D. García and L. Duro. 2021. Radionuclide Solubility Calculation (Phase 1). Nuclear Waste Management Organization Technical Report NWMO-TR-2021-02. Toronto, Canada.

Colàs, E., O. Riba, A. Valls, D. García and L. Duro. 2022. Radionuclide Solubility Calculations (Phase 2). NWMO-TR-2022-11. Toronto, Canada.

CSA. 2003. Guidelines for Calculating Radiation Doses to the Public from a Release of Airborne Radioactive Material under Hypothetical Accident Conditions in Nuclear Reactors. Canadian Standards Association CSA N288.2-M91. Toronto, Canada.

CSA. 2008. Guidelines for Calculating Derived Release Limits for Radioactive Material in Airborne and Liquid Effluents for Normal Operation of Nuclear Facilities. Canadian Standards Association CSA Guideline N288.1-08. Toronto, Canada.

CSA. 2014. Guidelines for Calculating the Radiological Consequences to the Public of a Release of Airborne Radioactive Material for Nuclear Reactor Accidents. Canadian Standards Association CSA N288.1-14. Toronto, Canada.

CSA. 2016. Quality Assurance of Analytical, Scientific and Design Computer Programs. Canadian Standards Association CSA N286.7-16. Toronto, Canada.

CSA. 2019. Guidelines for Calculating the Radiological Consequences to the Public of a Release of Airborne Radioactive Material for Nuclear Reactor Accidents. Canadian Standards Association CSA N288.2-19. Toronto, Canada.

CSA. 2020. Guidelines for Modelling Radionuclide Environmental Transport, Fate, and Exposure Associated with the Normal Operation of Nuclear Facilities. Canadian Standards Association CSA N288.1-20. Toronto, Canada.

Damiani, H. L., G. Kosakowski, A. Vinsot and S.V. Churakov. 2022. Hydrogen gas transfer between a borehole and claystone: experiment and geochemical model. Submitted to Environmental Geotechnics. doi:10.1680/jenge.21.00061.

Darcel, C., P. Davy, R. Le Goc and D. Mas Ivars. 2018. Rock mass effective properties from a DFN approach. Proceedings of 2nd International Discrete Fracture Network Engineering Conference, Seattle, USA, June 20-22, 2018. American Rock Mechanics Association.

Davy, P., C. Darcel, E. Lavoine, H. Kasani, D. Mas Ivars. 2022. The RED project: assessing stress fluctuations in fractured rock masses. NWMO Annual Geoscience Seminar, Toronto, Canada. June 2, 2022.

Davy, P., R. Le Goc, C. Darcel, J.O. Selroos, D. Mas Ivars. 2021. Permecability: Factoring Stress Dependency Into The Permeability Of Fractured Rocks. American Geophysical Union Fall Meeting 2021, Dec 2021, New Orleans, USA.

Davy, P., C. Darcel, R. Le Goc, and D. Mas Ivars. 2018. Elastic properties of fractured rock masses with frictional properties and power - law fracture size distributions. Journal of Geophysical Research: Solid Earth. 123, 6521-6539. doi:10.1029/2017JB015329

Davy, P., A. Hansen, E. Bonnet, S-Z. Zhang. 1995. Localization and fault growth in layered brittle-ductile systems: Implications for deformations of the continental lithosphere. Journal of Geophysical Research: Solid Earth. Volume 100, issue B4, p. 6281-6294.

De Simone, S., C. Darcel, R. Ghazal, P. Davy, H. Kasani, D. Mas Ivars, 2022. Defining equivalent Biot and Skempton coefficients for a fractured rock mass, CouFrac 2022, Berkeley (USA), November 14-16, 2022.

Diederichs, M., and J. Day. 2021. An illustrative study on the potential sensitivity of predicted long-term EDZ development to, layered and nodular sedimentary structure. Rock Mechanics and Rock Engineering. doi:10.1007/s00603-021-02602-z.

Dobkowska, A. et al. 2021. A comparison of the corrosion behaviour of copper materials in dilute nitric acid. Corrosion Science, 192, 109778.

Eriksen, T.E., D.W. Shoesmith and M. Jonsson. 2012. Radiation induced dissolution of UO2 based nuclear fuel – A critical review of predictive modelling approaches. Journal of Nuclear Materials, 420, 409–423.

Esmaieli K., J. Hadjigeorgiou and M. Grenon. 2010. Estimating geometrical and mechanical REV based on synthetic rock mass models at Brunswick Mine. International Journal of Rock Mechanics and Mining Sciences. 47(6), 915-926.

Fernandes, S., K. Woolhouse and N. Thackeray. 2019. Supplementary Non-Radiological Interim Acceptance Criteria for the Protection of Persons and the Environment. Nuclear Waste Management Organization Technical Report NWMO-TR-2017-05. Toronto, Canada.

Fischer, C. and M.S. Diederichs. 2021a. The use of explicit numerical models for the prediction of residual rockmass behaviour around a circular tunnel. GEONiagara – CGS conference 2021. Niagara Falls, Canada.

Fischer, C. and M.S. Diederichs. 2021b. Comparison between GSI-based implicit and explicit structure models. In The Evolution of Geotech-25 Years of Innovation p. 527-533. CRC Press.

Fischer, C. and Diederichs, M. (*submitted*). The Use of Explicit Numerical Models for the Representation of Elasto-Plastic and Post-Yield Weakening Rockmass Behaviour Around a Circular Tunnel. Canadian Geotechnical Journal.

Gagnon, É. and J.J. Day. 2022. Vein genesis and the emergent geomechanical behaviour of numerically simulated intact veined rock specimens under uniaxial compression. GeoCalgary2022, the 75th Canadian Geotechnical Society Annual Conference.

Gao, K. and J.P. Harrison. 2016. Mean and dispersion of stress tensors using Euclidean and Riemannian approaches. International Journal of Rock Mechanics and Mining Sciences. 85, 165-173.

Gao, K. and J. P. Harrison. 2018a. Multivariate distribution model for stress variability characterisation. International Journal of Rock Mechanics and Mining Sciences. 102, 144-154.

Gao, K. and J.P. Harrison. 2018b. Scalar-valued measures of stress dispersion. International Journal of Rock Mechanics and Mining Sciences. 106, 234-242.

Garnier-Laplace, J., R. Gilbin, A. Agüero, F Alonzo, M. Björk, Ph. Ciffroy, D. Copplestone, M. Gilek, T. Hertel-Aas, A. Jaworska, C-M. Larsson, D. Oughton and I. Zinger. 2006. Deliverable 5: Derivation of Predicted-No-Effect-Dose-Rate values for ecosystems (and their sub-organisational levels) exposure to radioactive substances. ERICA (Contract Number: FI6R-CT-2004-508847). Brussels, Belgium.

Gobien, M. and C. Medri. 2019. ISM v1.0 Theory Manual. Nuclear Waste Management Organization Technical Report NWMO-TR-2019-06. Toronto, Canada.

Gobien, M., K. Liberda, and C. Medri. 2022. Fuel Radiotoxicity and Screening Analysis. Nuclear Waste Management Organization Technical Report NWMO-TR-2021-16 R001. Toronto, Canada.

Goguen, J., A. Walker, J. Riddoch, S. Nagasaki. 2021. Sorption of Pd on illite, MX-80 and shale in Na-Ca-Cl solutions, Nuclear Engineering and Technology 53 (3), 894-900. doi: doi.org/10.1016/j.net.2020.09.001

Golder Associates Ltd. 2005. Hydrocarbon Resource Assessment of the Trenton-Black River Hydrothermal Dolomite Play in Ontario. Ontario Oil, Gas and Salt Resources Library. London, Canada.

Grenthe, I., X. Gaona, A.V. Plyasunov, L. Rao, W.H. Runde, B. Grambow, R.J.M. Konings, A.L. Smith and E.E. Moore. 2020. Second Update on the Chemical Thermodynamics of Uranium, Neptunium, Plutonium, Americium and Technetium. Vol 14. OECD Nuclear Energy Agency Data Bank, Eds., OECD Publications, Paris, France.

Grenthe, I., J. Fuger, R.J.M. Konings, R.J. Lemire, A.B. Muller, C. Nguyen-Trung and H. Wanner. 1992. Chemical Thermodynamics of Uranium. Elsevier Science Publishers, New York, United States.

Guglielmi, Y., Nussbaum, C., Cappa, F., De Barros, L., Rutqvist, J. and Birkholzer, J., 2021. Field-scale fault reactivation experiments by fluid injection highlight aseismic leakage in caprock analogs: Implications for CO2 sequestration. International Journal of Greenhouse Gas Control, 111, p.103471.

Hall, D.S., M. Behazin, W.J. Binns and P.G. Keech. 2021. An evaluation of corrosion processes affecting copper-coated nuclear waste containers in a deep geological repository. Progress in Materials Science, 118, 100766.

Harper, J., T. Meierbachtol, N. Humphrey, J. Saito and A. Stansberry. 2021. Generation and Fate of Basal Meltwater During Winter, Western Greenland Ice Sheet. The Cryosphere, 15, 5409–5421. doi:10.5194/tc-15-5409-2021

Harthong, B., L. Scholtès, F-V. Donzé. 2012. Strength characterization of rock masses, using a coupled DEM–DFN model. Geophysical Journal International. 191(2), 467-480. doi:10.1111/j.1365-246X.2012.05642.x

Health Canada. 2010. Part IV Guidance on Human Health Detailed Quantitative Radiological Risk Assessment. Ottawa, Canada.

Heckman, K. and J. Edward. 2020. Radionuclide Inventory for Reference CANDU Fuel Bundles. Nuclear Waste Management Organization Technical Report NWMO-TR-2020-05. Toronto, Canada.

Hegger, S., N. Vlacholpoulos and M. Diederichs. 2021a. A New Apparatus for Installing Distributed Optical Sensors onto Uniaxial Compression Test Specimens to Measure Full-Field Strain Responses. Geotechnical Testing Journal 45(1). doi:10.1520/GTJ20210021

Hegger, S., N. Vlachopoulos, T. Poles, and M. Diederichs. 2021b. Measuring the full-field strain response of uniaxial compression test specimens using distributed fiber optic sensing. Rock Mechanics and Rock Engineering. doi:10.1007/s00603-021-02643-4

Innocente, J., M. Diederichs, C. Paraskevopoulou. 2021. Long-term strength; time-dependency; time-dependent cracking; static load testing; Creep; time-to-failure. International Journal of Rock Mechanics and Mining Science. V147. 13p. doi:10.1016/j.ijrmms.2021.104900

IAEA. 2006. Safety Requirements: Geological Disposal of Radioactive Waste. International Atomic Energy Agency Safety Requirements WS-R-4. Vienna, Austria.

IAEA. 2011. Meteorological and Hydrological Hazards in Site Evaluation for Nuclear Installations, IAEA Safety Standards Series No. SSG-18, IAEA, Vienna, Austria.

IAEA. 2014. Radiation Protection and Safety of Radiation Sources: International Basic Safety Standards. General Safety Requirements Part 3. No. GSR Part 3. Vienna, Austria.

ICRP. 2007. The 2007 Recommendations of the International Commission on Radiological Protection. International Commission on Radiological Protection Publication 103, Annals of the ICRP (W2-4). Vienna, Austria.

ICRP. 2008. Environmental Protection: The Concept and Use of Reference Animals and Plants. ICRP Publication 108. Vienna, Austria.

ICRP. 2013. Radiological Protection in Geological Disposal of Long-lived Solid Radioactive Waste. International Commission on Radiological Protection Publication 122, Annals of the ICRP 42(3). Vienna, Austria.

INL. 2005. Damaged Spent Fuel at U.S. DOE Facilities, Experience and Lessons Learned. Idaho National Laboratory Report INL/EXT-05-00760. Idaho, USA.

Innocente, J., C. Paraskevopoulou, M. Diederichs. 2022. Time-Dependent Model for Brittle Rocks Considering the Long-Term Strength Determined from Lab Data. Mining 2022, 2, 463–486. doi:10.3390/mining2030025

Itasca Consulting Group, Inc. 2020. 3DEC — Three-Dimensional Distinct Element Code (Version 7.0). Minneapolis, MN.

ITASCA. 2015. Long-Term Stability Analysis of APM Conceptual Design in Sedimentary and Crystalline Rock Settings. Itasca Consulting Group, Inc. report for NWMO. Nuclear Waste Management Organization Technical Report NWMO-TR-2015-27. Toronto, Canada.

Jacobsson, L., D. Mas Ivars, H.A. Kasani, F. Johansson and T. Lam. 2021. Experimental program on mechanical properties of large rock fractures, EUROCK 2021, Torino, Italy, 20-25 September 2021, IOP Conf. Ser.: Earth Environ. Sci. 833 012015. doi.10.1088/1755-1315/833/1/012015

Janson, W., Zhang, X. and Doyle, D. 2022. Full-Scale External Pressure Test of Used Nuclear Fuel Container for Deep Geological Disposal – Phase 2. Proceedings of the 41st Annual Conference of the Canadian Nuclear Society and 46th Annual CNS/CNA Student Conference. Virtual Conference, June 5 – June 8, 2022.

Jaquenoud, M., T.E. William, T. Grundl, T. Gimmi, A. Jakob, S. Schefer, V. Cloet, P. De Canniere, L. R. Van Loon and O.X. Leupin. 2021. In-situ X-ray fluorescence to investigate iodide diffusion in opalinus clay: Demonstration of a novel experimental approach, Chemosphere 269, 128674

Javaid, M.A., J.P. Harrison, M.I. Diego and H. Kasani. 2021a. Assessing heterogeneity of in situ stress for the design of nuclear waste repositories. GeoNiagara 2021: 74th Canadian Geotechnical Conference & 14th Joint CGS/IAH-CNC Groundwater Conference, Niagara, Canada.

Javaid, M.A. and J.P. Harrison. 2021b. Heterogeneity of in situ stress: A Review. EUROCK 2021: ISRM Symposium on Mechanics and Rock Engineering from Theory to Practice, Torino, Italy.

Javaid, M.A., Harrison, J.P., Kasani, H.A. and Mas Ivars, D. (2022a) Incorporating an assessment of uncertainty into estimates of in situ stress in rock as a function of depth. GeoCalgary 2022: Canadian Geotechnical Society Conference on Reflection on Resources, Calgary, Alberta, Canada.

Javaid, M.A., Harrison, J.P., Mas Ivars, D. and Kasani, H.A. (2022b) A Bayesian regression analysis of in situ stress using overcoring data. EUROCK 2022: ISRM Symposium on Rock and Fracture Mechanics in Rock Engineering and Mining Espoo, Finland.

Jove-Colon, C., T. Wolery, J. Rard, A. Wijesinghe, R. Jareck and K. Helean. 2007. Pitzer database development: Description of the Pitzer Geochemical Thermodynamic Database data0.ypf.R2. Appendix I. In In-Drift Precipitates/Salts Model, Report ANL-EBS-MD-000045 REV 03, DOC.20070306.0037 Las Vegas, Nevada: Sandia National Laboratories.

Junkin, W., L. Fava, M. Cai, E. Ben Awuah. 2020. Using DFN models to improve ground control through wedge identification and hazard mapping. Extended abstract, geoconvention, May 11-13, Calgary, Canada.

Junkin, W., E. Ben-Awuah and L. Fava. 2019a. DFN variability analysis through voxelization. Proc. ARMA 2019, 53rd US Rock Mechanics/Geomechanics Symposium, New York, USA.

Junkin, W., E. Ben-Awuah and L. Fava. 2019b. Incorporating DFN analysis in rock engineering systems blast fragmentation models. Proc. ARMA 2019, 53rd US Rock Mechanics/Geomechanics Symposium, New York, USA.

Junkin, W., L. Fava, E. Ben-Awuah and R.M. Srivastava. 2018. Analysis of MoFrac-generated deterministic and stochastic Discrete Fracture Network models. Proc. DFNE 2018, 2nd International Discrete Fracture Network Engineering Conference, Seattle, USA.

Junkin W., D. Janeczek, S. Bastola, X. Wang, M. Cai, L. Fava, E. Sykes, R. Munier and R.M. Srivastava. 2017. Discrete Fracture Network generation for the Äspö TAS08 tunnel using MoFrac. Proc. ARMA 2017, 51st US Rock Mechanics/Geomechanics Symposium, San Francisco, USA.

Kanik, N.J., F.J. Longstaffe, A. Kuligiewicz and A. Derkowski. (*in press*). Systematics of smectite hydrogen-isotope composition: Structural hydrogen versus absorbed water. Submitted to Applied Clay Science.

Kasani, H.A., and A.P.S. Selvadurai. (*submitted*). A Review of Techniques for Measuring the Biot Coefficient and Other Effective Stress Parameters for Fluid-Saturated Rocks. Applied Mechanics Reviews, 75(2), 020801. doi:10.1115/1.4055888.

King, F. 2021. Natural Analogues and Their Use in Supporting the Prediction of the Long-Term Corrosion Behaviour of Copper-Coated UFC. Nuclear Waste Management Organization Report Technical Report NWMO-TR-2021-19. Toronto, Canada.

King, F. and M. Behazin. 2021. A Review of the Effect of Irradiation on the Corrosion of Copper-Coated Used Fuel Containers. Corrosion and Materials Degradation, 2, 678–707.

King, F. and S. Briggs. 2022. Development and Validation of a COMSOL Version of the Copper Corrosion Model. Nuclear Waste Management Organization Technical Report NWMO-TR-2022-08. Toronto, Canada.

King, F. and M. Kolář. 2000. The copper container corrosion model used in AECL's second case study. Ontario Power Generation, Nuclear Waste Management Division Report 06819-REP-01200-10041-R00.

King, F. and M. Kolář. 2006. Simulation of the consumption of oxygen in long-term in situ experiments and in the third case study repository using the copper corrosion model CCM-UC.1.1. Ontario Power Generation, Nuclear Waste Management Division Report, 06819-REP-01300-10084-R00.

Kremer, E.P., J.D. Avis, J. Chen, P.J. Gierszewski, M. Gobien, R. Guo and C. Medri. 2019. Postclosure Safety Assessment of a Canadian Used Fuel Repository. 4th Canadian Conference on Nuclear Waste Management, Decommissioning and Environmental Restoration. Ottawa, Canada.

Lampman, T. 2021. Update to Fuel Burnups and Power Ratings. Nuclear Waste Management Organization Technical Report NWMO-TR-2019-04. Toronto, Canada.

Larsson, J. 2021a. Experimental investigation of the system normal stiffness of a 5 MN direct shear test setup and the compensation of it in CNS direct shear tests, EUROCK 2021, Torino, Italy, 20-25 September 2021. IOP Conf. Ser.: Earth Environ. Sci. 833 012011. doi:10.1088/1755-1315/833/1/012011

Larsson, J. 2021b. Quality aspects in direct shear testing of rock joints, Licentiate thesis KTH Royal Institute of Technology, Stockholm, Sweden, TRITA-ABE-DLT, 2113.

Larsson J., Johansson F., Mas Ivars D., Johnson E., Flansbjer M., Portal N. W. (*submitted* a) A novel method for geometric quality assurance of rock joint replicas in direct shear testing – Part 1: derivation of quality assurance parameters and geometric reproducibility. Journal of Rock Mechanics and Geotechnical Engineering, accepted for publication.

Larsson J., Johansson F., Mas Ivars D., Johnson E., Flansbjer M., Portal N. W. (*submitted* b) A novel method for geometric quality assurance of rock joint replicas in direct shear testing – Part 2: validation and mechanical replicability. Journal of Rock Mechanics and Geotechnical Engineering. doi:10.1016/j.jrmge.2022.12.012

Lavoine, E., Darcel, C., Davy, P., Mas Ivars, D., and Kasani, H. 2022. Understanding and predicting stress fluctuations induced by multiscale fracture networks in naturally fractured rocks. Eurock 2022, Espoo, Finland. September 12-15, 2022.

Le Goc R., C. Darcel, P. Davy, M. Pierce and M.A. Brossault. 2014. Effective elastic properties of 3D fractured systems. Proceedings of Discrete Fracture Network Engineering. Vancouver, Canada.

Le Goc R., P. Davy, and C. Darcel. 2015. Scaling effects on elastic properties of jointed rock mass. Proceedings of Eurock. Salzburg, Austria.

Lemieux, J-M., R. Fortier, J. Molson, R. Therrien and M. Ouellet. 2020. Topical collection: Hydrogeology of a cold-region watershed near Umiujaq (Nunavik, Canada), Hydrogeology Journal, 28, p809–812, doi:10.1007/s10040-020-02131-z.

Lemire, R.J., D.A. Palmer, P. Taylor and H. Schlenz. 2020. Chemical Thermodynamics of Iron, Part 2, Vol 13b. OECD Nuclear Energy Agency Data Bank, Eds., OECD Publications. Paris, France.

Liberda, K. 2020. Preliminary Radon Assessment for a Used Fuel Deep Geological Repository. Nuclear Waste Management Organization Technical Report NWMO-TR-2019-09. Toronto, Canada.

Liebscher, A., I. Aaltonen, N. Diomidis, C. Lilja, S. Norris, H. Reijonen and L. Waffle. 2021. Michigan International Copper Analogue (MICA) project – recent advances [abstract]. In: safe ND: Interdisciplinary research symposium on the safety of nuclear disposal practices. November 10-12; Berlin, Germany. Saf. Nucl. Waste Disposal, 1, 129–130, 20.

Liljedahl, L. C., T. Meierbachtol, J. Harper, D. van As, J.O. Näslund, J.O. Selroos, J. Saito, S. Follin, T. Ruskeeniemi, A. Kontula and N. Humphrey. 2021. Rapid and sensitive response of Greenland's groundwater system to ice sheet change. Nature Geoscience. 14(10), pp.751-755. doi:10.1038/s41561-021-00813-1

Liu, L., S. Giger, D. Martin, R. Chalaturnyk and N. Deisman. 2021. Stress and strain dependencies of shear modulus from pressuremeter tests in Opalinus Clay. *In:* The 6th International Conference on Geotechnical and Geophysical Site Characterization. Budapest, Hungary.

Liu, N., H. He, J.J Noël and D.W. Shoesmith. 2017a. The electrochemical study of Dy_2O_3 doped UO_2 in slightly alkaline sodium carbonate/bicarbonate and phosphate solutions, Electrochimica Acta 235, 654-663.

Liu, N., J. Kim, J. Lee, Y-S. Youn, J-G. Kim, J-Y. Kim, J.J Noël and D.W. Shoesmith. 2017b. Influence of Gd doping on the structure and electrochemical behavior of UO2, Electrochimica Acta 247, 496-504.

Liu, N., Z. Qin, J.J Noël and D.W. Shoesmith. 2017c. Modelling the radiolytic corrosion of a-doped UO_2 and spent nuclear fuel, Journal of Nuclear Materials 494, 87-94.

Liu, N., Z. Zhu, J.J Noël and D.W. Shoesmith. 2018. Corrosion of nuclear fuel inside a failed waste container, Encyclopedia of Interfacial Chemistry, 2018, 172–182.

Liu, N., Z. Zhu, L. Wu, Z. Qin, J.J Noël and D.W. Shoesmith. 2019. Predicting radionuclide release rates from spent nuclear fuel inside a failed waste disposal container using a finite element model, Corrosion Journal 75, 302-308.

Liu, N., F. King, J.J Noël and D.W. Shoesmith. 2021. An electrochemical and radiolytic study of the effects of H_2 on the corrosion of UO_2-based materials, Corrosion Science 192 (3), 109776.

MacDonald, N.R., J.J. Day and M.S. Diederichs. 2021a. A Critical Review of Laboratory Multi-Stage Direct Shear Testing for Rock Fractures. GEONiagara – CGS conference 2021.

MacDonald, N., J.J. Day and M.S. Diederichs. 2021b. A critical review of multi-stage direct shear testing for rock joints. GeoNiagara: Creating a Sustainable and Smart Future, Canadian Geotechnical Society Annual Conference, 26-29 September 2021.

MacDonald, M., S. Gaines, M.S. Diederichs. 2021c. Estimation of dynamic elastic properties calculated using ultrasonic pulse waves in rock core and comparison to static elastic properties. GEONiagara – CGS conference 2021.

Markus, S., M.S. Diederichs, E. Almog, and A.M.T. Keita. 2021. A Review of Excavation Induced Coupled Consolidation Analysis in Jointed Rock. GEONiagara – CGS conference 2021.

Markus, S. and M.S. Diederichs. 2021. Use of continuum and pseudo-discontinuum FEM models in stepwise verification of the FDEM for simulating damage around tunnels in brittle rock, RocScience International Conference, April 20-21 2021, Toronto, Canada.

Mas Ivars, D., M. Pierce, C. Darcel, J. Reyes-Montes, D. Potyondy, R.P. Young, and P.A. Cundall. 2010. The synthetic rock mass approach for jointed rock mass modelling.

International Journal of Rock Mechanics and Mining Sciences. 48(2), 219-244. doi:10.1016/j.ijrmms.2010.11.014

Marty, N.C.M., P. Blanc, O. Bildstein, F. Claret, B. Cochepin, D. Su, E.C. Gaucher, D. Jacques, J.-E. Lartigue, K. U. Mayer, J.C.L Meeussen, I. Munier, I. Pointeau, S. Liu and C. Steefel. 2015. Benchmark for reactive transport codes in the context of complex cement/clay interactions, Computational Geosciences, Special Issue on: Subsurface Environmental Simulation Benchmarks. doi: 10.1007/s10596-014-9463-6

Mayer, K.U., E.O. Frind and D.W. Blowes. 2002. Multicomponent reactive transport modelling in variably saturated porous media using a generalized formulation for kinetically controlled reactions. Water Resources Research 38, 1174. doi: 10:1029/2001WR000862

Mayer, K.U. and K.T.B. MacQuarrie. 2010. Solution of the MoMaS reactive transport benchmark with MIN3P - Model formulation and simulation results, Computational Geosciences 14, 405-419. doi: 10.1007/s10596-009-9158-6

Min, K-B. and L. Jing. 2003. Numerical determination of the equivalent elastic compliance tensor for fractured rock masses using the distinct element method. International Journal of Rock Mechanics and Mining Sciences. 40(6), 795-816.

Medri, C. 2015. Non-Radiological Interim Acceptance Criteria for the Protection of Persons and the Environment. Nuclear Waste Management Organization Technical Report NWMO TR-2015-03. Toronto, Canada.

Medri, C. 2021. Proposed Post-Closure Non-Radiological Acceptance Criteria for the Protection of Persons and the Environment. Nuclear Waste Management Organization Technical Report NWMO-TR-2021-21. Toronto, Canada.

Md Abdullah, A., T. Rashwan, I. Molnar and M. Krol. 2022. Modelling Bisulfide Transport through the Engineered Barrier System under Repository Conditions: Coupling Unsaturated Flow and Refining Boundary Conditions. Nuclear Waste Management Organization Technical Report NWMO-TR-2022-06. Toronto, Canada.

Mikhailova, N. 2019. Developing the First Ever Facility for the Safe Disposal of Spent Fuel. IAEA Bulletin. Management of Spent Fuel from Nuclear Power Reactors (Vol. 60/2, June 2019). International Atomic Energy Agency. Vienna, Austria.

Mompeán, F.J and H. Wanner. 2003. The OECD Nuclear Energy Agency thermodynamic database project. Radiochimica Acta 91, 617-622.

Nagra. 2019. Implementation of the Full-scale Emplacement Experiment at Mont Terri: Design, Construction and Preliminary Results. Nagra Technical Report 15-02. Wettingen, Switzerland.

Nasir, O., M. Fall, T.S. Nguyen and E. Evgin. 2011. Modelling of the hydro-mechanical response of sedimentary rocks of southern Ontario to past glaciations. Engineering Geology, 123(4): 271–287.

NEA. 2018. Metadata for Radioactive Waste Management. Report NEA# 7378. OECD Nuclear Energy Agency. Paris, France.

NEA. 2019a. Preservation of Records, Knowledge and Memory across Generations: Developing a Key Information File for a Radioactive Waste Repository. Report NEA#7377. OECD Nuclear Energy Agency. Paris, France.

NEA. 2019b. Preservation of Records, Knowledge and Memory (RK&M) across Generations: Compiling a Set of Essential Records for a Radioactive Waste Repository. Report NEA#7423. OECD Nuclear Energy Agency. Paris, France.

NEA. 2019c. Preservation of Records, Knowledge and Memory across Generations: Final Report. Report NEA#7421. OECD Nuclear Energy Agency. Paris, France.

Neuzil, C.E. and A.M. Provost. 2014. Ice sheet load cycling and fluid underpressures in the Eastern Michigan Basin, Ontario, Canada. JGR Solid Earth. Volume 119, Issue 12, December 2014.

Norris, S.L., Gosse, J.C., Alley, R., et al. (*submitted*) Global estimate of contemporary glacial erosion and its drivers. Nature Geoscience.

Norris, S.L., Fast, J., Gosse, J.C. (*submitted*) Quaternary glacial erosion: A global review of measurement and rate. Earth Sciences Reviews.

NWMO. 2005. Choosing a Way Forward – The Future Management of Canada's Nuclear Fuel – Final Study. Toronto, Canada.

NWMO. 2010. Moving Forward Together: Process for Selecting a Site for Canada's Deep Geological Repository for Used Nuclear Fuel. Toronto. Canada.

NWMO. 2011. Geosynthesis: Nuclear Waste Management Organization NWMO DGR-TR-2011-11, 448 p.

NWMO. 2018. Postclosure Safety Assessment of a Used Fuel Repository in Sedimentary Rock. Nuclear Waste Management Organization Technical Report NWMO-TR-2018-08. Toronto, Canada.

NWMO. 2019. RD 2019 – NWMO's Program for research and development for long term management of used nuclear fuel. Nuclear Waste Management Organization Technical Report NWMO-TR-2019-18. Toronto, Canada.

NWMO. 2021a. Characterization of Optimized Low Heat High Performance Concrete. Nuclear Waste Management Organization Technical Report NWMO-TR-2021-20. Toronto, Canada.

NWMO. 2021b. Technical Program for Long-Term Management of Canada's Used Nuclear Fuel - Annual Report 2020. Ed. S. Briggs. Nuclear Waste Management Organization Technical Report NWMO-TR-2021-01. Toronto, Canada.

NWMO. 2022a. Technical Program for Long-Term Management of Canada's Used Nuclear Fuel - Annual Report 2021. Ed. S. Briggs. Nuclear Waste Management Organization Technical Report NWMO-TR-2022-01. Toronto, Canada.

NWMO. 2022b. Confidence in Safety – South Bruce Site. Nuclear Waste Management Organization Technical Report NWMO-TR-2022-15.

NWMO. 2022c. Confidence in Safety – Revell Site. Nuclear Waste Management Organization Technical Report NWMO-TR-2022-14.

NWMO. 2023. Implementing Adaptive Phased Management 2023-2027. Toronto, Canada.

NWMO and AECOM. 2011. Regional Geomechanics -Southern Ontario: AECOM Canada Ltd. and Nuclear Waste Management Organization. Report NWMO DGR-TR-2011-13 R000.

OHN. 1994. The disposal of Canada's nuclear fuel waste: Preclosure assessment of a conceptual system. Ontario Hydro Nuclear Report N-03784-940010 (UFMED), COG-93-6. Toronto, Canada.

Packulak, T.R.M., J.J. Day, M. T. Ahmed Labeid and M. Diederichs. 2021. New Data Processing Protocols to Isolate Fracture Deformations to Measure Normal and Shear Joint Stiffness. Rock Mech Rock Eng. doi:10.1007/s00603-021-02632-7

Packulak, T.R.M., J.J. Day, M.S. Diederichs. 2022. Enhancement of constant normal stiffness direct shear testing protocols for determining geomechanical properties of fractures. Canadian Geotechnical Journal. 59(9): 1643-1659. doi:10.1139/cgj-2021-0576.

Packulak, T.R.M., J.J. Day. (*submitted*). The impact of axial load distribution on Brazilian tensile testing on rock. Rock Mechanics and Rock Engineering

Packulak, T.R.M., J.J Day, M.S. Diederichs. 2022. Examination of the variation in intact material geomechanical properties on anisotropic rock materials. GeoCalgary2022, the 75th Canadian Geotechnical Society Annual Conference.

Packulak, T.R.M., J.J. Day, M.S. Diederichs. 2022. Tensile strength of anisotropic rocks from enhanced Brazilian laboratory testing and data analysis protocols. EUROCK 2022 Conference, Helsinki.

Persaud, A. 2021. The Aqueous Chloride Complexes of Antimony(III) and Lanthanum(III) from 25°C up to 300°C by Raman Spectroscopy. PhD Thesis, University of Guelph.

Plampin, M.R. 2019. Glacially Induced Hydromechanical Coupling in Shale May Have Caused Underpressured Water in the Eastern Michigan Basin Despite the Possible Presence of Gas Phase Methane. Geophysical Research Letters. Volume 46, Issue 1428 July 2019.

Plampin, M.R. and C.E. Neuzil. 2018. Multiphase flow and underpressured shale at the Bruce nuclear site, Ontario, Canada. Geological Society, London, Special Publications, 482(1), –114.

Plampin, M.R., A.M. Provost, and E.A. Morrissey, 2022, Model of potential multiphase methane evolution in the subsurface of Southern Ontario across a wide range of initial gas contents: USGS Data Release. doi:10.5066/P9I7O770.

Plampin, M.R, A.M. Provost, and C.E. Neuzil. 2021. What Causes Underpressures in Multiphase Subsurface Systems? Possible Mechanisms Elucidated by Modeling Southern Ontario. Hydrogeomechanics. Journal of Geophysical Research – Solid Earth.

Poulsen, B., D. Adhikary, M. Elmouttie and A. Wilkins. 2015. Convergence of synthetic rock mass modelling and the Hoek–Brown strength criterion. International Journal of Rock Mechanics and Mining Sciences. 80, 171-180.

Prasianakis, N.I., G. Kosakowski, Th. Gimmi, P. Luraschi, G.D. Miron, W. Pfingsten and S.V. Churskov. 2022. Cement-Clay Synthesis of Transport Across the Cement-Clay Interface. Nagra Arbeitsbericht NAB 22-34. Wettingen, Switzerland.

Racette, J., A. Walker, T. Yang and S. Nagasaki. 2019. Sorption of Se(-II): Batch Sorption Experiments on Limestone and Multi-site Sorption Modelling on Illite and Montmorillonite. Proceedings of 39th Annual Conference of the Canadian Nuclear Society and 43rd Annual CNS/CAN Student Conference. Ottawa, Canada, June 23-29, 2019.

Radakovic-Guzina, Z., B. Damjanac, T Lam and H. A. Kasani. 2022. DEM-Based Methodology for Simulation of Long-Term Geomechanical Performance of a Placement Room in a Deep Geological Repository. Rock Mechanics and Rock Engineering. doi:10.1007/s00603-022-03188-w

Radakovic-Guzina, Z., B. Damjanac, T Lam and H. A. Kasani. (*submitted*). Numerical Simulation of Long-term Performance of Deep Geological Repository Placement Rooms in Crystalline and Sedimentary Rocks. Submitted to Computers and Geotechnics.

Rashwan, T.L., Md.A. Asad, I.L. Molnar, M. Behazin, P.G. Keech and M.M. Krol. 2022. Exploring the governing transport mechanisms of corrosive agents in a Canadian deep geological repository. Science of The Total Environment, 828, 153944.

Reijonen, H., T. Karvonen and J.L. Cormenzana. 2014. Preliminary ALARA dose assessment for three APM DGR concepts. Nuclear Waste Management Organization Technical Report NWMO-TR-2014-18. Toronto, Canada.

Reijonen, H., J.L. Cormenzana and T. Karvonen. 2016. Preliminary hazard identification for the Mark II conceptual design. Nuclear Waste Management Organization Technical Report NWMO-TR-2016-02. Toronto, Canada.

Reilly, T. 2022. Nuclear Fuel Waste Projections in Canada – 2022 Update, Nuclear Waste Management Organization Technical Report NWMO-TR-2022-17, Toronto, Canada.

Rodriguez, A. and R. Brown. 2021. Preliminary Flood Hazard Assessment at the Ignace Study Area. Nuclear Waste Management Organization Technical Report NWMO-TR-2021-26. Toronto, Canada.

Rodriguez, A. and R. Brown. 2022. Preliminary Flood Hazard Assessment at South Bruce Study Area. Nuclear Waste Management Organization Technical Report NWMO-TR-2022-16. Toronto, Canada.

Rose, C. and T. Al. 2018. Poster (2018 NWMO Geoscience Seminar). Porewater chemical and isotopic compositions in clay rich rocks: extractions with cellulose. Department of Earth Sciences, University of Ottawa, Canada

Saito, J., Meierbachtol, T. and Harper, J., 2023. Multi-decadal elevation changes of the land terminating sector of West Greenland. Journal of Glaciology, 69(273), pp.120-128.

Salehi Alaei, E., M. Guo, J. Chen, M. Behazin, E. Bergendal, C. Lilja, D.W. Shoesmith, and J.J. Noël. s*ubmitted.* The transition from used fuel container corrosion under oxic conditions to corrosion in an anoxic environment. Materials and Corrosion.

Schardong, A., P. Breach, J. Kelly and S. Capstick. 2020. Climate Change Impacts on Climate Variables for a Deep Geological Repository (Ignace Study Area). Nuclear Waste Management Organization Technical Report NWMO-TR-2020-04 R001. Toronto, Canada.

Schneider, A., M. A. Friedl, D. K. McIver, and C. E. Woodcock. 2003. Mapping urban areas by fusing multiple sources of coarse resolution remotely sensed data. Photogrammetric Engineering and Remote Sensing, volume 69, pages 1377-1386.

Selvadurai, P.A. 2010. Permeability of Indiana limestone: experiments and theoretical concepts for interpretation of results. MEng Thesis, McGill University.

Selvadurai, A.P.S. 2019a. A multi-phasic perspective of the intact permeability of the heterogeneous argillaceous Cobourg limestone, Scientific Reports, 9: 17388. doi:10.1038/s41598-019-53343-7

Selvadurai, A.P.S. 2019b. The Biot coefficient for a low permeability heterogeneous limestone, Continuum Mechanics and Thermodynamics, 31, 939-953. doi:10.1007/s00161-018-0653-7

Selvadurai, A.P.S. and P.A. Selvadurai. 2010. Surface permeability tests: Experiments and modelling for estimating effective permeability, Proceedings of the Royal Society, Mathematical and Physical Sciences Series A, 466, 2819-2846.

Selvadurai, A.P.S., A. Blain-Coallier and PA Selvadurai. 2020. Estimates for the effective permeabilities of intact granite obtained from the eastern and western flanks of the Canadian Shield. Minerals: Special Issue on Hydro-Mechanics of Crystalline Rocks, 10(8), 667.

Selvadurai, A.P.S., and A. Głowacki. 2017. Stress-induced permeability alterations in an argillaceous limestone. Rock Mechanics and Rock Engineering, 50(5), 1079-1096.

Selvadurai, A.P.S. and S.M. Rezaei Niya. 2020. Effective thermal conductivity of an intact heterogeneous limestone, Rock Mechanics and Geotechnical Engineering, 12, 682-692. doi:10.1016/j.jrmge.2020.04.001

Selvadurai, A.P.S. and A.P. Suvorov. 2020. Influence of pore shape on the bulk modulus and the Biot coefficient of fluid-saturated porous rocks. Scientific Reports, 10:18959.

Selvadurai, A.P.S. 2021. On the poroelastic Biot coefficient for a granitic rock. Geosciences,11, 219. doi:10.3390/geosciences11050219

Selvadurai, A.P.S. and A.P Suvorov. 2022. Poroelastic properties of rocks with a comparison of theoretical estimates and typical experimental results. Scientific Reports, 12(1), pp.1-11. doi:10.1038/s41598-022-14912-5.

Seyedi, D.M., C. Plua, M. Vitel, G. Armand, J. Rutqvist, J. Birkholzer, H. Xu, R. Guo, K.E. Thatcher, A.E. Bond, W. Wang, T. Nagel, H. Shao and O. Kolditz. 2021. Upscaling THM modeling from small-scale to full-scale in-situ experiments in the Callovo-Oxfordian claystone. International Journal of Rock Mechanics and Mining Sciences 144: 104582.

Snowdon, A.P., S.D. Normani and J.F. Sykes. 2021. Analysis of Crystalline Rock Permeability Versus Depth in a Canadian Precambrian Rock Setting. JGR Solid Earth, 125(5). doi:10.1029/2020JB020998

Standish, T., J. Chen, R. Jacklin, P. Jakupi, S. Ramamurthy, D. Zagidulin, P. Keech and D. Shoesmith. 2016. Corrosion of copper-coated steel high level nuclear waste containers under permanent disposal conditions. Electrochimica Acta, 211, 331–342.

Standish, T., D. Zagidulin, S. Ramamurthy, P. Keech, D. Shoesmith and J. Noël. 2018. Synchrotron-Based Micro-CT Investigation of Oxic Corrosion of Copper-Coated Carbon Steel for Potential Use in a Deep Geological Repository for Used Nuclear Fuel. Geosciences, 8, 360.

Standish, T.E., L.J. Braithwaite, D.W. Shoesmith and J.J. Noël. 2019. Influence of Area Ratio and Chloride Concentration on the Galvanic Coupling of Copper and Carbon Steel. Journal of The Electrochemical Society, 166, C3448–C3455.

Stansberry, A., J. Harper, J. Johnson, and T. Meierbachtol. 2022. Millennial-scale migration of the frozen/melted basal boundary, western Greenland ice sheet. Journal of Glaciology, 68(270), 775-784. doi:10.1017/jog.2021.134

Stuhne G., and W.R. Peltier. 2015. Reconciling the ICE-6G_C reconstruction of glacial chronology with ice sheet dynamics: the cases of Greenland and Antarctica, J. geophys. Res., 120(9), 1841–1865.

Su, D., K.U. Mayer and K.T.B. MacQuarrie. 2020. Numerical investigation of flow instabilities using fully unstructured discretization for variably saturated flow problems, Advances in Water Resources, 143:103673. doi: 10.1016/j.advwatres.2020.103673

Su, D., K.U. Mayer and K.T.B. MacQuarrie. 2021. MIN3P-HPC: a high-performance unstructured grid code for subsurface flow and reactive transport simulation. Mathematical Geosciences. 53, 517-550.

Su, D., K.U. Mayer and K.T.B. MacQuarrie. 2022a. Implementation of 2D/3D-unstructured Grid Capabilities into MIN3P-THCm, Nuclear Waste Management Organization Technical Report NWMO-TR-2022-10. Toronto, Canada.

Su, D., M. Xie, K.U. Mayer and K.T.B. MacQuarrie. 2022b. Simulation of diffusive solute transport in heterogeneous porous media with dipping anisotropy. Frontiers in Water 4, 974145. doi: 10.3389/frwa.2022.974145.

Tam, J., B. Yu, W. Li, D. Poirier, J-G. Legoux, J.D. Giallonardo, J. Howe, and U. Erb. 2022. The Effect of Annealing on Trapped Copper Oxides in Particle-Particle Interfaces of Cold-Sprayed Cu Coatings. Submitted to Scripta Materialia, 208: 114333.

Tortola M., I.S. Al-Aasm and R Crowe. 2020. Diagenetic Pore Fluid Evolution and Dolomitization of the Silurian and Devonian Carbonates, Huron Domain of Southwestern Ontario: Petrographic, Geochemical and Fluid Inclusion Evidence. Minerals 2020, 10(2), 140. doi: 10.3390/min10020140

Turnbull, J., M. Behazin, J. Smith and P.G. Keech. 2022. The impact of 40 years of radiation on the integrity of copper. Journal of Nuclear Materials, 559, 153411.

US DOE. 1994. Airborne release fractions/rates and respirable fractions for non-reactor nuclear facilities. U.S. Department of Energy DOE-HDBK-3010-94. USA.

US DOE. 2007. Preparation of safety basis documents for transuranic waste facilities. U.S. Department of Energy, DOE-STD-5506-2007. USA.

US DOE. 2009. Yucca Mountain Repository SAR. U.S. Department of Energy, DOE/RW-0573, Rev. 1. USA.

Vachon, M.A., K. Engel, R.C. Beaver, G.F. Slater, W.J. Binns, J.D. Neufeld. 2021. Fifteen shades of clay: distinct microbial community profiles obtained from bentonite samples by cultivation and direct nucleic acid extraction. Scientific Reports 11 (1).

Velay-Vitow, J., W. R. Peltier and G. R. Stuhne. 2021. An investigation of the possibility of non-Laurentide ice stream contributions to Heinrich event 3. Quaternary Research, 101, 13-25.

Vilks, P. 2011. Sorption of Selected Radionuclides on Sedimentary Rocks in Saline Conditions - Literature Review. Nuclear Waste Management Organization Technical Report NWMO-TR-2011-12. Toronto, Canada.

Vilks, P. and T. Yang. 2018. Sorption of Selected Radionuclides on Sedimentary Rocks in Saline Conditions – Updated Sorption Values. Nuclear Waste Management Organization Technical Report NWMO-TR-2018-03. Toronto, Canada.

Walker, A., J. Racette, T. Saito, T. Yang and S. Nagasaki. 2021. Sorption of Se(-II) on Illite, MX-80 Bentonite, Shale, and Limestone in Na-Ca-Cl Solutions, Nuclear Engineering and Technology. doi:10.1016/j.net.2021.10.039

Walker, A., J. Racette, J. Goguen and S. Nagasaki. 2018. Ionic Strength and pH Dependence of Sorption of Se(-II) onto Illite, Bentonite and Shale. Proceedings of 38th Annual Conference of the Canadian Nuclear Society and 42nd Annual CNS/CAN Student Conference, Saskatoon, SK, Canada, June 3-6, 2018.

Walker, A., J. Racette, T. Saito, T. Yang and S. Nagasaki. 2022. Sorption of Se(-II) on Illite, MX-80 Bentonite, Shale, and Limestone in Na-Ca-Cl Solutions. Nuclear Engineering and Technology 54 (5), 1616-1622.

Wersin, P., Mazurek, M. and Gimmi, T., 2022. Porewater chemistry of Opalinus Clay revisited: Findings from 25 years of data collection at the Mont Terri Rock Laboratory. Applied geochemistry, 138, p.105234.

Wilk, L. and G. Cantello. 2006. Used fuel burnups and power ratings for OPG owned used fuel. Ontario Power Generation Report 06819-REP-01300-10121. Toronto, Canada.

Wilk, L. 2013. CANDU fuel burnup and power rating 2012 update. Nuclear Waste Management Organization Technical Report NWMO-TR-2013-02. Toronto, Canada.

Wood. 2019. Climate Change Impacts Review and Method Development. NWMO-TR-2019-05. Toronto, Canada.

Xie, M., P. Rasouli, K.U. Mayer and K.T.B. MacQuarrie. 2014. Reactive Transport Modelling of Diffusion in Low Permeable Media – MIN3P-THcm Simulations of EBS TF-C Compacted Bentonite Diffusion Experiments. Nuclear Waste Management Organization Technical Report NWMO-TR-2014-23. Toronto, Canada.

Xie, M., D. Su, K.U. Mayer and K.T.B. MacQuarrie. 2018. Reactive Transport Modelling Investigation of Elevated Dissolved Sulphide Concentrations in Sedimentary Basin Rocks. Nuclear Waste Management Organization Technical Report NWMO-TR-2018-07. Toronto, Canada.

Xie, M., K.U. Mayer and K.T.B. MacQuarrie. 2021. Reactive Transport Simulations of the Alteration of Interfaces between Bentonite/LHHPC/Host Rock and the Impact on Radionuclide Migration. Nuclear Waste Management Organization Technical Report NWMO-TR-2021-14. Toronto, Canada.

Xie, M., D. Su, K.U. Mayer and K.T.B. MacQuarrie. 2022. Reactive transport investigations of the long-term geochemical evolution of a multibarrier system including bentonite, low-alkali concrete and host rock. Applied Geochemistry 143, 105385.

Yang, J., J. Racette, F.G. Garcia, S. Nagasaki and T. Yang. 2022. Sorption of Eu on MX-80 bentonite in Na-Ca-Cl brine solutions. Journal of Nuclear Fuel Cycle and Waste Technology 20 (2), 151-160.

You, C., S. Briggs and M.E. Orazem. 2021. A Mathematical Model for Localized Corrosion of Copper Under a Droplet. In ECS Meeting Abstracts (No. 10, p. 575). IOP Publishing.

You, C., Briggs, S. and Orazem, M.E., 2022. An Advanced Model for Long-Term Localized Corrosion of Copper. In Electrochemical Society Meeting Abstracts 242 (No. 11, pp. 714-714).

Zappone, A. Pio Rinaldi, A. Grab, M. Wenning, Q. Roques, C. Madonna, C. Obermann, A, Bernasconi, A. Soom, F. Cook, P.Guglielmi, Y. Nussbaum. C. Giardini, D. Wiemer, S. 2020. Fault sealing and caprock integrity for CO2 storage: an in-situ injection experiment. AGU Solid Earth.

Zhu, Z., L. Wu, J.J Noël and D.W. Shoesmith. 2019. Anodic reactions occurring on simulated spent nuclear fuel (SIMFUEL) in hydrogen peroxide solutions containing bicarbonate/carbonate – The effect of fission products. Electrochimica Acta 320, 134546.

Zhu, Z., J.J Noël, D.W. Shoesmith. 2020. Hydrogen peroxide decomposition on simulated spent nuclear fuel in bicarbonate/carbonate solutions. Electrochimica Acta 340, 135980.

Zhu, Z, M. Ly, N. Liu, J.J. Noël and D.W. Shoesmith. 2022. The kinetics of hydrogen peroxide reduction on rare earth doped UO2 and SIMFUEL. Frontiers in Materials 9:1038310. doi: 10.3389/fmats.2022.1038310

Zuo, E., A. Lapp, J.J. Jautzy and I. D. Clark. 2021. Crustal Noble Gas Isotopic Characteristics in Low-Permeability Ordovician Sedimentary Rock, Eastern Flank of the Michigan Basin December 2021, ACS Earth and Space Chemistry doi:10.1021/acsearthspacechem.1c00346

APPENDIX A: **NWMO TECHNICAL REPORTS AND REFEREED JOURNAL ARTICLES**

A.1   NWMO TECHNICAL REPORTS

Ariani, I. 2022a. Dose Rate Analysis to Support Radiolysis Assessment of Used CANDU Fuel. Nuclear Waste Management Organization Technical Report NWMO-TR-2022-02. Toronto, Canada.

Ariani, I. 2022b. Dose Rate Analysis to Support Radiological Characterization of Used CANDU Fuel. Nuclear Waste Management Organization Technical Report NWMO-TR-2022-03. Toronto, Canada.

Badley, M. and D.W. Shoesmith. 2022. The Corrosion/Dissolution of Used Nuclear Fuel in a Deep Geological Repository. Nuclear Waste Management Organization Technical Report NWMO-TR-2022-09. Toronto, Canada.

Boucher C., N. Ackerley, V. Peci. 2020. Seismic Activity in the Northern Ontario Portion of the Canadian Shield: Annual Progress Report for the Period January 01, 2020 – December 31, 2021. Nuclear Waste Management Organization Technical Report NWMO-TR-2022-23. Toronto, Canada.

Colàs, E., O. Riba, A. Valls, D. García and L. Duro. 2022. Radionuclide Solubility Calculations (Phase 2). NWMO-TR-2022-11. Toronto, Canada.

Gobien, M., K. Liberda, and C. Medri. 2022. Fuel Radiotoxicity and Screening Analysis. Nuclear Waste Management Organization Technical Report NWMO-TR-2021-16 R001. Toronto, Canada.

King, F., and S. Briggs. 2022. Development and Validation of a COMSOL Version of the Copper Corrosion Model. Nuclear Waste Management Organization Technical Report NWMO-TR-2022-08. Toronto, Canada.

Md Abdullah, A., T. Rashwan, I. Molnar and M. Krol. 2022. Modelling Bisulfide Transport through the Engineered Barrier System under Repository Conditions: Coupling Unsaturated Flow and Refining Boundary Conditions. Nuclear Waste Management Organization Technical Report NWMO-TR-2022-06. Toronto, Canada.

NWMO. 2022a. Technical Program for Long-Term Management of Canada's Used Nuclear Fuel - Annual Report 2021. Ed. S. Briggs. Nuclear Waste Management Organization Technical Report NWMO-TR-2022-01. Toronto, Canada.

NWMO. 2022b. Confidence in Safety – South Bruce Site. Nuclear Waste Management Organization Technical Report NWMO-TR-2022-15. Toronto, Canada.

NWMO. 2022c. Confidence in Safety – Revell Site. Nuclear Waste Management Organization Technical Report NWMO-TR-2022-14. Toronto, Canada.

Rodriguez, A. and R. Brown. 2022. Preliminary Flood Hazard Assessment at South Bruce Study Area. Nuclear Waste Management Organization Technical Report NWMO-TR-2022-16. Toronto, Canada.

Su, D., K.U. Mayer and K.T.B. MacQuarrie. 2022. Implementation of 2D/3D-unstructured Grid Capabilities into MIN3P-THCm, Nuclear Waste Management Organization Technical Report NWMO-TR-2022-10. Toronto, Canada.

Reilly, T. 2022. Nuclear Fuel Waste Projections in Canada – 2022 Update. 2022. Nuclear Waste Management Organization Technical Report NWMO-TR-2022-17. Toronto, Canada.

A.2 REFEREED JOURNAL ARTICLES

Beaver, R., K. Engel, J. Binns and J. Neufeld. 2022. Microbiology of barrier component analogues of a deep geological repository. Canadian Journal of Microbiology, 68(2), 73-90. doi: 10.1139/cjm-2021-0225

Carter, T. R., C. Logan, J. Clark, H. Russell, E. Priebe, S. Sun. 2022. A three-dimensional bedrock hydrostratigraphic model of southern Ontario. Geological Survey of Canada, Open File 8927. doi.org/10.4095/331098

Blanksma, D., J. Hazzard, B. Damjanac, T. Lam, and H. A. Kasani. 2022. Effect of fault reactivation on deformation of off-fault fractures near a generic deep geological repository in crystalline rock in Canada. Journal of Seismology, 26:987–1002. doi:10.1007/s10950-022-10096-7.

Kanik, N., F. Longstaffe, A Kuligiewicz and A Derkowski. 2022. Systematics of smectite hydrogen-isotope composition: Structural hydrogen versus adsorbed water Applied Clay Science, 216 106338. doi: 10.1016/j.clay.2021.106338

Radakovic-Guzina, Z., B. Damjanac, T Lam and H. A. Kasani. 2022. DEM-Based Methodology for Simulation of Long-Term Geomechanical Performance of a Placement Room in a Deep Geological Repository. Rock Mechanics and Rock Engineering. doi:10.1007/s00603-022-03188-w

Rashwan, T.L., Md.A. Asad, I.L. Molnar, M. Behazin, P.G. Keech and M.M. Krol. 2022. Exploring the governing transport mechanisms of corrosive agents in a Canadian deep geological repository. Science of The Total Environment, 828, 153944.

Stansberry, A., J. Harper, J. Johnson and T. Meierbachtol. 2022. Millenial-scale migration of thfrozen/melted basal boundary, western Greenland Ice Sheet. Journal of Glaciology. 68(270) 775-784. doi.org/10.1017/jog.2021.134.

Saito, J., T. Meierbachtol and J. Harper. 2022. Multi-decadal elevation changes of the land terminating sector of West Greenland. Journal of Glaciology. 1-9. doi.org/10/1017/jog.2022.47

Su, D., M. Xie, K. U. Mayer and K.T.B. MacQuarrie. 2022. The impact of ice sheet geometry on meltwater ingress and reactive solute transport in sedimentary basins, Water Resources Research 58 (10), e2022WR032353, doi:10.1029/2022WR032353.

Su, D., M. Xie, K. U. Mayer and K.T.B. MacQuarrie. 2022. Simulation of diffusive solute transport in heterogeneous porous media with dipping anisotropy, Frontiers in Water, 4, 974145, doi:10.3389/frwa.2022.974145.

Tam, J., B. Yu, W. Li, D. Poirier, J-G. Legoux, J.D. Giallonardo, J. Howe, and U. Erb. 2022. The Effect of Annealing on Trapped Copper Oxides in Particle-Particle Interfaces of Cold-Sprayed Cu Coatings. Scripta Materialia, 208: 114333.

Turnbull, J., M. Behazin, J. Smith and P.G. Keech. 2022. The impact of 40 years of radiation on the integrity of copper. Journal of Nuclear Materials, 559, 153411.

Walker, A., J. Racette, T. Saito, T. Yang and S. Nagasaki. 2022. Sorption of Se(-II) on illite, MX-80 bentonite, shale, and limestone in Na-Ca-Cl solution, Nuclear Engineering and Technology 54 (5), 1616-1622.

Winkelmann, R., M. Martin, M. Haseloff, T. Albrecht, E. Bueler, C. Khroulev, and A. Levermann. 2011. The Potsdam parallel ice sheet model (PISM-PIK)–Part 1: Model description, The Cryosphere, 5(3), 715–726.

Xie, M., D. Su, K.U. Mayer and K.T.B. MacQuarrie. 2022. Reactive transport investigations of the long-term geochemical evolution of a multibarrier system including bentonite, low-alkali concrete and host rock. Applied Geochemistry 143, 105385.

Yang, J., J. Racette, F. Guido-Garcia, S. Nagasaki and T. Yang. 2022. Sorption of Eu on MX-80 bentonite in Na-Ca-Cl solutions, Journal of Nuclear Fuel Cycle and Waste Technology 20 (2), 151-160.

Zhu Z, M. Ly, N. Liu, J.J. Noël and D.W. Shoesmith. 2022. The kinetics of hydrogen peroxide reduction on rare earth doped UO2 and SIMFUEL. Frontiers in Materials 9:1038310. doi: 10.3389/fmats.2022.1038310.